**Restricting cell movement: The role of Tspan18 in neural crest migration**

A DISSERTATION
SUBMITTED TO THE FACULTY OF THE GRADUATE SCHOOL
OF THE UNIVERSITY OF MINNESOTA
BY

Corinne Leigh Alinea Fairchild

IN PARTIAL FULFILLMENT OF THE REQUIREMENTS
FOR THE DEGREE OF
DOCTOR OF PHILOSOPHY

Laura S. Gammill, Ph.D Advisor

July, 2013

## Acknowledgements

I am sincerely grateful to the members of the Gammill Lab. Without their endless support and advice I would not have been able to complete this thesis. Julaine Roffers-Agarwal and Bridget Jacques-Fricke, thanks for always giving me great professional and personal life advice, and for always being willing to listen to and critique my practice talks (over and over again, even via FaceTime). Katie Vermillion and Dan Kretzschmar, thanks for being my partners through this journey they call graduate school, and always providing great lunch-time conversations and/or entertainment. Joe Conway and Kevin Lidberg, we would be lost without you both. Finally, I would like to give a crap-ton of thanks to Laura, who has taught me so much. Thanks for showing me that I am an embryologist and teaching me how to write, give a talk, mentor, and become an independent, confident scientist. Also, thanks for always having my back, regardless of the barriers I faced as a graduate student. I couldn't have asked for a better advisor.

To my wonderful thesis committee, David Zarkower, Steve McLoon, Paul Letourneau, Yasuhiko Kawakami and Naoko Koyano; thanks for always providing me with perceptive input and thoughtful criticisms that greatly shaped my thesis work.

Thanks, Lindsey Bade and Tina Hellberg, for sharing the pain of graduate school, and always distracting me from lab-life and grad school woes. Thanks Roooomies (Amanda, Caroline and Kelsey) for reminding me, on our yearly apple-picking get-together, that life can still be fun.

To my family (Tim, Mom, Dad, Danielle, TJ, Pam and Tom) thanks for always being my number one supporters. Thanks for always encouraging me to continue, even when I didn't think it possible. Thanks for always pointing out my exceptional "geeky-ness", even when I had lost all confidence. And lastly, thanks for always keeping me grounded, it is with you that I am most happy and most myself. A special thanks to my parents, who have always provided me with the opportunity to be anything I could ever want to be; I know you worked hard to make it so, and I can't express in words how grateful I am.

I would not have had the strength to finish graduate school if it wasn't for Tim. Thanks for always being at my side, even when I was unrecognizable. Thanks for putting up with flying chairs, tearful nights, and crazy behavior; only to remind me I'm worth it. Thanks for making sure I never forgot what I really wanted from life. Thanks for reminding me who I am, and taking me on fun adventures to take my mind off the stress. Thanks for not laughing (too hard) at my excitement over little, sometimes nerdy, things. Your unwavering support kept me going. I love you.

## Abstract

The neural crest is a unique population of stem cells that arise from the developing central nervous system of vertebrate embryos. Unlike surrounding neuroepithelial cells, neural crest cells undergo an epithelial-to-mesenchymal transition (EMT) and migrate into the periphery of the embryo where they contribute to diverse adult lineages, including the central nervous system, craniofacial skeleton and melanocytes. Despite the fundamental importance of the neural crest, our understanding of the molecular events controlling neural crest migration is incomplete. My thesis focuses on how the transmembrane scaffolding protein, Tetraspanin18 (Tspan18) regulates neural crest EMT. Here I show that Tspan18 is expressed in premigratory, cranial neural crest cells, but is downregulated prior to migration. Sustained expression of Tspan18 maintains the epithelial cell adhesion molecule cadherin-6B (Cad6B) post-translationally, without affecting *Cad6B* mRNA levels, and in turn inhibits cranial neural crest migration. In contrast, morpholino-mediated knockdown of Tspan18 reduces Cad6B protein levels. Unexpectedly, this does not lead to precocious migration, emphasizing that although loss of Tspan18 is required for migration, loss of Tspan18 alone is not sufficient to trigger neural crest migration. This is, at least in part, because EMT is a multiple step process, and the other steps of EMT are not affected by Tspan18 knockdown. Together these findings suggest that Tspan18 antagonizes neural crest EMT by supporting cell adhesion. Additionally, I show here that *Tspan18* downregulation at the onset of migration is achieved by the winged-helix transcription factor, FoxD3. FoxD3 knockdown sustains *Tspan18* mRNA levels and inhibits neural crest formation and migration. Importantly, Tspan18 knockdown rescues the FoxD3 loss-of-function migration defect without rescuing the reduction in neural crest cell number. This suggests that FoxD3 independently regulates neural crest formation and migration, and effects migration through its regulation of *Tspan18*. Overall, the work in this thesis has defined a novel, Tspan18-dependent maintenance of Cad6B protein levels in epithelial cranial neural crest cells that is relieved, via FoxD3, to support migration. This work provides important insight into how cell adhesion molecules are regulated during EMT and increases our understanding for how neural crest transcription factors, like FoxD3, impact the cellular events that lead to migration.

## Table of Contents

## List of Figures

## Abbreviations

**NNE:** non neural ectoderm

**NP:** neural plate

**NPB:** neural plate border

**BMP:** Bone morphogenetic protein; a cell-signaling pathway

**FGF:** Fibroblast growth factor; a cell-signaling pathway

**Wnt:** Wingless/INT; a cell-signaling pathway

**GRN:** gene regulatory network

**EMT:** epithelial-to-mesenchymal transition

**AJ:** adherens junction

**Cad6B:** cadherin-6B

**ADAM:** A disintegrin and metalloproteinase; a family of proteases

**MMP:** matrix metalloproteinase

**Tspan18 or TS18:** tetraspanin18

**s:** somite

**MO:** morpholino oligonucleotide

# Chapter 1

# Background

## 1.1 Overview of the neural crest

The neural crest is a unique, transient population of cells that originates from the developing central nervous system of vertebrate embryos. Unlike their neighbors, neural crest cells detach from the developing neural tube and undergo an extensive migratory phase, during which they actively explore the far reaches of the embryo. Furthermore, individual neural crest cells display an incredible ability to differentiate into diverse cell types of multiple lineages (Bronner-Fraser and Fraser, 1988), leading to their nickname "the fourth germ layer" (Hall, 2000). For example, neural crest cells form not only ectodermal derivatives such as the neurons and glia that form our peripheral nervous system and the melanocytes that pigment our skin, but also, in spite of their ectodermal heritage, mesodermal derivatives including the bone and cartilage shaping our craniofacial skeleton and the outflow tract of the heart. Given that they contribute to essential adult structures, the neural crest is fundamental to vertebrate success. As a result, problems during neural crest development cause a wide array of devastating developmental disorders including cleft lip and palate and Hirschprung's disease (Etchevers et al., 2006). Furthermore, their invasive characteristics in the embryo are thought to contribute to the metastatic severity of neural crest-derived adult cancers, such as melanoma (Gupta et al., 2005). Given its impressive impact on vertebrate development, the neural crest has long been an intriguing model for studying many cellular behaviors including induction and cell fate decisions as well as cell adhesion and migration.

## 1.2 Neural crest induction

### *1.2.1 Participating tissue types*

The formation of a neural crest precursor cell is a long, complex process that occurs as the embryo is undergoing extensive morphological changes (Fig. 1-1). Neural crest formation begins during gastrulation when inductive signals from the sparse underlying mesoderm segregate the ectoderm into three distinct regions. The distal ectoderm forms the future epidermis, and is referred to as the non-neural ectoderm (NNE), while the proximal region forms the presumptive neural plate (NP) and will eventually become the brain and spinal cord. At the margin of the NNE and NP is the neural plate border (NPB), the region from which neural crest cells will eventually arise. As neurulation commences, the neural plate elevates and the neural folds bend inward towards the midline of the embryo. Afterwards, an enclosed neural tube is formed following the fusion of the NPB regions from adjacent sides of the embryo and separation of the neural ectoderm from the overlying NNE. In chick embryos, neural crest cells subsequently migrate from the dorsal portion of the closed neural tube.

The location of the NPB at the margin of the NNE and the NP suggests that inductive signals from both directions might promote neural crest fate. In fact, in chick and amphibian embryos and *in vitro* models, juxtaposing NP tissue with NNE tissue is sufficient to induce neural crest fate, with cells of both lineages contributing to neural crest derivatives (Dickinson et al., 1995; Moury and Jacobson, 1990; Rollhauser-ter Horst, 1979; Selleck and Bronner-Fraser, 1995). Identifying the molecular cues controlling this interaction-dependent induction, however, has been more complicated and seems to vary between species (for a review see (Stuhlmiller and Garcia-Castro,

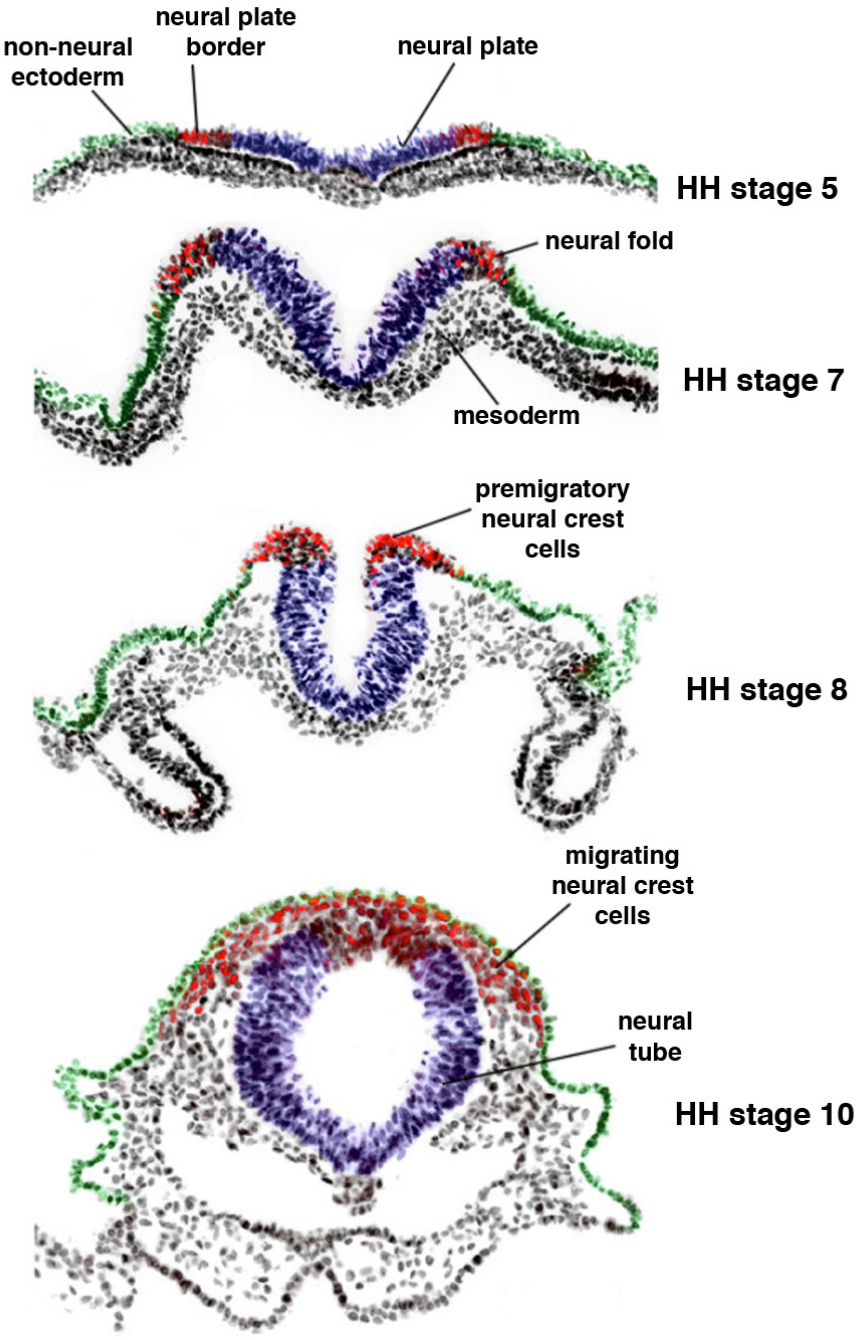
non-neural ectoderm
neural plate border
neural plate
HH stage 5
neural fold
mesoderm
HH stage 7
premigratory neural crest cells
HH stage 8
migrating neural crest cells
neural tube
HH stage 10

**Fig. 1-1. An overview of neural crest development using the chick embryo as a model system**

The formation of neural crest precursors takes place as the embryo is undergoing major morphological changes. During gastrulation, presumptive neural crest cells (red) can be found at the neural plate border, a region molecularly distinct from the adjacent neural plate (blue) and non-nerual ectoderm (green). As neurulation progresses the neural folds elevate and fold inward towards the embryo midline. Meanwhile, specified premigratory neural crest cells are present in the dorsal neural folds. Upon neural tube closure, neural crest cells leave the dorsal neural tube and migrate into the periphery of the embryo. Image adapted from (Stuhlmiller and Garcia-Castro, 2012a).

2012a)). Furthermore, neural crest induction occurs in close spatial and temporal proximity with induction of neural tissue, making it hard to distinguish the two processes. Nonetheless, extensive investigation spanning the last two decades has elucidated some of the molecular mechanisms controlling neural crest formation and, as a result, neural crest induction has been organized into three hierarchical, collaborative steps.

### ***1.2.2 Initial inducing cues***

The first step of neural crest formation requires presumptive NPB cells to integrate multiple environmental cues, in turn distinguishing themselves from the surrounding ectoderm. The requirement for the bone morphogenetic protein (BMP) signaling pathway (for review see (Nohe et al., 2004)) during this early step of neural crest induction has been extensively studied, however its exact role has been highly debated. In *Xenopus*, BMPs play a key role in dorsal-ventral patterning and modulation of BMP signaling distinguishes NNE from NP during early neural induction. High levels of BMP activity specify NNE and low levels, maintained by endogenous BMP inhibitors from the underlying mesoderm, specify NP (Wilson and Hemmati-Brivanlou, 1995). Meanwhile, intermediate levels of BMP activity specify the formation of NPB (LaBonne and Bronner-Fraser, 1998; Marchant et al., 1998). However, in contrast to *Xenopus* embryos, the NNE in chick embryos expresses BMP4 and BMP7, and both molecules are necessary and sufficient to mimic the NPB-inductive activity of the NNE on NP cells (Liem et al., 1997; Liem et al., 1995), suggesting that a higher level of BMP activity might be required for neural crest induction in avian embryos. Although this discrepancy could be solely because of species variation, these conflicting findings could also reflect temporal complexity in the requirement for BMP activity. This idea is consistent with the

finding that BMP activity only affects chick neural crest specification at later steps: around the time of neural tube closure but after initial induction (Selleck et al., 1998). To accommodate these conflicting observations, more recently a two-step model has been proposed that suggests that BMP **inhibition** is first required during gastrulation and subsequently BMP **activity** is required during neurulation to maintain the neural crest precursor pool (Steventon et al., 2009). Importantly, however, in zebrafish embryos, morpholino knockdown of all three endogenously-expressed BMP inhibitors still results in a small pool of neural crest (Ragland and Raible, 2004), suggesting that neural crest induction requires the activity of additional signaling pathways.

In addition to the BMPs, both the fibroblast growth factor (FGF) and Wnt signaling pathways (for reviews see (Dorey and Amaya, 2010; MacDonald et al., 2009)) have been implicated in neural crest induction. FGF signaling is required for the formation of neural crest in both *Xenopus* and chick embryos, as blocking FGF signaling prevents mesoderm-induced neural crest formation *in vitro* (Monsoro-Burq et al., 2003) and inhibiting FGF signaling *in vivo* results in an extensive loss of neural crest markers (Mayor et al., 1997; Stuhlmiller and Garcia-Castro, 2012b; Villanueva et al., 2002). Likewise, active Wnt signaling is a requirement for neural crest induction and Wnt inhibition in *Xenopus*, zebrafish and chick embryos or *in vitro* culture leads to loss of neural crest markers (Deardorff et al., 2001; Garcia-Castro et al., 2002; LaBonne and Bronner-Fraser, 1998; Lewis et al., 2004; Saint-Jeannet et al., 1997; Steventon et al., 2009). Although both of these signaling pathways are required for neural crest induction, a recent study suggests FGFs may actually be required indirectly to activate Wnt signaling (Hong et al., 2008). This is consistent with the documented evidence of cross-

talk between these three signaling pathways (Betancur et al., 2010; Rogers et al., 2012; Stuhlmiller and Garcia-Castro, 2012a), emphasizing the fact that neural crest induction is highly complex, and likely the result of the convergence of multiple environmental cues, rather than the activity of one individual "inducer".

### *1.2.3 The neural crest gene regulatory network*

The combined activity of the BMP, FGF, and Wnt signaling pathways converge to induce the expression of an extensive array of highly conserved transcription factors that have been assembled into a complex gene regulatory network (GRN; Fig. 1-2) (Betancur et al., 2010). There are two transcriptional modules within the GRN that collaborate in a step-wise fashion to promote neural crest development. The first transcriptional module, the NPB specifiers, discriminate the NPB region from the surrounding NP and NNE and provide the NPB region with the competence to activate the expression of the second transcriptional module, the neural crest specifiers. Neural crest specifiers distinguish neural crest precursors within the dorsal neural tube and promote the transition between premigratory and migratory neural crest cells by regulating the expression of neural crest effectors. Each module is described in more detail below.

### *1.2.4 Neural plate border specifiers*

The NPB specifiers, including the homeobox transcription factors *Msx1/2*, *Pax3/7*, and *Gbx2* as well as the zinc finger transcription factor *Zic1*, are activated by a unique combination of signals from the BMP, Wnt, and FGF signaling pathways. Although rare, there is some evidence of NPB specifier expression being the direct result of one neural crest inducer. For example, *Gbx2*, the earliest expressed NPB specifier

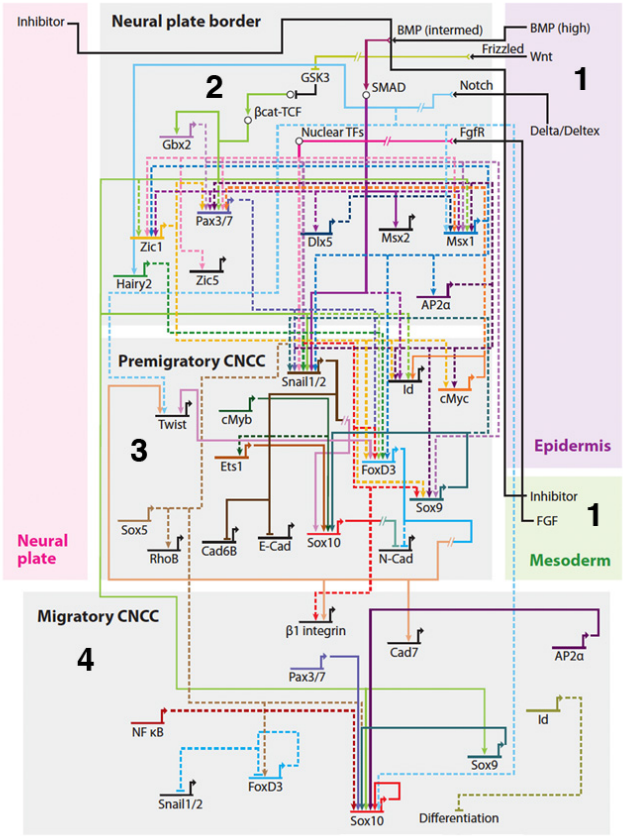
Inhibitor
Neural plate border
BMP (intermed)
BMP (high)
Frizzled
Wnt
1
2
GSK3
SMAD
Notch
βcat-TCF
Nuclear TFs
FgfR
Delta/Deltex
Gbx2
Pax3/7
Zic1
Dlx5
Msx2
Msx1
Hairy2
Zic5
AP2α
Premigratory CNCC
Snail1/2
Id
cMyc
Twist
cMyb
3
Ets1
FoxD3
Epidermis
Sox9
Inhibitor
FGF
1
Sox5
RhoB
Cad6B
E-Cad
Sox10
N-Cad
Neural plate
Mesoderm
Migratory CNCC
β1 integrin
Cad7
AP2α
4
Pax3/7
NF κB
Id
Sox9
FoxD3
Snail1/2
Sox10
Differentiation

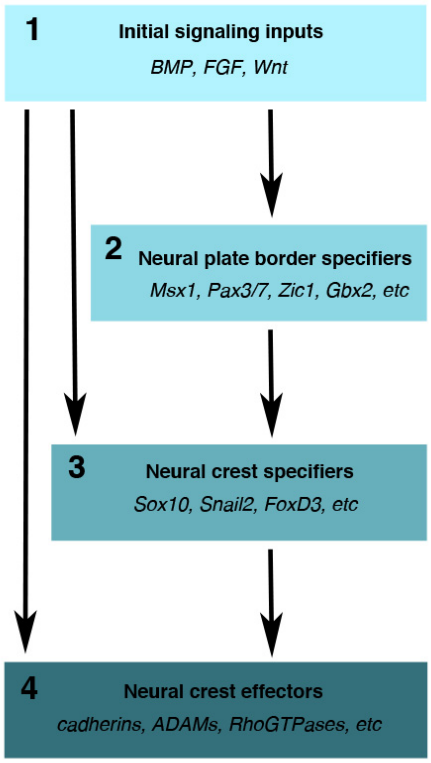
1
Initial signaling inputs
BMP, FGF, Wnt
2
Neural plate border specifiers
Msx1, Pax3/7, Zic1, Gbx2, etc
3
Neural crest specifiers
Sox10, Snail2, FoxD3, etc
4
Neural crest effectors
cadherins, ADAMs, RhoGTPases, etc

**Fig. 1-2. The neural crest gene regulatory network**

The complex gene regulatory network (GRN) that establishes neural crest fate includes environmental inducing cues, transcription factors, and effectors. Environmental signaling inputs (1) initiate neural crest development. After initial induction, two distinct modules of GRN transcription factors collaborate in a step-wise fashion to specify neural crest precursor identity. First, neural plate border specifiers (2) distinguish neural plate border cells from the surrounding ectoderm and promote the expression of neural crest specifiers (3). The expression of neural crest specifiers marks the end of neural crest specification and promotes the activity of neural crest effectors (4) that prepare neural crest cells for migration. Image adapted from (Betancur et al., 2010).

characterized to date, is a direct target of the Wnt signaling pathway (Li et al., 2009). However, as they are the first genes activated downstream of the complex environmental cues controlling neural crest induction, it is not surprising that the expression of the majority of NPB specifiers is a result of the simultaneous activity of more than one signaling pathway (Garnett et al., 2012; Monsoro-Burq et al., 2005; Sato et al., 2005; Tribulo et al., 2003). Additionally, there is evidence for interplay between NPB specifiers. For instance, although *Pax3* and *Zic1* are independently regulated, both need to be present in the NPB at a precise balance in order to achieve neural crest specification, as increased levels of either *Pax3* or *Zic1* promote alternative cell fates at the expense of neural crest (Hong and Saint-Jeannet, 2007).

### ***1.2.5 Neural crest specifiers***

Once NPB identity is established, neural crest specifiers distinguish the identity of neural crest precursors within the dorsal neural tube. The neural crest specifiers, including *AP-2*, *Snail1/2*, *Sox10*, *FoxD3 and Twist*, are required in premigratory neural crest cells to maintain neural crest precursor fate, number and potency (Betancur et al., 2010; Prasad et al., 2012). The expression of these genes is the result of synergistic regulation by environmental inducing pathways as well as NPB specificer activity. One prime example of this regulatory convergence is *Snail2* (previously known as *Slug*). *Snail2* contains cis-regulatory elements for both Smad1 and TCF/Lef, which clues us into its direct regulation by the BMP and Wnt signaling pathways, however, its expression also requires the activity of the NPB specifiers *Zic1*, *Msx1*, and *Pax3/7* (Sakai et al., 2005; Sato et al., 2005; Tribulo et al., 2003; Vallin et al., 2001). Additionally, in *Xenopus*, it appears that many, if not all neural crest specifiers studied to date are both

necessary and sufficient to promote the expression of the other neural crest specifiers (Meulemans and Bronner-Fraser, 2004). For example, morpholino-knockdown of *Sox10* leads to a dramatic loss of *Snail2* and *FoxD3* expression, whereas *Sox10* overexpression expands the *Snail2*- and *FoxD3*-positive domains (Aoki et al., 2003; Honore et al., 2003). It is not currently known whether the regulatory cross-talk between neural crest specifiers is direct.

Many neural crest specifiers are required reiteratively at more than one step of the neural crest developmental pathway (Prasad et al., 2012). One example is the winged helix transcription factor FoxD3, which is first required during neural crest specification to control neural crest precursor survival, multipotency and cell fate (Kos et al., 2001; Lister et al., 2006; Montero-Balaguer et al., 2006; Mundell and Labosky, 2011; Nitzan et al., 2013; Sasai et al., 2001; Stewart et al., 2006; Thomas and Erickson, 2009). However, FoxD3 also regulates neural crest migration later in development. Elevated expression of FoxD3 in the trunk neural tube increases the number of emigrating cells and impacts the expression of cell-cell adhesion molecules (Cheung et al., 2005; Dottori et al., 2001; Kos et al., 2001). However, because FoxD3 is required for neural crest specification, it has been hard to determine whether its effect on migration is direct or a consequence of altered neural crest specification. Furthermore, although the reiterative nature of some neural crest transcription factors can be explained, in part, by the temporal control of their stability (Lander et al., 2011; Vernon and LaBonne, 2006), the post-translational regulation of many neural crest specifiers remains uninvestigated. Thus we are only beginning to understand how neural crest specifiers control multiple steps of the neural crest developmental pathway.

## 1.3 The making of a migratory neural crest cell

Although the expression of neural crest specifiers marks the completion of neural crest specification, it is just the beginning of the process to produce a migratory neural crest cell. The progression from premigratory to migratory neural crest cell is an event that is still not entirely understood, and contemplating this process clearly illustrates the gaps in our current knowledge. For example, although a cell is present in the dorsal neural tube, and may express neural crest cell markers like *Snail2* or *Sox10* it is not guaranteed to ever become a migratory neural crest cell. In fact, marking individual dorsal neural tube cells with lineage-tracing dyes has clearly shown that one cell produces daughter cells that remain in the neural tube and contribute to roof plate lineages in addition to daughter cells that migrate and eventually differentiate into expected neural crest derivatives (Bronner-Fraser and Fraser, 1988; McKinney et al., 2013; Selleck and Bronner-Fraser, 1995). Supporting this finding is the fact that dorsal neural tube cells coexpress both the neural crest marker Snail2 and roof plate marker Lmx1a (Chizhikov and Millen, 2004), suggesting that the transcriptional activity of neural crest specifiers alone is insufficient for the production of a migratory neural crest cell. What, then, *is* the trigger for neural crest migration? This question will most likely be answered when the identity, mechanism, and regulation of neural crest effector genes becomes more clear. Unfortunately, despite the longstanding scrutiny of the regulatory inputs controlling neural crest specifier expression, few of their direct downstream targets have been verified. As a result, we are only beginning to understand how neural crest specifiers impact the dynamic cellular behaviors that are required for their migration in the later steps of the neural crest developmental pathway.

### *1.3.1 Epithelial-to-mesenchymal transition*

Premigratory neural crest cells are epithelial in nature, but to migrate they modify their cellular characteristics and become individual mesenchymal cells through a process called epithelial-to-mesenchymal transition (EMT; Fig. 1-3). Epithelial cells are tightly associated to one another via specialized junctions, exhibit an apical-basal polarity and are anchored to the underlying basement membrane. In turn, epithelial cells form a selectively penetrable barrier that separates distinct embryonic tissues and adult organs while providing structural integrity and protection from external contaminants (Hay, 2005). Epithelial tissue is the first embryonic tissue type formed, but because of their rigid, adherent nature, epithelial sheets are unable to perform the vast number cellular movements required during embryogenesis. In contrast to epithelial cells, mesenchymal cells, such as migratory neural crest cells, are loosely associated with surrounding tissue, exhibit a front-to-back polarity required for locomotion and are capable of diverse morphological movements (Hay, 2005). Embryologists have long appreciated the remarkable difference between epithelial and mesenchymal cells and the process of EMT has been rigorously investigated.

EMT occurs at multiple times throughout development and during disease progression (Hay, 1968; Hay, 2005; Micalizzi et al., 2010; Powell et al., 2013; Thiery et al., 2009). Developmental EMT is required to produce many of the intricate adult structures formed during embryogenesis. In addition to neural crest cells, gastrulation in early amniote embryos requires EMT in order for epiblast cells to internalize and produce the mesoderm and endoderm lineages (Thiery et al., 2009). Furthermore, the mesenchymal cells produced during gastrulation eventually undergo the reverse process,

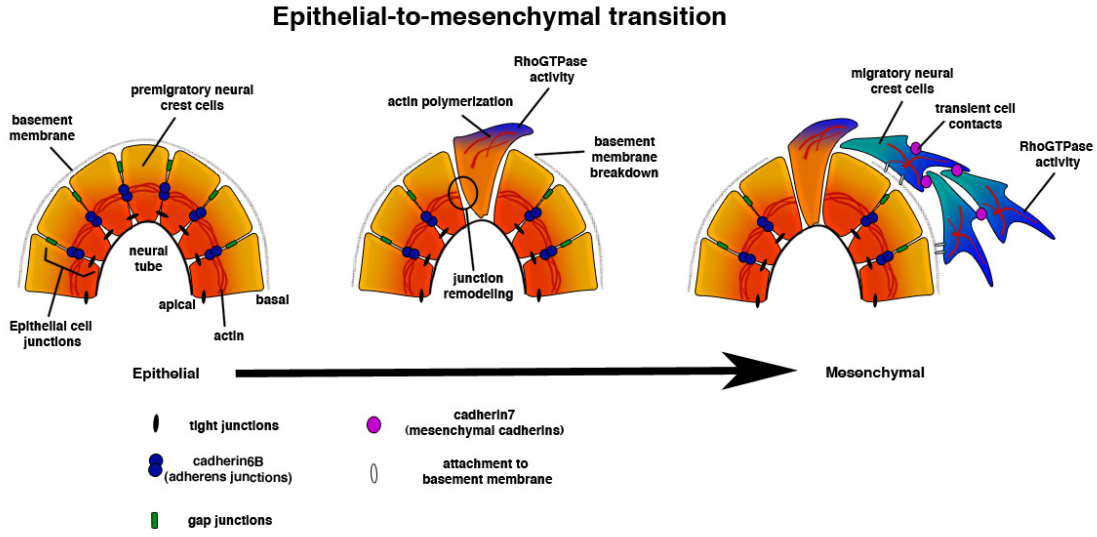
Epithelial-to-mesenchymal transition
basement membrane
premigratory neural crest cells
neural tube
apical
basal
actin
Epithelial cell junctions
RhoGTPase activity
actin polymerization
basement membrane breakdown
junction remodeling
migratory neural crest cells
transient cell contacts
RhoGTPase activity
Epithelial
Mesenchymal
tight junctions
cadherin6B (adherens junctions)
gap junctions
cadherin7 (mesenchymal cadherins)
attachment to basement membrane

**Fig. 1-3. An epithelial-to-mesenchymal transition facilitates neural crest migration.**

In order to leave the neural tube, neural crest cells undergo an epithelial-to-mesenchymal transition (EMT). EMT is a complex process by which rigid, adherent epithelial cells transition into individual mesenchymal cells that are capable of migrating. EMT involves dynamic changes in cell polarity and cell-cell adhesion, the breakdown of the restrictive basement membrane, and major cytoskeletal rearrangements.

MET (mesenchymal-to-epithelial transition), to give rise to transient, mesodermally-derived epithelial structures like the somites and notochord. In addition to being essential to development, EMT has also been implicated in cancer metastasis (Micalizzi et al., 2010; Nieto, 2011), during which cells from adult epithelial structures, such as the mammary gland, detach from the primary tumor and spread throughout the body resulting in secondary tumors. Although EMT occurs in distinct tissues and at various times during development and disease progression, many of the cellular events that occur during EMT are conserved, and the molecular players involved are closely related (Micalizzi et al., 2010; Nieto, 2011; Powell et al., 2013; Thiery et al., 2009).

During EMT cells undergo a complex series of events that include changes in cell-cell adhesion, breakdown of the underlying basement membrane, and reorganization of the actin cytoskeleton (Fig. 1-3). Together these changes allow epithelial cells to detach from their neighbors, invade their surrounding environment and acquire the motility they need to migrate. Some of the molecular players that control these cellular behaviors, as well as their function specifically during neural crest EMT, are outlined below.

## 1.4 Molecules involved in EMT

### *1.4.1 Cadherins*

One of the defining characteristics of epithelial cells is the presence of specialized cell-cell junctions that give epithelial cells their adherent, rigid organization. Three distinct structures comprise these specialized junctions: tight junctions, adherens junctions (AJs) and gap junctions, which are located in that order along the apical-basal axis of an epithelial cell (Fig. 1-3; for review see (Meng and Takeichi, 2009; Oda and

Takeichi, 2011)). AJs are the only junctional structures conserved in all metazoans (Oda and Takeichi, 2011) and are believed to be the main source of physical associations between epithelial cells. Therefore, it is not surprising that during EMT, AJs must be remodeled to allow for individual mesenchymal cell movement.

The main functional component of AJs are cell adhesion molecules of the cadherin superfamily (Fig. 1-4; for review see (Meng and Takeichi, 2009)). Cadherins are integral membrane proteins that provide cell-cell adhesions via their extracellular cadherin (EC) domains that, upon binding $Ca^{++}$, undergo a conformational change and interact strongly with cadherins on adjacent cells (Overduin et al., 1995; Pokutta et al., 1994). Additionally, through intracellular interactions with β-catenin, and subsequently α-catenin, cadherins link AJs to the actin cytoskeleton (Yonemura, 2011) providing additional structural support to epithelial cells. The cadherin family is extremely diverse, but the stereotypical cadherins that provide cell-cell adhesions are called classical cadherins, and to date approximately 20 distinct classical cadherins have been identified (Oda and Takeichi, 2011). Classical cadherins have been organized into two main categories, type I and type II, based on their adhesive properties and phylogenic relationships (Oda and Takeichi, 2011). Type I cadherins (cadherin-1 to -5) play a major role in epithelial AJs, and include the widely expressed E-cadherin (E-cad; cadherin-1) and N-cadherin (N-cad; cadherin-2). Interestingly the role of type II cadherins (cadherin-6 and higher) in AJs is still unclear, leading to their implication in more transient cell-cell adhesions such as those found in migrating mesenchymal cells.

Many cadherins interact homophilically, for example E-cad binds preferentially to E-cad while N-cad prefers N-cad. This observation lead to the idea that cadherin

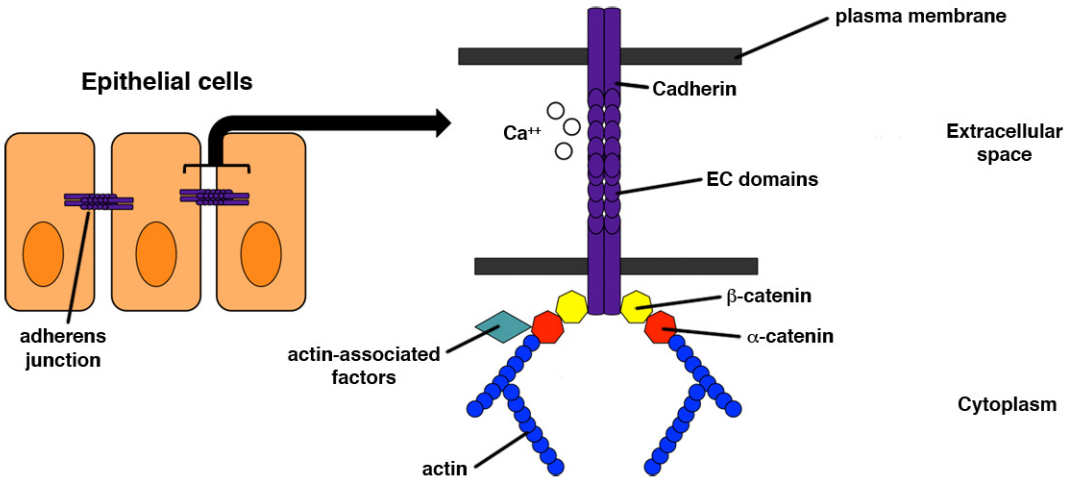
Epithelial cells
adherens junction
plasma membrane
Cadherin
Ca++
Extracellular space
EC domains
β-catenin
α-catenin
actin-associated factors
Cytoplasm
actin

**Fig. 1-4. Cadherin structure**

Adherens junctions are specialized structures found at points of epithelial cell-cell contacts. Cadherins, $Ca^{2++}$-dependent cell adhesion molecules, are the major component of adherens junctions. Upon binding $Ca^{2++}$, cadherins interact homophillically with cadherin molecules on adjacent cells, forming strong cell-cell adhesions. Furthermore, cadherins are linked to the actin cytoskeleton via interactions with β-catenin, providing additional structural support to epithelial cells.

expression promotes cell sorting, with cells expressing similar cadherins segregating from those expressing different cadherins (Nose et al., 1988; Takeichi et al., 1988). However, heterophillic interactions can occur. Cells expressing cadherin-7 or -14 can associate with each other just as strongly as they can with cells expressing cadherin-7 or -14 respectively (Shimoyama et al., 2000). Nonetheless, changes in expression, for example from strong, type I cadherins to more transient and flexible type II cadherins is a common theme during EMT (Gheldof and Berx, 2013; Wheelock et al., 2008). Such cadherin switching presumably leads to reduced epithelial adhesions and perhaps aids in cell sorting during EMT.

### ***1.4.2 Cadherins relevant to neural crest EMT***

Neural crest cells express different cadherins as they progress through development, and the expression of an individual cadherin often varies along the rostral-caudal axis. Prior to migration in chick embryos, N-cad is expressed throughout most of the neural tube, but it is downregulated in the dorsal neural folds in the head well before cranial neural crest cells migrate and is also downregulated in trunk neural crest cells as they exit the neural tube (Akitaya and Bronner-Fraser, 1992; Dady et al., 2012; Nakagawa and Takeichi, 1998; Shoval et al., 2007). Additionally premigratory chick neural crest cells express cadherin-6B (Cad6B), and its expression is downregulated prior to migration in cranial neural crest cells but it is retained in early migrating trunk neural crest cells (Coles et al., 2007; Nakagawa and Takeichi, 1995; Park and Gumbiner, 2010). Strikingly, recent studies in chick showed that E-cad is expressed throughout the entire cranial neural tube, even in early migrating neural crest cells (Dady et al., 2012). However, in the trunk E-cad is absent from the neural tube and is instead restricted to the

NNE following neural tube closure (Dady et al., 2012). Once migration commences, neural crest cells gain the expression of cadherin-7 (Cad7) in chick embryos (Nakagawa and Takeichi, 1995) and cadherin-11 (Cad11) in *Xenopus* embryos (Vallin et al., 1998). Thus, as neural crest cells become migratory, they transition from expressing premigratory cadherins, like N-cad or Cad6B, to migratory cadherins, such as Cad7 and Cad11, indicating that a cadherin switch is involved in neural crest EMT. Furthermore, blocking this cadherin switch inhibits migration (Borchers et al., 2001; Coles et al., 2007; Dufour et al., 1999; Nakagawa and Takeichi, 1998; Shoval et al., 2007), emphasizing the requirement for strict regulation of cadherin expression during neural crest EMT.

In addition to regional differences in cadherin expression, the function of individual cadherins varies along the rostral-caudal axis. For example, Cad6B plays a distinct role in cranial and trunk neural crest cells. In chick cranial premigratory neural crest, Cad6B appears to be a source of epithelial cell-cell adhesions, as loss of Cad6B augments neural crest migration while overexpression of Cad6B inhibits migration (Coles et al., 2007). Furthermore, the neural crest specifier Snail2 directly represses *Cad6B* transcription, alleviating Cad6B-dependent cell-cell adhesions and in turn promoting migration (Taneyhill et al., 2007). As transcriptional repression of cadherins is a recurring observation of EMTs during development and disease, this finding is consistent with our generalized understanding of how cells disrupt epithelial adhesions during EMT (Gheldof and Berx, 2013; Micalizzi et al., 2010; Peinado et al., 2004; Thiery et al., 2009). Meanwhile, early migrating trunk neural crest cells retain Cad6B protein, and in this case Cad6B is actually required to promote de-epithelialization by activating a non-canonical BMP signaling pathway (Park and Gumbiner, 2010; Park and Gumbiner, 2012).

Consistent with this finding, blocking Cad6B function in trunk neural crest cells actually inhibits migration (Park and Gumbiner, 2010). This finding suggests that in the trunk Cad6B may function in more than just a cell adhesive capacity, and emphasizes that it most likely acts through distinct mechanisms in the trunk and head. Further investigation into the regional differences in cadherin regulation is required for a more complete understanding of how individual cadherins play such distinct roles in cranial and trunk neural crest EMT.

### *1.4.3 ADAM proteases*

The "A disintegrin and metalloproteinase" (ADAM) family of membrane proteins are a diverse group of proteases that have unique roles in regulating cell adhesion, cell migration, cell fusion and intercellular signaling (Edwards et al., 2008; Tousseyn et al., 2006). ADAMs are primary facilitators in protein ectodomain shedding, a process by which integral membrane proteins or membrane associated proteins are cleaved to produce a soluble extracellular domain and resulting membrane-associated fragment (Weber and Saftig, 2012). This can drastically change the function of shed proteins by downregulating their presence at the membrane or by liberating soluble ligands or cytoplasmic fragments that modulate cell signaling (Blobel, 2005; Weber and Saftig, 2012). For example, Notch signaling is transduced by multiple cleavages of the Notch receptor, the first of which is mediated by ADAM10-dependent ectodomain shedding, which removes the Notch extracellular domain and frees up the membrane associated portion for further clevage by γ-secretase (Kopan, 2012; Pan and Rubin, 1997; Weber and Saftig, 2012). In addition to cell signaling molecules, ADAMs can also cleave cell

adhesion molecules including cadherins (Tousseyn et al., 2006), and have thus become interesting genes for study during EMT.

### ***1.4.4 ADAMs relevant to neural crest EMT***

The activity of neural crest cadherins is modulated via proteolytic processing by ADAMs. For example, cleavage of Cad11 by ADAM13 is required for migration of *Xenopus* cranial neural crest cells (McCusker et al., 2009). Interestingly, this processing produces an extracellular, membrane-associated cleavage product that retains only some cell-cell adhesive activity (McCusker et al., 2009) and presumably supports migration by promoting transient, mesenchymal cell-cell adhesions in exchange for stronger, epithelial adhesions. Such cadherin processing can also act as a switch between cell-cell adhesion and cell signaling activity. In chick, loss of N-cad protein is a prerequisite for migration, but its downregulation is not mediated transcriptionally, as *N-cad* mRNA levels are unchanged in the dorsal neural tube when trunk neural crest cells begin to migrate (Shoval et al., 2007). Instead, cleavage of N-cad by the BMP-responsive metalloproteinase, ADAM10, mediates loss of N-cad protein levels (Shoval et al., 2007). This cleavage presumably alters N-cad dependent cell-cell adhesions as expected, but also produces a soluble C-terminal fragment (CTF2). Furthermore, CTF2 translocates to the nucleus and leads to transcriptional changes that promote exit from the neural tube (Shoval et al., 2007). This finding suggests that ADAM-dependent cleavage of cadherins might serve to communicate disruption of adhesions with the rest of the cell, thus coordinating changes in cell-cell adhesion with other cellular events that occur during EMT. Unfortunately, ADAM-dependent processing of many neural crest cadherins has not been evaluated. Future investigation into this processing will help us gain a more

comprehensive understanding for the unique roles cadherins play in neural crest EMT, and may help clarify some of the distinct regional differences in cadherin function.

### *1.4.5 Matrix metalloproteinases (MMPs)*

Like all epithelia, the basal surface of the neural tube is surrounded by an intact basement membrane (Tosney, 1982), and even when neural crest cells have completed other cellular changes that occur during EMT, they will not invade an intact lamina (Erickson, 1987). Therefore, during EMT it is crucial that migrating cells breakdown their restricting basement membrane. Invading cells do this, in part, via the activity of matrix metalloproteinases (MMPs). MMPs are extracellular or cell-surface expressed proteins that, upon interaction with metal ions, can enzymatically degrade components of the extracellular matrix (ECM), including laminin, as well as cell surface adhesion molecules (Sternlicht and Werb, 2001). Although the requirement for MMPs in degradation of the tumor microenvironment during cancer progression has been well studied (Micalizzi et al., 2010; Przybylo and Radisky, 2007), less is known about how specific MMPs impact neural crest development.

### *1.4.6 MMPs relevant to neural crest EMT*

To date, the activity of two MMPs have been implicated in chick neural crest EMT. The first, MMP2/gelatinase A, is expressed transiently in early migrating chick neural crest cells, and blocking MMP2 activity leads to a drastic loss of migratory neural crest cells (Duong and Erickson, 2004). Although MMP2 is known to digest laminin (McCawley and Matrisian, 2001), this study did not show a direct effect on the laminin surrounding the neural tube. Meanwhile, a later study showed that another gelatinase, MMP9/gelatinaseB is also expressed in early migrating chick neural crest cells and its

expression in turn promotes the breakdown of both the laminin basement membrane and N-cad, while its loss inhibits migration (Monsonego-Ornan et al., 2012). Similarly, the activity of a related MMP, MMP14 (MT1-MMP), expressed in *Xenopus* neural crest cells is required to promote migration in that context (Harrison et al., 2004; Tomlinson et al., 2009), suggesting similar mechanisms control basement membrane breakdown in both species. Thus, MMPs appear to be important for promoting neural crest cell invasive abilities, however more investigation is required to gain a complete understanding for how they are involved in EMT as compared to their involvement during migration.

### ***1.4.7 RhoGTPases***

In the final stages of EMT, neural crest cells become motile, retract their apical tails and propel themselves out of the neural tube. To complete these actions, neural crest cells produce a remarkable amount of mechanical force. In fact, live cell imaging has shown that sometimes neural crest cells leaving the neural tube produce enough force to rupture their apical tail and leave behind intact cell-cell adhesions (Ahlstrom and Erickson, 2009). Such mechanical forces are provided by dynamic cytoskeletal rearrangements that are regulated in part by the Rho family of GTPases. The three main RhoGTPase family members are Rho, Rac and Cdc42, and all are molecular switches of the Ras superfamily that alternate between GDP-bound (off) and GTP-bound (on) conformational states (Etienne-Manneville and Hall, 2002; Wennerberg and Der, 2004). When bound to GTP, RhoGTPases activate a number of downstream effectors including, but not limited to, Rho kinase (ROCK) and cytoskeletal regulators like WASPs and mDia (Vega and Ridley, 2007), that in turn lead to the dynamic cytoskeletal rearrangements that specify cell shape or enhance motility. For example, constitutively active Rho leads

to the formation of actin stress fibers, active Rac results in the formation of lamellipodia and Cdc42 promotes the assembly of filopodia (Kozma et al., 1995; Nobes and Hall, 1995; Ridley and Hall, 1992; Ridley et al., 1992). In addition to providing the mechanical force required for leaving the neural tube, RhoGTPases impact the dissolution of adherens junctions during EMT and regulate cell motility during migration (Menke and Giehl, 2012; Savagner, 2001).

### ***1.4.8 RhoGTPases relevant to neural crest EMT***

Multiple RhoGTPases have been implicated in regulating various aspects of neural crest EMT, including RhoA, RhoB, RhoU and Rac1 (Berndt et al., 2008; Faure and Fort, 2011; Fort et al., 2011; Groysman et al., 2008; Liu and Jessell, 1998; Matthews et al., 2008; Notarnicola et al., 2008; Shoval and Kalcheim, 2012). Despite conflicting findings on the exact requirement for RhoGTPases as neural crest cells exit the neural tube and actively migrate (Berndt et al., 2008; Groysman et al., 2008; Liu and Jessell, 1998), there is strong evidence that RhoGTPases regulate cell-cell adhesions during neural crest EMT. In fact, inhibiting Rho signaling via ROCK inhibitors in chick trunk neural crest cells prematurely downregulated N-cad in the dorsal neural tube and promoted migration, while overexpression of RhoA or RhoB maintained N-cad levels and inhibited migration (Groysman et al., 2008), suggesting that Rho stabilizes N-cad protein levels and antagonizes EMT. This is consistent with the general idea that RhoGTPase activity is required to assemble and maintain mature adherens junctions (Menke and Giehl, 2012). These findings suggest that RhoGTPases, a protein family that is best known for their role in regulating cytoskeletal dynamics in actively migrating

cells, also functionally interacts with proteins responsible for neural crest cell-cell adhesion.

### *1.4.9 The consequence of EMT*

As a consequence of EMT, the cellular characteristics of epithelial premigratory neural crest cells are remodeled and neural crest cells transition into motile mesenchymal cells that are capable of migration. Although EMT involves independent changes in cell adhesion, invasiveness, and motility, these cellular events occur simultaneously and are inter-connected rather than linear. Recent studies using live cell imaging in chick neural tube slice cultures stress this point and show that at times cells exit the neural tube without completing all the steps of EMT. For example, some cells acquired enough mechanical force to exit the neural tube without completely dissociating their cell adhesions (Ahlstrom and Erickson, 2009). Further investigation into the dynamic regulation of key EMT modulators will help us answer remaining questions about how neural crest cell-cell adhesions are regulated and how the independent steps of EMT are coordinated. New studies involving live cell imaging in addition to identifying new EMT regulators will be crucial to increasing our understanding of how neural crest cells become migratory.

## 1.5 Insight into the differences between cranial and trunk neural crest cells

Neural crest cells arise from nearly the entire neural tube, however there are distinct differences between neural crest cells in different regions (Kuo and Erickson, 2010). For example, neural crest potential is not equivalent along the anterior-posterior axis. Although neural crest cells from all regions of the neural tube can produce neural, glial and melanocyte derivatives, the ability of neural crest cells to contribute to bone and

cartilage is restricted to cranial and rostral trunk neural crest cells anterior to the fifth somite (Le Lievre and Le Douarin, 1975; Nakamura and Ayer-le Lievre, 1982). Moreover, the dorsal neural tube anterior to the mid-diencephalon does not produce migratory neural crest cells (Creuzet et al., 2005). This suggests that there are innate differences in neural crest cells in different regions of the embryo (Kuo and Erickson, 2010).

Perhaps the most striking difference between cranial and trunk neural crest cells is their modes of migration away from the neural tube. Cranial neural crest delamination occurs quickly, with large numbers of cells leaving the neural tube *en masse*, while trunk neural crest cells leave the neural tube one at a time, over a period of 2-3 days (Duband, 2006; Kalcheim and Burstyn-Cohen, 2005; Kuo and Erickson, 2010; Tosney, 1978; Tosney, 1982). Furthermore, once cranial neural crest cells leave the neural tube they migrate collectively in broad streams, with contacts between them essential for directing their migration (Carmona-Fontaine et al., 2008; McCusker et al., 2009). In contrast, trunk neural crest cells migrate individually, although similar transient contacts form between individual migratory trunk neural crest cells (Kasemeier-Kulesa et al., 2005; Kulesa and Fraser, 2000). The unique environment to which cranial and trunk neural crest cells are exposed may play a crucial role in mediating their modes of migration, but the mechanism dictating this striking difference is currently unknown.

Recent studies in chick embryos have identified a few molecular differences between cranial and trunk neural crest cells. As previously mentioned, there are a number of key differences in cadherin expression and individual cadherin function in different regions of the neural tube (see section 1.4.2). This emphasizes that EMT regulators, such

as cell adhesion molecules, are likely to play a prominent role in mediating the migratory dissimilarities between cranial and trunk neural crest cells. Further investigation into neural crest cadherin regulation will help define some of the regional differences in EMT and help to determine whether different EMT mechanisms are central to the cranial versus trunk mode of migration. Additionally, the transcription factor *Ets-1* is involved in regulating cranial-specific migratory characteristics. Cranial neural crest cells alone express *Ets-1*, and its misexpression in the trunk induces basement membrane breakdown and the "all at once" mode of migration typically restricted to the head (Theveneau et al., 2007). Unfortunately, since the targets of *Ets-1* are unknown, we do not how *Ets-1* impacts the cellular events that promote the cranial mode of migration. Together these findings emphasize that the mechanisms controlling the migration of cranial and trunk neural crest cells are clearly distinct, and we cannot study one population and assume the outcome applies for all neural crest cells.

## 1.6 Thesis goals

### *1.6.1 Identifying new regulators of neural crest EMT*

Despite the importance of understanding neural crest EMT, identifying novel EMT regulators has proven difficult. One reason for this is the fact that neural crest precursors are present within a mixed population of dorsal neural tube cells and some of these cells will never migrate. Thus, distinguishing the cells that will migrate is virtually impossible, given that the expression of neural crest specifiers does not guarantee migration. Nonetheless, a recent screen has provided a much-needed profile of genes that are expressed as a consequence of neural crest induction (Adams et al., 2008; Gammill and Bronner-Fraser, 2002). One of the genes resulting from this screen was

*Tetraspanin18* (*Tspan18*). *Tspan18* encodes a small, transmembrane protein that was first cloned from developing chick spinal cord (Perron and Bixby, 1999), whose function remained unknown. Interestingly, the role of tetraspanins during neural crest development has never been investigated, making the finding that *Tspan18* is upregulated upon neural crest induction an important one for further investigation.

### ***1.6.2 The tetraspanin family***

*Tspan18* is a member of the tetraspanin family, a large and diverse group of integral membrane proteins consisting of at least 32 mammalian homologues, one of which has been discovered in every cell type examined (Hemler, 2003). In addition to the four characteristic transmembrane domains that give tetraspanins their name, they share a number of other essential features (Fig. 1-5; (Levy and Shoham, 2005)). These include two stereotypical extracellular domains, the small extracellular loop (SEL, ECL1) and long extracellular loop (LEL, ECL2), as well as multiple intracellular, juxtamembrane cysteines that are commonly modified by the reversible addition of the fatty acid palmitate via palmitoylation. The unique features of tetraspanins allow them to interact with their binding partners, which include cadherins, integrins, receptors, and other tetraspanins, to form complex membrane microdomains called tetraspanin webs. Tetraspanins have no known enzymatic activity, and as a result were historically thought to play mainly a structural role. However, recent evidence supports the idea that tetraspanins are capable of actively regulating the stability, localization and processing of associated proteins within the tetraspanin web (Hemler, 2005; Tsai and Weissman, 2011; Wakabayashi et al., 2009). As a result, tetraspanins impact many diverse cellular

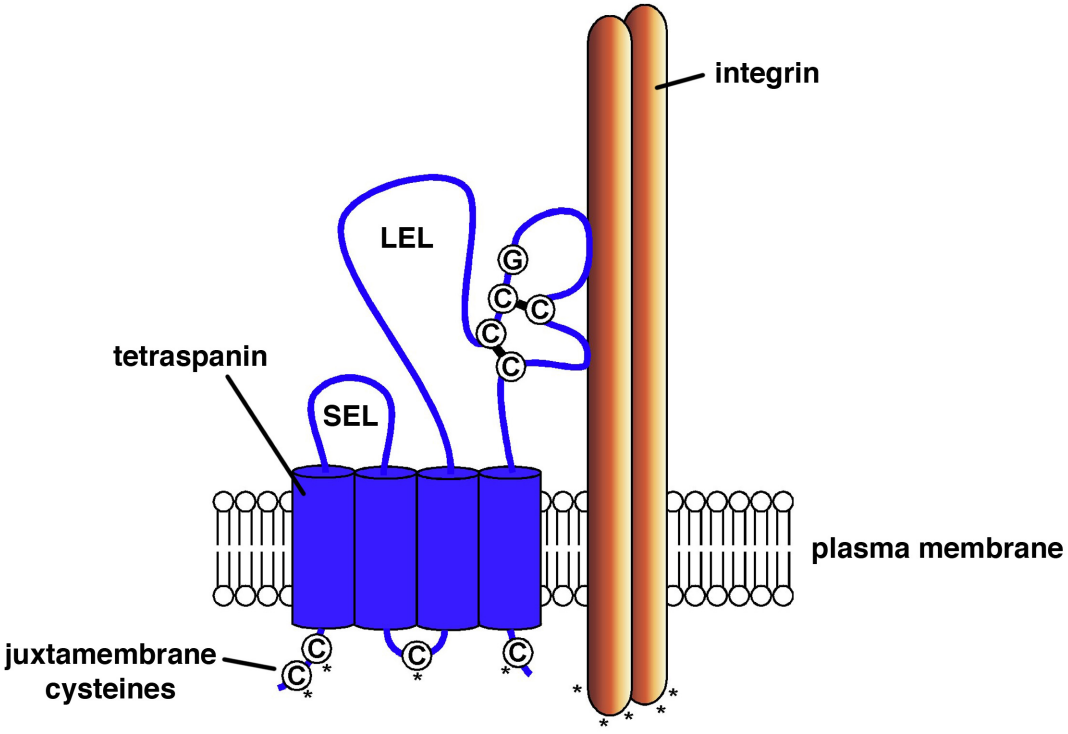
integrin
LEL
G
C
C
C
C
tetraspanin
SEL
plasma membrane
juxtamembrane
cysteines
C
C
C
C
*
*
*
*
*
*
*
*
*

**Fig. 1-5. Tetraspanin structure**

Tetraspanins (blue) are small transmembrane proteins that span the membrane four times. They contain a number of defining structural features; including two extraceullular loops the SEL and LEL and juxtamembrane cysteines that are commonly modified by the addition of the fatty acid palmitate (*). These structural features facilitate interactions with nearby membrane proteins including cell adhesion molecules like integrins (orange) and cadherins as well as other tetraspanins and some receptors. With their binding partners they form unique membrane microdomains called tetraspanin webs and regulate diverse cellular processes including migration. Image modeled after (Levy and Shoham, 2005).

processes, including cell adhesion, migration, invasion and fusion (Hemler, 2003; Hemler, 2005). Because the tetraspanin family is large and diverse, their actions are also diverse and the activity of an individual tetraspanin is commonly distinct in different cellular contexts (Hemler, 2005).

### *1.6.3 Tetraspanins are excellent candidate regulators of neural crest EMT*

Tetraspanins have been known to both suppress and promote cancer metastasis (Zoller, 2009). For example, the tetraspanin CD82, a well-known metastasis suppressor, regulates cadherin-dependent cell adhesion and the localized activity of extracellular proteases (Tsai and Weissman, 2011), two events that similarly occur during neural crest EMT. Specifically, in non-small cell lung carcinoma, CD82 strengthens the interaction of E-cad with β-catenin, in turn promoting cell-cell adhesion to maintain an epithelial barrier that prevents cancer cell dissemination from the primary tumor (Abe et al., 2008). Meanwhile, expression of CD82 in a mammary epithelial cancer cell line significantly reduces the activation of urokinase plasminogen activator surface receptor (uPAR; (Bass et al., 2005)), a molecule that directly regulates the invasiveness of many metastatic cancer cells by activating localized proteolysis of ECM components. Although these mechanisms for CD82 are functionally distinct, they both reflect an overall role in suppressing metastasis. In contrast, another tetraspanin CD151 actually promotes metastasis by activating MMPs or modulating integrin function (Winterwood et al., 2006; Zoller, 2009). Given the similarities between cancer metastasis and neural crest EMT (Nieto, 2011; Powell et al., 2013; Thiery et al., 2009), tetraspanins are intriguing candidate regulators of neural crest EMT. In fact, tetraspanins have already been implicated in modulating known neural crest EMT regulators. For example, Tspan12

promotes the maturation of ADAM10, a protease that has been implicated in neural crest EMT (see section 1.4.4), in multiple cancer cell lines and subsequently regulates the cleavage of amyloid precursor protein (Xu et al., 2009). Thus, investigating the role of tetraspanins during neural crest EMT may help clarify how the molecular players of EMT are regulated.

### ***1.6.4 Overview of thesis chapters***

The goal of this thesis was to gain a better understanding of how the molecular players involved in neural crest EMT, such as cadherins, are regulated. Because it's expression was a consequence of neural crest induction *in vitro* (Adams et al., 2008; Gammill and Bronner-Fraser, 2002), I more specifically aimed to evaluate the role of Tspan18 during neural crest EMT. Given that other tetraspanins have been widely implicated in regulating cell-cell adhesion in cancer metastasis, I hypothesized that Tspan18 regulates cell-cell adhesions during cranial neural crest EMT by modulating the activity of the neural crest cadherin, Cad6B.

In Chapter 2, I summarize the findings of multiple Tspan18 gain- and loss-of-function experiments that reveal Tspan18's involvement in neural crest cell adhesion and provide a clearer picture of the regulation of cranial neural crest EMT. Specifically, I show that Tspan18 maintains Cad6B post-translationally, and conclude that alleviating this Tspan18-mediated stabilization is required, in parallel to transcriptional repression by Snail2, for migration. I find that this parallel pathway includes the neural crest specifier FoxD3, and report that *Tspan18* lies downstream of FoxD3. This is the first study showing that Cad6B is post-translationally regulated, and importantly provides new insight into the requirement for simultaneous transcriptional and post-translational

regulation of cadherins during EMT. I also add to previous findings emphasizing that neural crest EMT is a complex process that involves many independent events, increase our understanding for how neural crest specifiers modulate EMT, and provide new insight into some of the regional differences exhibited by neural crest cells as they migrate.

Chapter 3 is a follow-up of the experiments performed in Chapter 2, and provides a more in depth analysis behind the transcriptional regulation of *Tspan18* by FoxD3. FoxD3 loss-of-function experiments in this chapter show that FoxD3 is required for *Tspan18* downregulation, but suggest it does not work alone in regulating *Tspan18* mRNA expression. Furthermore I report that FoxD3 is required for cranial neural crest specification and migration. Importantly, the FoxD3 loss-of-function migration defect, but not specification defect, is partially rescued by Tspan18 knock down. This finding suggests that FoxD3 plays an independent role in regulating cranial neural crest migration, and this role is achieved by promoting *Tspan18* downregulation. This study provides crucial new insight into how the neural crest specifiers impact cellular behaviors during EMT, identifies one of the few downstream targets of a neural crest specifier, and highlights for the first time an independent role of FoxD3 in chick cranial neural crest specification and migration.

Following my summary of the main conclusions of this thesis and proposed future directions in Chapter 4, I have outlined preliminary data I have obtained in an attempt to understand the mechanism behind Tspan18's maintenance of Cad6B protein levels in Appendix I. In this section, I propose that Tspan18 might support Cad6B protein levels by modulating ADAM-dependent Cad6B processing. Although these data do not provide

conclusive evidence for this mechanism, they do support continuing investigation into Tspan18's potential role in regulating ADAM maturity, trafficking, or activity and how this might mediate Cad6B function. Altogether the work described in this thesis has provided new insight into our understanding of how neural crest cells become migratory, and has interesting implications for cancer cell metastasis.

# Chapter 2

## Tetraspanin18 is a FoxD3-responsive antagonist of cranial neural crest epithelial-to-mesenchymal transition that maintains cadherin-6B protein

[Reprinted from: Farichild, C. L. and Gammill, L. S. (2013). Tetraspanin18 is a FoxD3-responsive antagonist of cranial neural crest epithelial-to-mesenchymal transition that maintains cadherin-6B protein. J Cell Sci **126**, 1464-76.]

## 2.1 Summary:

During epithelial to mesenchymal transition (EMT), tightly associated, polarized epithelial cells become individual mesenchymal cells capable of migrating. Here, we investigate the role of the transmembrane protein tetraspanin18 (Tspan18) in cranial neural crest EMT. *Tspan18* mRNA is expressed in premigratory cranial neural crest cells, but is absent from actively migrating neural crest cells. Tspan18 knock down leads to a concomitant loss of Cadherin6B (Cad6B) protein, while Cad6B protein persists when Tspan18 expression is extended. As the temporal profile of *Cad6B* mRNA downregulation is unaffected in these embryos, this indicates that Tspan18 maintains Cad6B protein levels and reveals that Cad6B is regulated by post-translational mechanisms. Although downregulation of Tspan18 is necessary, it is not sufficient for neural crest migration: the timing of neural crest emigration, basal lamina break down and Cad7 upregulation proceed normally in Tspan18-deficient cells. This emphasizes the need for coordinated transcriptional and post-translational regulation of Cad6B during EMT and illustrates that Tspan18-antagonized remodeling of cell-cell adhesions is only one step in preparing for cranial neural crest migration. Unlike Cad6B, which is transcriptionally repressed by Snail2, Tspan18 expression is downstream of the winged-helix transcription factor FoxD3, providing a new transcriptional input into cranial neural crest EMT. Altogether our data reveal post-translational regulation of Cad6B protein levels by Tspan18 that must be relieved by a FoxD3-dependent mechanism in order for cranial neural crest cells to migrate. These results offer novel insight into the molecular mechanisms of cranial neural crest EMT and expand our understanding of tetraspanin function relevant to metastasis.

## 2.2 Introduction:

Epithelial-to-mesenchymal transition (EMT) is a complex, multiple step process during which tightly joined epithelial cells undergo dramatic changes in cell polarity, cell-cell adhesion, and cytoskeletal arrangement to become motile, invasive mesenchymal cells (Hay, 2005; Thiery and Sleeman, 2006). Many of the events that create the intricate adult body plan during embryogenesis require EMT, including the formation of migratory neural crest cells (Nieto, 2011; Polyak and Weinberg, 2009; Thiery et al., 2009). Neural crest cells are a unique developmental cell population that arises in the developing CNS but disperses throughout the embryo to form diverse cell types that are crucial for vertebrate organisms (LeDouarin and Kalcheim, 1999). Despite the importance of migration for neural crest development, our understanding of neural crest EMT is incomplete. In fact, a recent study using time lapse imaging to track neural crest cells as they emigrate has revealed that our current model of neural crest EMT is oversimplified and emphasizes the need for closer examination (Ahlstrom and Erickson, 2009).

During EMT, cell-cell adhesion is disrupted by the altered expression of cadherins, $Ca^{2+}$ dependent adhesion molecules that are the main structural component of epithelial cell membrane structures called adherens junctions (AJs; (Meng and Takeichi, 2009; Oda and Takeichi, 2011). In the chick embryo, cadherins relevant to neural crest EMT vary along the rostrocaudal axis. Cranial neural folds express Cadherin6B (Cad6B) and E-cadherin (E-cad), but not N-cadherin (N-cad). At cranial levels, Cad6B downregulation is necessary for neural crest EMT, while E-cad expression persists in migratory cells (Coles et al., 2007; Dady et al., 2012; Nakagawa and Takeichi, 1995;

Nakagawa and Takeichi, 1998). On the other hand, trunk neural crest cells express Cad6B and N-cad but not E-cad, and N-cad is lost during EMT but Cad6B persists during migration (Dady et al., 2012; Nakagawa and Takeichi, 1995; Park and Gumbiner, 2010; Shoval et al., 2007). Subsequently, the less adhesive, type II Cadherin-7 (Cad7) is upregulated in migratory neural crest cells all along the axis (Chu et al., 2006; Nakagawa and Takeichi, 1995; Nakagawa and Takeichi, 1998). As a result of this AJ remodeling, neural crest cells transition from tightly adherent epithelial cells to mesenchymal cells capable of distinct adhesive interactions including chain formations and collective cell migration (Alfandari et al., 2003; Carmona-Fontaine et al., 2011; Friedl and Wolf, 2003; Kulesa and Fraser, 2000; Nishimura and Takeichi, 2009; Theveneau and Mayor, 2012).

While AJ remodeling is the first step in EMT (Thiery et al., 2009), the mechanisms that regulate cadherin levels in neural crest cells during this transition remain incomplete. Transcriptional downregulation of cadherin expression is crucial to EMT (Nieto, 2011), and in the cranial neural crest, the well-documented EMT transcription factor Snail2 directly binds and represses the *Cad6B* promoter (Taneyhill et al., 2007). Meanwhile, in the trunk neural tube, ectopic expression of the neural crest transcription factor FoxD3 leads to N-cad downregulation and elicits features of EMT (Cheung et al., 2005; Dottori et al., 2001; Kos et al., 2001). However, FoxD3 is not a classical EMT transcription factor (Yang and Weinberg, 2008) and a role for FoxD3 in cranial neural crest EMT has not been evaluated. Moreover, cadherins typically undergo post-translational regulation through processing, trafficking, or stabilization (Nishimura and Takeichi, 2009; Thiery et al., 2009). For example, N-cad levels in chick trunk neural crest cells are regulated by processing prior to EMT (Shoval et al., 2007), and cadherin-

11 cleavage is required for *Xenopus* cranial neural crest migration (McCusker et al., 2009). However, post-translational regulation of cadherins during cranial neural crest EMT has not been determined.

Tetraspanins are transmembrane scaffolding proteins that have been implicated in the control of cell-cell adhesion and motility (Hemler, 2005). Tetraspanins organize membrane microdomains through intracellular interactions with other membrane proteins, including cadherins, integrins, membrane-bound proteases, and cell surface receptors (Levy and Shoham, 2005). By clustering proteins and facilitating their interactions, tetraspanins affect protein function (Yanez-Mo et al., 2009). Despite evidence that tetraspanins promote cadherin-dependent cell-cell adhesion and act as metastasis suppressors (Abe et al., 2008; Chattopadhyay et al., 2003; Greco et al., 2010; Johnson et al., 2009; Tsai and Weissman, 2011; Zoller, 2009), the role of tetraspanins in preventing EMT, and in regulating cadherins during neural crest development, has not been investigated.

We identified *Tetraspanin18* (*Tspan18*) in a screen for genes upregulated as a consequence of neural crest induction (Adams et al., 2008; Gammill and Bronner-Fraser, 2002). *Tspan18* was originally cloned from chick spinal cord, however, its function was unknown (Perron and Bixby, 1999). Here we report that *Tspan18* is expressed in chick cranial premigratory neural crest cells in a pattern similar to that of *Cad6B*. Our analysis of Tspan18 knock down and overexpression reveals a novel role for Tspan18 in stabilizing Cad6B protein levels to antagonize EMT and subsequent neural crest migration. Strikingly, Tspan18 must be downregulated for cranial neural crest cells to migrate, but FoxD3, rather than Snail2, is required for this repression. Collectively, our

data reveal post-translational regulation of Cad6B protein levels by Tspan18, and identify FoxD3 as a novel transcriptional regulator of cranial neural crest EMT, providing new insight into the complex regulation of neural crest EMT.

## 2.3 Results:

### *Tspan18*, like *Cad6B*, is expressed by premigratory neural crest cells, but is down regulated prior to migration.

To determine whether *Tspan18* is expressed at the correct time and place to regulate neural crest cadherins, we visualized *Tspan18* mRNA localization in chick embryos by whole mount in situ hybridization. Between 5 and 8 somites (s), *Tspan18* transcripts were apparent in the neural tube, head mesenchyme, epithelial somites, and developing vasculature (Fig. 2-1A-D). Transverse sections revealed that *Tspan18* was abundantly expressed in cranial premigratory neural crest cells in the neural folds at 3s (Fig. 2-S1B) and the dorsal neural tube at 5, 6 and 7s (Fig. 2-1A'-C', arrowheads). However *Tspan18* was absent in the dorsal neural tube at 8s (Fig. 2-1D', arrow), after cranial neural crest cells have emigrated. This expression pattern resembled that of the epithelial cell adhesion molecule *Cad6B* that must be downregulated in order for cranial neural crest cells to migrate (Fig. 2-1E-H'; (Coles et al., 2007; Taneyhill et al., 2007). Interestingly, both *Tspan18* and *Cad6B* persisted in the forebrain, which does not produce neural crest cells (Fig. 2-1D,H). *Tspan18* expression was never apparent in neural crest cells migrating away from the neural tube, and was absent from HNK-1-positive neural crest cells in the head mesenchyme (Fig. 2-S1D,E) and branchial arches, a cranial target (Fig. 2-S1G,H). *Tspan18* transcripts were not detectable by in situ hybridization in premigratory trunk neural crest cells at any stage examined (Fig. 2-S1F and C.L. Fairchild, unpublished). *Tspan18* mRNA expression persisted in the head mesenchyme, epithelial somites, and developing vasculature at both 10 and 16s (Fig. 2-S1). However, *Tspan18* was downregulated in rostral somites that had dissociated into sclerotome and

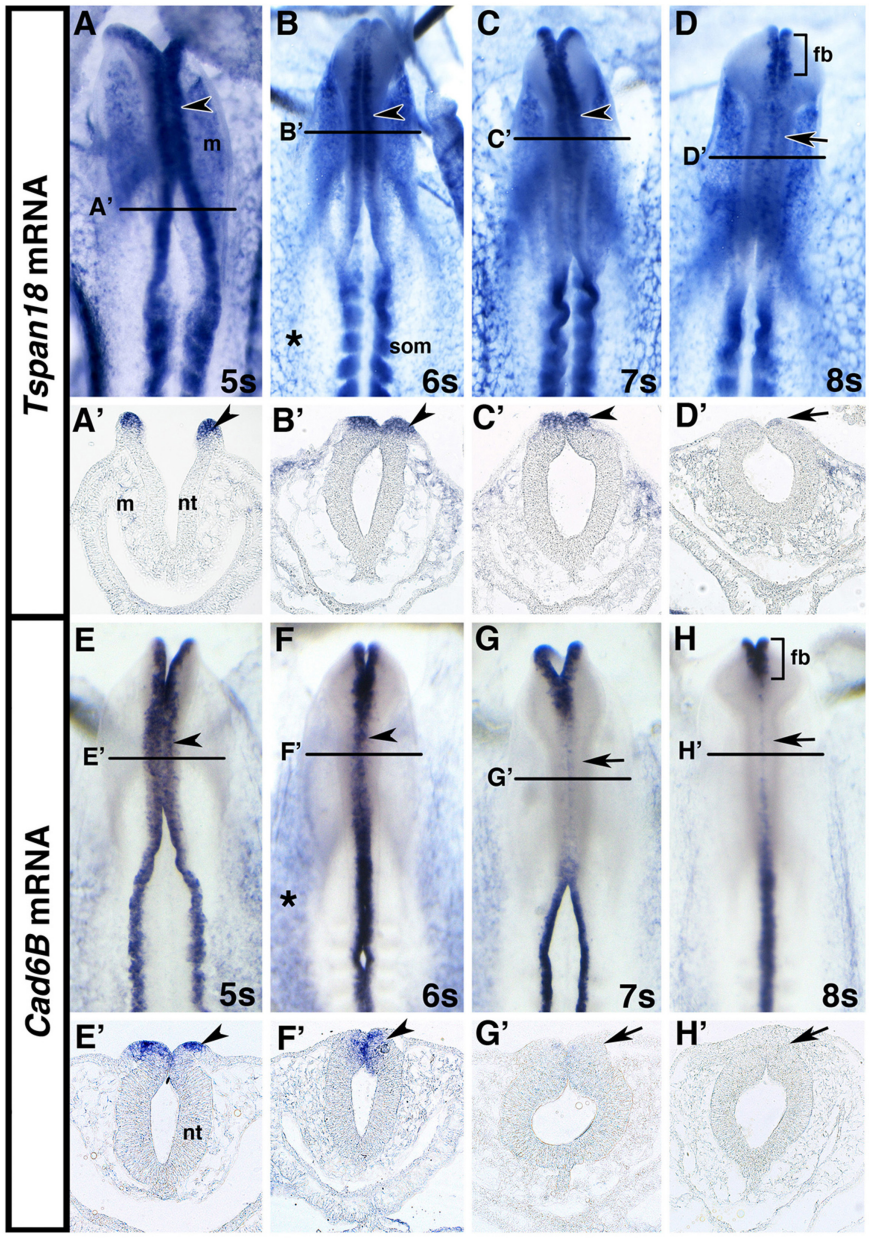
Tspan18 mRNA
Cad6B mRNA
A
B
C
D
fb
m
A'
B'
C'
D'
som
5s
6s
7s
8s
nt
E
F
G
H
E'
F'
G'
H'

**Fig. 2-1. *Tspan18* and *Cad6B* expression in cranial premigratory neural crest cells is downregulated prior to migration.**

(A-H) Whole mount in situ hybridization for *Tspan18* (A-D) or *Cad6B* (E-H) in 5 somite (s; A,E), 6s (B,F), 7s (C,G) and 8s (D,H) embryos (dorsal view, anterior embryo half). *Tspan18* and *Cad6B* expression in the cranial dorsal neural tube (A-C,E,F; arrowheads) is downregulated (D,G,H; arrows) prior to neural crest migration. *Tspan18* and *Cad6B* expression in the forebrain (fb; brackets in D,H) persists during midbrain neural crest migration. *Tspan18* and *Cad6B* are also expressed in the developing vasculature (asterisks in B,F), and *Tspan18* is expressed in the head mesenchyme (m) and epithelial somites (som). (A'-H') Transverse sections at the levels indicated in A-H reveal *Tspan18* (A'-D') and *Cad6B* (E'-H') expression in premigratory neural crest cells in the dorsal neural tube (nt; arrowheads in A'-C' and E',F') that is downregulated upon neural crest migration (D',G',H'; arrows). *Tspan18* expression in the cranial mesenchyme (m) is also apparent.

dermomyotome (Fig. 2-S1D,G). Thus, *Tspan18* is expressed by premigratory cranial neural crest cells and generally correlates with epithelial and not mesenchymal cell types.

**Tspan18 knock down leads to premature loss of Cad6B protein.**

Given that *Tspan18* and *Cad6B* were similarly expressed (Fig. 2-1), and that tetraspanins are known to influence cadherin localization and function (Abe et al., 2008; Greco et al., 2010; Hemler, 2005), we postulated that Tspan18 would affect Cad6B. To investigate this possibility, we designed a FITC-tagged, antisense morpholino oligonucleotide (MO) to block Tspan18 translation (TS18MO). FITC-tagged standard control MO (ContMO) or TS18MO were electroporated into presumptive neural crest cells and Cad6B protein was visualized by immunofluorescence at 5-7s in whole mount and cryosections. Electroporation of ContMO had no effect on Cad6B protein levels (Fig. 2-2A-C; equivalent average fluorescence intensity on targeted and untargeted sides, O). However, when Tspan18 was knocked down, Cad6B protein was diminished in the forebrain (Fig. 2-2D; 81.3% of embryos; $p=2.2x10^{-4}$, n=16), a region that continuously expressed *Tspan18* and *Cad6B* (Fig. 2-1) and does not produce neural crest cells. Meanwhile, following TS18MO electroporation into the premigratory neural crest-containing midbrain, Cad6B protein was largely depleted (Fig. 2-2E; 68.7% of embryos; $p=6.5x10^{-4}$, n=16) and the average intensity of Cad6B immunofluorescence on the targeted side was significantly reduced (Fig. 2-2O; n=5; $p=8.0x10^{-3}$). Whole mount images of TS18MO-electroporated embryos further confirmed the reduction of Cad6B protein levels throughout the cranial premigratory neural crest (Fig. 2-2F). Embryos electroporated with a TS18MO containing a 5 base pair mismatch (mmTS18MO) did not

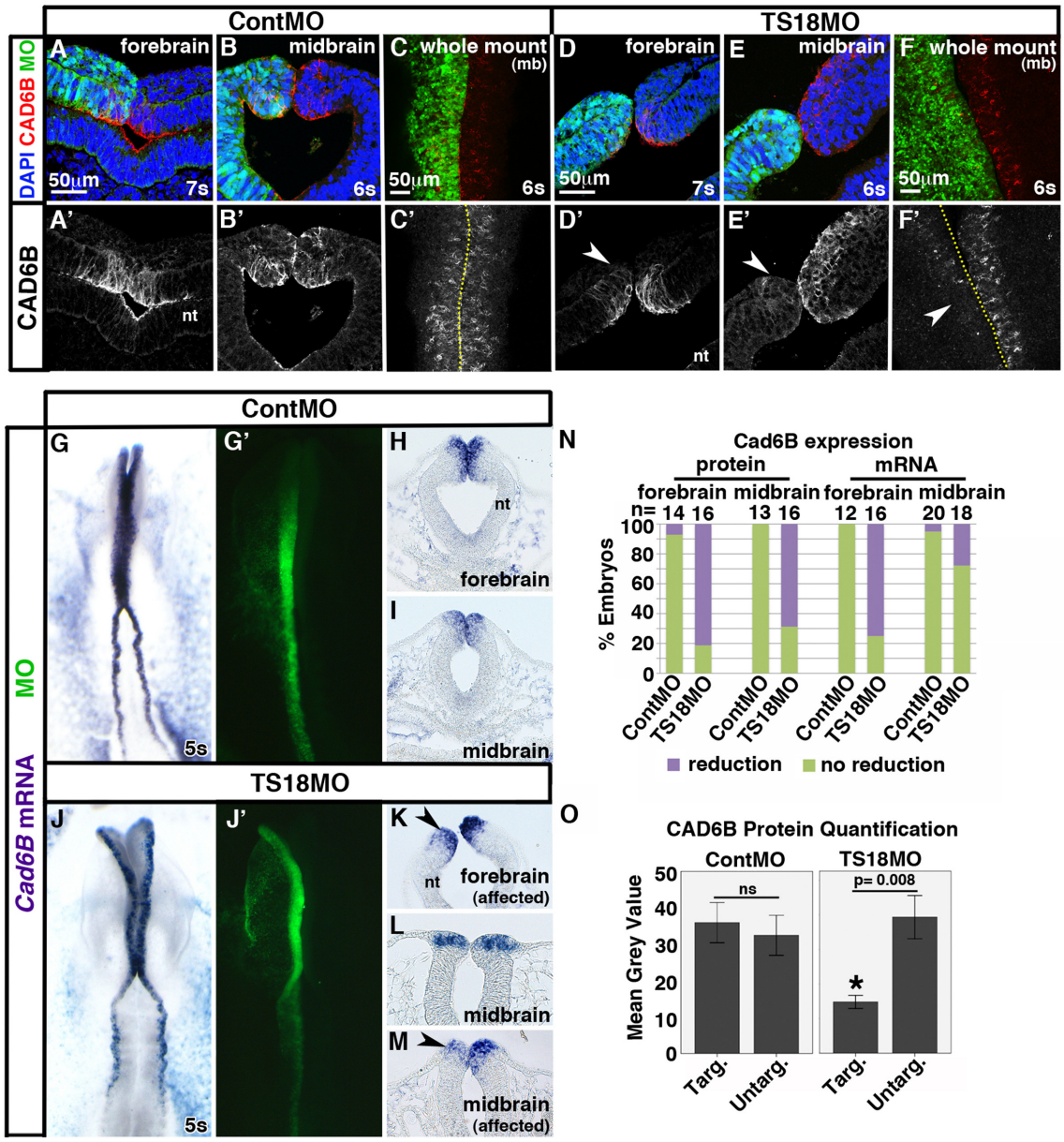
ContMO
TS18MO
DAPI CAD6B MO
CAD6B
A forebrain
B midbrain
C whole mount (mb)
D forebrain
E midbrain
F whole mount (mb)
50μm
7s
6s
A'
B'
C'
D'
E'
F'
nt
Cad6B mRNA MO
G
G'
H
I
J
J'
K
L
M
5s
forebrain
midbrain
forebrain (affected)
midbrain (affected)
N
Cad6B expression
protein
mRNA
forebrain midbrain forebrain midbrain
n= 14 16 13 16 12 16 20 18
% Embryos
ContMO TS18MO
reduction
no reduction
O
CAD6B Protein Quantification
ContMO
TS18MO
Mean Grey Value
ns
p= 0.008
Targ.
Untarg.

**Fig. 2-2. Tspan18 knock down leads to a reduction in Cad6B protein levels with variable effects on *Cad6B* mRNA expression.**

(A-F) Transverse sections (A,B,D,E) and whole mount images (C,F; midbrain dorsal view) reveal that Cad6B immunofluorescence (A-F, red; A'-F') is reduced on the targeted side of the neural tube (green) in the forebrain (arrowhead in D') and midbrain (arrowheads in E',F') of 6-7s embryos unilaterally electroporated with TS18MO (D-F) but not with ContMO (A-C). (G-M) Whole mount in situ hybridization (G,J; dorsal view, anterior embryo half) and transverse sections (H,I,K,L,M) reveal that *Cad6B* mRNA expression (purple) is reduced on the targeted side (green) compared to the untargeted side in the forebrain (arrowhead in K) but is unaffected in the midbrain of the majority of TS18MO-electroporated embryos (L). In 27.8% of embryos, *Cad6B* mRNA was reduced in neural folds electroporated with TS18MO (arrowhead in M). (N) Bar graph representing the frequency of electroporated embryos exhibiting affected versus unaffected Cad6B protein levels or mRNA expression. (O) Quantification of Cad6B immunofluorescence intensity comparing the MO-targeted (targ) and untargeted (untarg) sides of the midbrain neural tube in individual sections (n=5). nt, neural tube; mb, midbrain; ns, not significant. Scale bars in A,C,D,F= 50 μm. Dotted lines in (C',F') indicate embryo midline.

exhibit this severe phenotype (7/9 unaffected; 2/9 mildly affected; C.L. Fairchild, unpublished), indicating the TS18MO concentration was in the effective and specific dose range (Moulton and Yan, 2008). Furthermore, these effects were specific to Cad6B as electroporation of TS18MO did not affect the level or localization of N-cad (Fig. 2-S2; n=4) or E-cad (Fig. 2-S3; n=16). These results indicate that Tspan18 is required to maintain premigratory Cad6B protein levels.

To verify that the loss of Cad6B protein in TS18MO-electroporated embryos was efficient and not due to off-target effects of TS18MO, we assessed efficacy and specificity of the knock down phenotype, and also visualized cell proliferation and survival. Because commercially available human Tspan18 antibodies do not cross-react with chick Tspan18 and the chick Tspan18 antibody we raised was ineffective, we were unable to visualize endogenous Tspan18 knock down. However, as TS18MO anneals to nucleotides +1 to +25 of the Tspan18 open reading frame, we could assess knock down of C-terminal myc-tagged Tspan18 expressed from a DNA construct (pCIG-Tspan18MT). Co-electroporation of 1 µg/µl pCIG-Tspan18MT with TS18MO dramatically reduced translation of the tagged protein (Fig. 2-S4). To assess the specificity of TS18MO, we co-electroporated 1 µg/µl untagged pCIG-Tspan18 with TS18MO, and evaluated Cad6B protein levels. Driving additional Tspan18 expression in TS18MO electroporated cells rescued Cad6B protein levels on the targeted side of the neural tube (Fig. 2-S5; Cad6B protein levels reduced in 13.6% of TS18MO + Tspan18 coelectroporated embryos and 88.9% of TS18MO electroporated embryos; $p=4.9x10^{-4}$, n=22). Moreover, embryos electroporated with either ContMO or TS18MO exhibited no statistically significant difference in the number of phospho-histone H3 (pH3) positive

proliferating cells between the targeted and untargeted sides of the neural tube (Fig. 2-S6A-C; p= 0.27; n=3). Likewise, no change in cell death, visualized by TUNEL staining, was apparent between the targeted and untargeted sides of the neural tube (Fig. 2-S6D-F; p=0.42; n=4). These data indicate that Tspan18 knock down is efficient, and TS18MO phenotypes are not due to off-target effects or changes in cell number through proliferation or death.

**Tspan18 knock down has variable effects on *Cad6B* mRNA expression that may be a consequence of increased nuclear β-catenin.**

Tetraspanins can modulate membrane proteins that elicit intracellular signaling cascades and lead to indirect transcriptional changes in the nucleus (Berditchevski, 2001; Chairoungdua et al., 2010; Hemler, 2005; Huang et al., 2004). To determine whether loss of Cad6B protein following Tspan18 knock down (Fig. 2-2E,F) was due to reduced *Cad6B* mRNA expression, we electroporated embryos with either ContMO or TS18MO and assessed *Cad6B* mRNA levels by whole mount in situ hybridization. Although *Cad6B* expression was unaffected in ContMO-electroporated embryos at 5s (Fig. 2-2G-I), *Cad6B* mRNA levels were reduced on the targeted side of the neural tube in the forebrain of TS18MO-electroporated embryos (Fig. 2-2N; $p=3.4x10^{-4}$, n=16). Interestingly, midbrain *Cad6B* mRNA expression was unaffected in the majority of TS18MO-electroporated embryos, and the infrequent inhibition was not statistically significant (Fig. 2-2J-N; p=0.14, n=18). Thus, although Tspan18 knock down can impact *Cad6B* gene expression, it does not account for the significant decrease in midbrain Cad6B protein levels in the majority of embryos (Fig. 2-2E',F',N). Furthermore, the differential

effect in the forebrain and midbrain suggest that *Cad6B* mRNA expression is differentially regulated along the rostrocaudal axis.

To understand how a membrane protein like Tspan18 with no known signaling domains might affect *Cad6B* transcription in the nucleus (Fig. 2-2), we investigated two potential scenarios. We first assessed whether Tspan18 knock down increased levels of the Cad6B transcriptional repressor Snail2 (Taneyhill et al., 2007). On the contrary, Snail2 protein levels were reduced in TS18MO-electroporated cells (Fig. 2-S7A-E), inconsistent with a reduction in *Cad6B* mRNA. Next we determined whether Tspan18 knock down indirectly increased nuclear β-catenin levels. β-catenin interacts with cadherins in AJs (Meng and Takeichi, 2009) and additionally regulates gene expression, including repression of cadherin transcription (Huber et al., 1996; Jamora et al., 2003), as a downstream effector of the Wnt signaling pathway (Heuberger and Birchmeier, 2010). Because AJ disassembly can indirectly affect nuclear β-catenin levels (Heuberger and Birchmeier, 2010; Kam and Quaranta, 2009; Kuphal and Behrens, 2006; Onder et al., 2008; Orsulic et al., 1999; Shtutman et al., 2006), we reasoned that loss of Cad6B protein could lead to increased nuclear β-catenin. Interestingly, line scans revealed increased nuclear-localized β-catenin in TS18MO-targeted compared to untargeted neural fold cells (Fig. 2-S7F-H), providing a possible mechanism by which Tspan18 knock down sometimes leads to reduced *Cad6B* transcription.

**Tspan18 knock down does not trigger neural crest migration.**

A previous report showed that Cad6B knock down enhances neural crest migration (Coles et al., 2007). In turn, we reasoned that Tspan18 knock down, which

leads to premature loss of Cad6B protein (Fig. 2-2), would also promote neural crest migration. Specifically, we postulated that Tspan18-deficient embryos would exhibit precocious cranial neural crest migration. To investigate this possibility, neural crest cells electroporated with either ContMO or TS18MO were visualized by *Sox10* in situ hybridization at 8-10s. Neural crest migration was unaffected in ContMO-electroporated embryos (Fig. 2-3A,B; n=22). In 28.1% of TS18MO-electroporated embryos, *Sox10*-positive neural crest cells migrated noticeably farther on the targeted side compared to the untargeted side of the neural tube (Fig. 2-3D,F; n=32). Unexpectedly, neural crest migration distance in the remaining 71.9% of TS18MO-electroporated embryos was similar to controls (Fig. 2-3C,E,G) and the enhanced migration phenotype we occasionally observed was not statistically significant (p=0.11). Therefore, while Tspan18 knock down leads to premature loss of Cad6B protein, in most embryos this is insufficient to stimulate cranial neural crest migration.

**Loss of Tspan18 does not interfere with the timing of subsequent steps in EMT.**

Although downregulation of Cad6B is required for cranial neural crest migration (Coles et al., 2007), AJ remodeling is not the only step in EMT; cells must also break down their restrictive basal lamina and express genes that establish their motility and mesenchymal characteristics (Hay, 2005). Thus, we reasoned that most Tspan18-deficient embryos did not migrate precociously because other steps in EMT were unaffected. Normally, cranial premigratory neural crest cells were enclosed within a basal lamina extending from the basal surface of the neural tube to the non-neural ectoderm (Fig. 2-S8A); at 8-10s, this basal lamina broke down, leaving a laminin-deficient void where

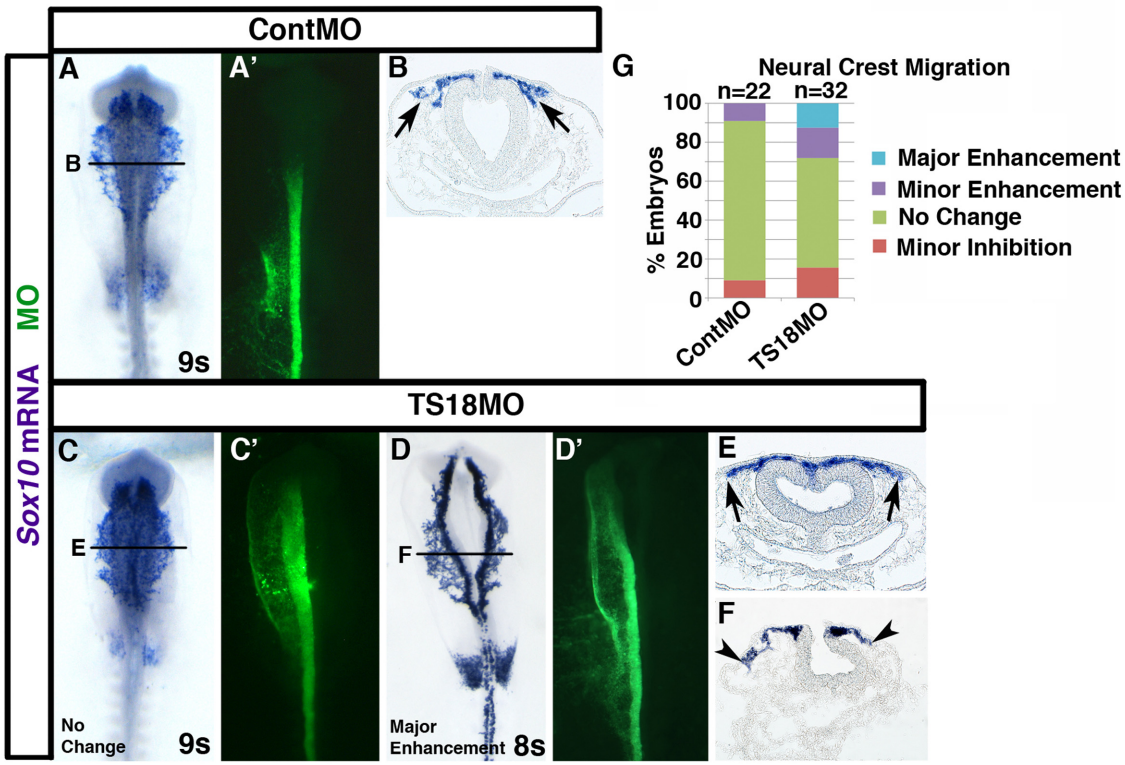
ContMO
A
A'
B
9s
TS18MO
C
C'
D
D'
E
F
No Change
9s
Major Enhancement
8s
Sox10 mRNA MO
G
Neural Crest Migration
n=22
n=32
100
80
60
40
20
0
% Embryos
ContMO
TS18MO
Major Enhancement
Minor Enhancement
No Change
Minor Inhibition

**Fig. 2-3. Tspan18 knock down inconsistently enhances neural crest migration.**

(A-F) Embryos unilaterally electroporated with ContMO (A,B) or TS18MO (C-F) were processed by whole mount in situ hybridization for *Sox10* at 8 or 9s (A,C,D, dorsal view, anterior embryo half; A',C',D', construct targeting; B,E,F, midbrain transverse sections at the level indicated). Neural crest migration is unaffected by ContMO (A,B, arrows). TS18MO-electroporated neural crest cells migrated normally in most embryos (C, E, arrows), but was enhanced in 28.1% of embryos (D, F, arrowheads). (G) Bar graph representing the frequency of embryos with enhanced or normal migration.

HNK-1-positive migratory neural crest cells escaped the neural tube (Fig. 2-S8B,C; (Tosney, 1982)). The same spatiotemporal pattern of laminin immunostaining was observed in embryos electroporated with either ContMO (Fig. 2-4A,B; n=13) or TS18MO (Fig. 2-4C,D; n=12). This indicates Tspan18 knock down does not alter basal lamina integrity during cranial neural crest delamination.

Once neural crest cells downregulate Cad6B, they activate expression of the mesenchymal cell adhesion molecule, Cad7 (Nakagawa and Takeichi, 1998). Although Cad7 protein was undetectable in early migrating cranial neural crest cells at 8s (Fig. 2-S8D), Cad7 protein was apparent in HNK-1-positive migratory neural crest cells by 10s (Fig. 2-S8E; staining was variable at 9s). This was consistent with the pattern of Cad7 expression in trunk migratory neural crest cells, although levels are higher in the trunk (Fig 2-S8F; (Nakagawa and Takeichi, 1998)). The timing of Cad7 protein accumulation was unaffected by Tspan18 knock down: Cad7 was undetectable at 8s in migratory cranial neural crest cells electroporated with ContMO (Fig. 2-4E; n=9) or TS18MO (Fig. 2-4H; n=9), but present at 10s in cranial neural crest cells electroporated with either ContMO (Fig. 2-4F,G; n=4) or TS18MO (Fig. 2-4I,J; n=4). Altogether, these results suggest that Tspan18 regulates Cad6B protein levels specifically, and is not required for other steps in EMT like delamination and acquisition of mesenchymal fate.

**Sustained expression of Tspan18 prevents neural crest migration.**

*Tspan18* mRNA was absent in migratory neural crest cells (Fig. 2-1, 2-S1). To determine whether downregulation of Tspan18 was a prerequisite for cranial neural crest migration, we forced Tspan18 expression in neural crest cells past the stage it is normally

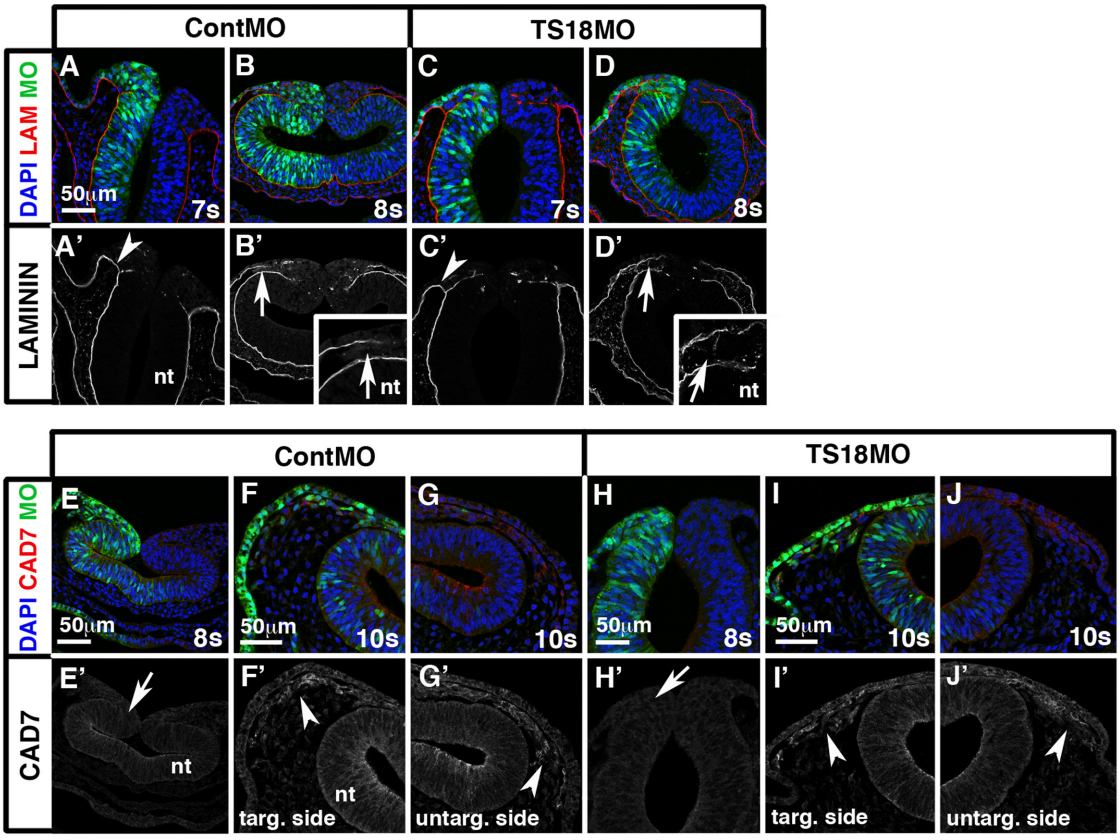
ContMO
TS18MO
DAPI LAM MO
A
B
C
D
50μm
7s
8s
7s
8s
LAMININ
A'
B'
C'
D'
nt
nt
nt
ContMO
TS18MO
DAPI CAD7 MO
E
F
G
H
I
J
50μm
8s
50μm
10s
10s
50μm
8s
50μm
10s
10s
CAD7
E'
F'
G'
H'
I'
J'
nt
nt
targ. side
untarg. side
targ. side
untarg. side

**Fig. 2-4. Loss of Tspan18 does not alter basal lamina break down or the acquisition of mesenchymal character.**

Transverse midbrain sections of ContMO (A,B,E-G) or TS18MO (C,D,H-J) electroporated embryos immunostained for Laminin (A-D, red; A'-D') or Cad7 (E-J, red; E'-J'). (A-D) In all conditions, the intact basal lamina connecting the basal surface of the neural tube with the non-neural ectoderm at 7s (arrowheads in A',C') becomes discontinuous at 8s (arrows in B',D', insets in B' and D') in the region that cranial neural crest cells will exit the neural tube. (E-J) Cad7 protein is undetectable in early migrating neural crest cells at 8s (arrows in E' and H') but accumulates by 10s in both ContMO and TS18MO targeted and untargeted migratory cranial neural crest cells (arrowheads in F',G',I',J'). G and J are the unelectroporated halves of embryos shown in F and G. nt, neural tube. Scale bars= 50 μm.

lost. Electroporation of the chick expression construct pCIG (Megason and McMahon, 2002) at low (3 μg/μl) or high (5 μg/μl) concentrations did not affect migration of *Sox10*- or HNK-1-positive neural crest cells (Fig. 2-5A,B,E,G,K). In contrast, neural crest migration was inhibited on the targeted side of the neural tube in over 90% of embryos electroporated with pCIG-TS18 at either concentration (Fig. 2-5C,D,F,H,K, arrowheads; $p=5.3x10^{-6}$ (low); $p=1.9x10^{-6}$ (high)). When analyzed by HNK-1 immunofluorescence, it was apparent that sometimes all neural crest migration was blocked (Fig. 2-5F, arrowhead) compared to the unelectroporated side (arrow). Meanwhile in other embryos, GFP-positive Tspan18-expressing cells were stopped near the dorsal neural tube (Fig. 2-5H, arrowhead), while GFP-negative neural crest cells migrated normally (Fig. 2-5H, arrow). This suggests that scoring migration without distinguishing between electroporated and unelectroporated cells (as in Fig. 2-5C,D,K) under-represents the severity of the phenotype. These effects were not due to changes in cell proliferation or death, as no differences were observed between targeted and untargeted sides of the neural tube in pCIG or pCIG-TS18 electroporated embryos (Fig. 2-S9). Together, these data indicate that Tspan18 expression is incompatible with migration.

While sustained Tspan18 expression dorsally in the neural folds prevented neural crest migration, ectopic expression of Tspan18 in the ventral neural tube altered neural tube morphogenesis. In about 55% of 3 μg/μl pCIG-TS18-electroporated embryos ($p=5.9x10^{-7}$, n=37) and 95% of, 5 μg/μl pCIG-TS18-electroporated embryos ($p=2.2x10^{-16}$, n=29), the neuroepithelium on the targeted side remained flat and exhibited a severe neural tube defect (Fig. 2-5D",J; asterisks). This phenotype was never observed in control embryos (Fig. 2-5B",I,L). Even when a neural tube formed, more subtle effects on neural

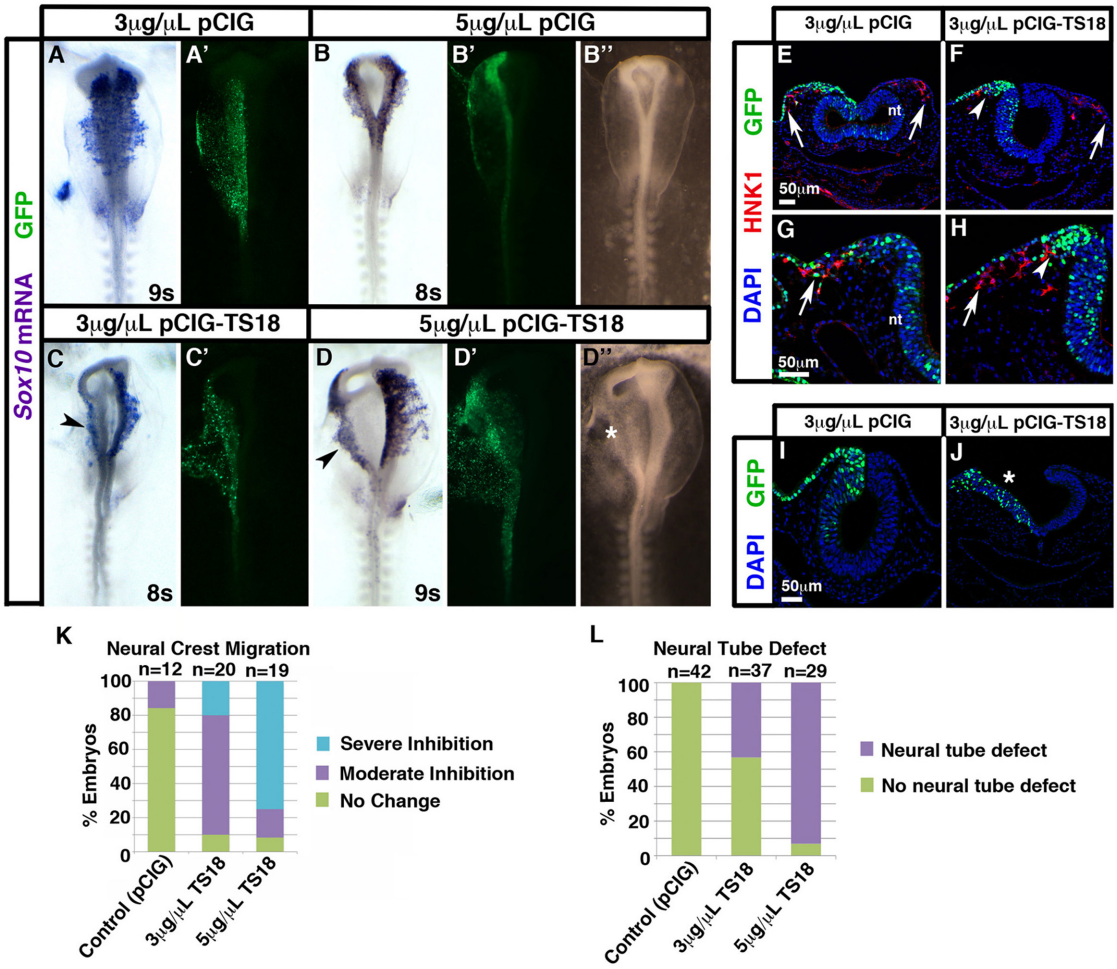
3μg/μL pCIG
5μg/μL pCIG
3μg/μL pCIG-TS18
5μg/μL pCIG-TS18
Sox10 mRNA
GFP
A
A'
B
B'
B''
C
C'
D
D'
D''
9s
8s
8s
9s
*
3μg/μL pCIG
3μg/μL pCIG-TS18
GFP
HNK1
DAPI
E
F
G
H
nt
nt
50μm
50μm
3μg/μL pCIG
3μg/μL pCIG-TS18
GFP
DAPI
I
J
*
50μm
K
Neural Crest Migration
n=12 n=20 n=19
% Embryos
100
80
60
40
20
0
Control (pCIG)
3μg/μL TS18
5μg/μL TS18
Severe Inhibition
Moderate Inhibition
No Change
L
Neural Tube Defect
n=42 n=37 n=29
% Embryos
100
80
60
40
20
0
Control (pCIG)
3μg/μL TS18
5μg/μL TS18
Neural tube defect
No neural tube defect

**Fig. 2-5. Tspan18 prevents neural crest migration.**

(A-D) Whole mount in situ hybridization for *Sox10* in 8-9s embryos unilaterally electroporated with low (A,C; 3μg/μl) or high (B,D; 5 μg/μl) concentrations of empty pCIG (A,B) or pCIG-TS18 (C,D; dorsal view, anterior embryo half; A'-D', construct targeting). pCIG-TS18 impedes neural crest migration (arrowheads in C,D). Bright field images (B",D") reveal an additional neural tube defect (D", asterisk) in embryos electroporated with pCIG-TS18. (E-J) Transverse sections of 9-10s embryos electroporated with 3μg/μl pCIG (E,G,I) or pCIG-TS18 (F,H,J). pCIG-TS18-electroporated cells (F,H; green, arrowhead) clump near the neural fold, while pCIG-electroporated (E,G, green, arrow) and unelectroporated (F,H, arrows) HNK-1 positive (red) neural crest cells migrate normally. In contrast to pCIG-electroporated embryos (I), pCIG-TS18-electroporated embryos sometimes exhibit flat, open neural tubes (J, asterisk). (K) Bar graph representing the frequency of neural crest migration defects. (L) Bar graph representing the frequency of neural tube defects. nt, neural tube. Scale bars= 50 μm.

fold shape were sometimes apparent (see for example Fig. 2-5F,H). However, morphogenetic abnormalities did not account for neural crest migration defects since pCIG-TS18-electroporated neural folds produced migratory neural crest cells (Fig. 2-5F,H, arrow).

**Cad6B protein persists following Tspan18 overexpression, while Cad6B mRNA is downregulated on time.**

Tspan18 knock down reduced Cad6B protein levels (Fig. 2-2) while Tspan18 overexpression impeded neural crest migration (Fig. 2-5). Because Cad6B overexpression inhibits neural crest migration (Coles et al., 2007), we postulated that sustained Tspan18 expression prevented neural crest migration through effects on Cad6B. Cad6B protein was absent in the midbrain neural folds of 7s embryos electroporated with 3 μg/μl pCIG (Fig. 2-6A,D; n=10). However, we detected Cad6B protein in 92.5% of 7-10s embryos electroporated with 3 μg/μl pCIG-TS18 (Fig. 2-6B-D; $p=4.4x10^{-5}$, n=14 embryos). Importantly, Cad6B protein was still restricted to the dorsal neural tube in pCIG-TS18 electroporated embryos, suggesting that Tspan18 overexpression maintains existing protein and does not induce de novo Cad6B translation in the neurectoderm (Fig. 2-6C).

To determine whether maintenance of Cad6B protein in the neural folds reflected persistent *Cad6B* transcription, we visualized *Cad6B* mRNA by in situ hybridization after electroporation with either pCIG or pCIG-TS18. In unmanipulated embryos (Fig. 2-1E-G) or embryos electroporated with 3 μg/μl pCIG (Fig. 2-6E,G; n=16), *Cad6B* mRNA was expressed at 5s, but downregulated by 7s. Likewise, *Cad6B* expression was present,

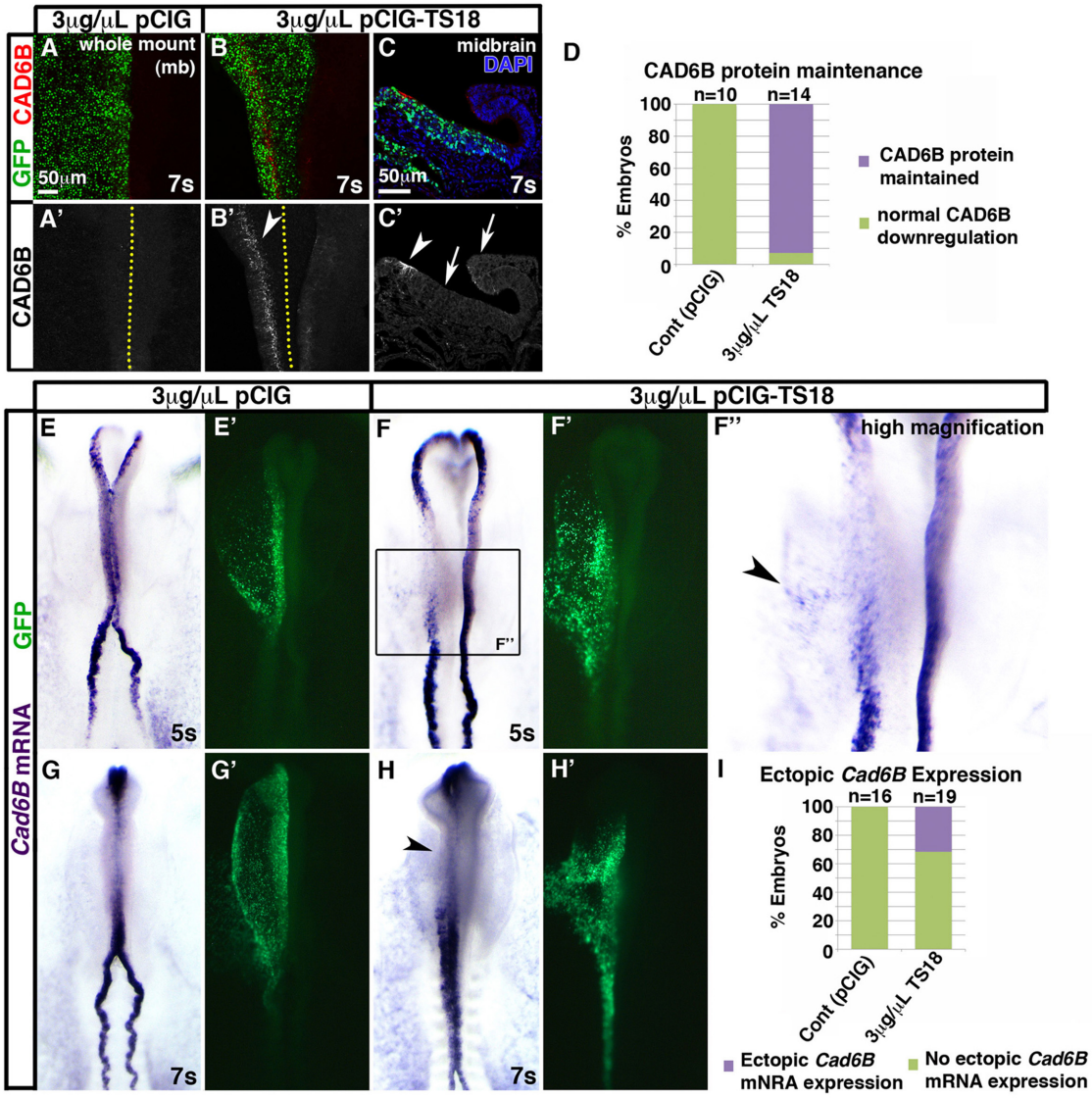
3μg/μL pCIG
3μg/μL pCIG-TS18
A whole mount (mb)
B
C midbrain DAPI
GFP CAD6B
50μm
7s
A'
B'
C'
CAD6B
D
CAD6B protein maintenance
n=10
n=14
% Embryos
100
80
60
40
20
0
Cont (pCIG)
3μg/μL TS18
CAD6B protein maintained
normal CAD6B downregulation
E
E'
F
F'
F''
high magnification
5s
Cad6B mRNA
GFP
G
G'
H
H'
I
Ectopic Cad6B Expression
n=16
n=19
Ectopic Cad6B mNRA expression
No ectopic Cad6B mRNA expression

**Fig. 2-6. Tspan18 overexpression maintains Cad6B protein, while *Cad6B* mRNA downregulates on schedule.**

Embryos unilaterally electroporated with empty pCIG (A,E,G) or pCIG-TS18 (B,C,F,H) were immunostained for Cad6B protein at 7s (A-B; wholemount midbrain dorsal view, C; transverse midbrain section) or processed by whole mount in situ hybridization for *Cad6B* mRNA (E-H, dorsal view, anterior embryo half; green in A-C,E'-H', construct targeting). (A-C) Cad6B protein (A-C, red; A'-C') is downregulated normally in pCIG electroporated embryos (A') but maintained in the midbrain dorsal neural tube of pCIG-TS18 electroporated embryos (white arrowheads in B',C'). Ectopic Cad6B protein was not observed in the ventral neural tube or unelectroporated side of the embryo (white arrows in C'). (D) Bar graph representing the number of 7-10s embryos exhibiting normal downregulation versus maintenance of Cad6B protein. (E-H) Although 5s pCIG-TS18-electroporated embryos exhibit *Cad6B* mRNA expression in the neural folds that is dispersed (F) and sometimes ectopic (arrowhead in F") compared to pCIG electroporated embryos (E), Cad6B mRNA is downregulated at 7s with the same temporal profile in pCIG (G) and TS18MO-electroporated embryos (H). (I) Bar graph representing the number of embryos exhibiting ectopic *Cad6B* mRNA expression. Scale bar in A,C= 50 μm. Dotted lines in (A',B') indicate embryo midline.

albeit dispersed, on the targeted side of the neural tube in 5s embryos electroporated with pCIG-TS18 (Fig. 2-6F; n=22). In turn, *Cad6B* mRNA expression in the midbrain was downregulated on time at 7s on both the pCIG-TS18 targeted and untargeted sides of the neural tube (Fig. 2-6H; n=11). Because *Cad6B* mRNA downregulated normally following Tspan18 overexpression (Fig. 2-6H), but Cad6B protein persisted (Fig. 2-6B-D), these results indicate that Tspan18 maintains Cad6B protein levels directly, without indirectly modulating *Cad6B* mRNA expression. Moreover, expression of neural crest markers *Cad6B* (Fig. 2-6B-D, F, H), *Sox10* (Fig. 2-5C, D, F), and HNK1 (Fig. 2-5F, H) indicate that neural crest cells form following Tspan18 overexpression, but simply fail to migrate.

Interestingly, 31.6% of pCIG-TS18 targeted embryos exhibited ectopic *Cad6B* mRNA expression in the adjacent non-neural ectoderm (arrowhead in Fig. 2-6F",I; $p=4.3x10^{-2}$, n=19). Since pCIG-TS18 embryos are electroporated at HH4+, it is possible that the ectopic *Cad6B* expressing cells reflect incomplete morphogenetic movements and displacement of neural crest precursors that are specified during gastrulation (Basch et al., 2006). Alternatively, if *Cad6B* mRNA expression is induced, only the non-neural ectoderm is competent to respond, as ectopic *Cad6B* mRNA was never observed in the neural tube. In either case, we cannot detect ectopic Cad6B protein, indicating it is below the limits of detection, some factor is missing, and/or Cad6B translation is repressed outside the neural folds.

**FoxD3 negatively regulates *Tspan18* expression.**

Downregulation of Tspan18 was required for neural crest cells to migrate (Fig. 2-5). Thus, characterizing the transcriptional regulation of *Tspan18* is essential to understanding how neural crest cells prepare for migration. During cranial neural crest EMT, Snail2 represses transcription of *Cad6B* (Taneyhill et al., 2007). Given the role of Tspan18 in stabilizing Cad6B protein (Fig. 2-6), we investigated whether *Tspan18* expression, like *Cad6B*, was repressed by Snail2. However, real time qRT-PCR analysis of *Tspan18* mRNA expression after knock down of Snail2 suggests that *Tspan18* is not a Snail2 target (L.A. Taneyhill, personal communication), leading us to investigate other possible regulators of *Tspan18* expression.

Previous studies have shown that ectopic expression of the winged helix transcription factor FoxD3 in trunk neural tube leads to changes in cell-cell adhesion and promotes neural crest delamination (Cheung et al., 2005; Dottori et al., 2001; Kos et al., 2001); thus FoxD3 was also a candidate to regulate *Tspan18*. To investigate this possibility, we examined the effect of FoxD3 overexpression on *Tspan18* mRNA expression at 5-8s. As expected, *Tspan18* mRNA levels were unaffected by electroporation with 5 μg/μL of the chick expression construct pMES ((Swartz et al., 2001); Fig. 2-7A; n=16). However, *Tspan18* mRNA expression was dramatically reduced on the targeted side of the dorsal neural tube in 76.5% of embryos electroporated with 5 μg/μL pMES-FoxD3 (Fig. 2-7C; $p=5.1x10^{-6}$, n=17). Transverse sections of the midbrain confirmed this observation (compare arrowhead in Fig. 2-7D to arrow in Fig. 2-7B) and furthermore revealed a neural tube defect similar to that of pCIG-TS18 electroporated embryos (Fig. 2-5D",J). These results suggest that Tspan18 lies downstream of FoxD3.

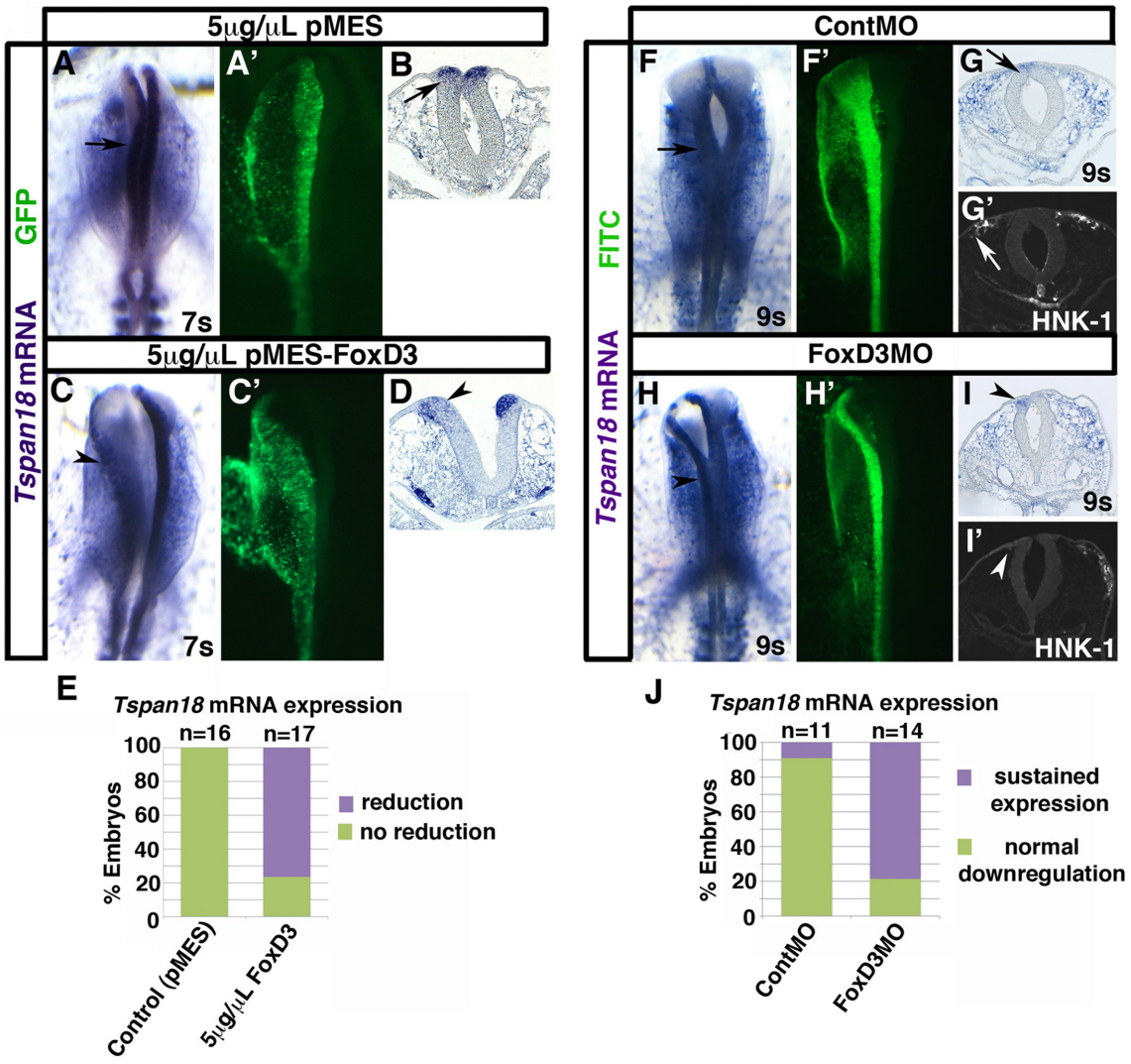
5μg/μL pMES
A
A'
B
7s
5μg/μL pMES-FoxD3
C
C'
D
7s
GFP
Tspan18 mRNA
ContMO
F
F'
G
9s
G'
HNK-1
FoxD3MO
H
H'
I
9s
I'
HNK-1
FITC
Tspan18 mRNA
E
Tspan18 mRNA expression
n=16
n=17
100
80
60
40
20
0
% Embryos
reduction
no reduction
Control (pMES)
5μg/μL FoxD3
J
Tspan18 mRNA expression
n=11
n=14
100
80
60
40
20
0
% Embryos
sustained expression
normal downregulation
ContMO
FoxD3MO

**Fig. 2-7. FoxD3 negatively regulates *Tspan18*.**

Embryos unilaterally electroporated with 5μg/μL of empty pMES (A,B) or pMES-FoxD3 (C,D), or with ContMO (F,G) or FoxD3MO (H,I) were processed by whole mount in situ hybridization for *Tspan18* at 7s (A-D) or 9s (F-I). A,C,F,H dorsal view, anterior embryo half; A',C',F',H', construct targeting; B,D,G,I, midbrain transverse sections. (A-D) *Tspan18* expression in the neural folds (A,B, arrow) is drastically reduced on the targeted side of the neural tube in pMES-FoxD3 electroporated embryos (C,D, arrowheads). (F-I) *Tspan18* expression is normally downregulated at 9s (F,G, arrow), but is maintained on the targeted side of FoxD3MO-electroporated embryos (H,I, arrowheads). Neural crest migration was inhibited in FoxD3MO-electroporated embryos (I'; arrowhead). (E) Bar graph representing the frequency of pMES-FoxD3-electroporated embryos exhibiting reduced *Tspan18* mRNA expression. (J) Bar graph representing the frequency of FoxD3MO-electroporated embryos with persistent *Tspan18* expression.

To confirm that FoxD3 negatively impacts *Tspan18* expression, we also determined whether FoxD3 was necessary for *Tspan18* mRNA downregulation. To this end, we electroporated neural crest precursors with the previously characterized FoxD3 MO (Kos et al., 2001) and analyzed expression of *Tspan18* mRNA at 9-10s. While *Tspan18* mRNA was absent from the midbrain of ContMO electroporated embryos (Fig. 2-7F,G), *Tspan18* transcripts persisted following FoxD3 knock down (Fig. 2-7H,I; $p=9.8x10^{-4}$, n=14). Moreover, these FoxD3-deficient, *Tspan18*-expressing cells failed to migrate (Fig. 2-7I'; (Kos et al., 2001). This indicates that FoxD3 is required for *Tspan18* transcriptional downregulation, and moreover, suggests that persistent endogenous Tspan18 expression, like Tspan18 overexpression (Fig. 2-5), prevents neural crest migration.

## 2.4 Discussion:

Although neural crest cells must undergo EMT to become motile and AJ remodeling is a crucial step in this process, a complete understanding of cadherin regulation in neural crest cells is lacking. In this study, we have revealed Tspan18 as a novel post-translational regulator of Cad6B in cranial neural crest cells. We show that Tspan18 is abundantly expressed in premigratory but not in migratory cranial neural crest cells, and that Tspan18 downregulation is required for cranial neural crest cells to migrate. Because Tspan18 overexpression maintains, and Tspan18 knock down leads to premature loss of Cad6B protein without affecting *Cad6B* mRNA expression, we conclude that Tspan18 post-translationally regulates Cad6B-dependent cell adhesion to antagonize cranial neural crest EMT. Snail2 does not regulate *Tspan18*, as it does *Cad6B*; rather *Tspan18* is downstream of FoxD3. Taken together, our data suggest that Tspan18 post-translationally regulates Cad6B protein levels and must be downregulated by FoxD3 during neural crest EMT in a pathway parallel to Snail2-dependent *Cad6B* transcriptional regulation.

### Tspan18 prevents neural crest migration.

Tspan18 overexpression blocks neural crest migration (Fig. 2-5C,D,F,H) and affects neural tube morphogenesis (Fig. 2-5D",J), however, these effects are unlikely to be interdependent. First of all, migration defects are more common than neural tube defects and there is not a one-to-one correlation between these phenotypes (Fig. 2-5K,L). Second, abnormal neural folds produce migratory neural crest cells (Fig. 2-5H, arrow); it is the expression of Tspan18 that prevents migration (Fig. 2-5H, arrowhead). Third,

generally speaking, neural crest migration does not require neural tube closure either developmentally (e.g., mouse cranial neural tube) or experimentally (C.L. Fairchild and L.S. Gammill, unpublished observations). Thus, persistent Tspan18 expression prevents neural crest migration. Since *Tspan18* is not normally expressed in the ventral neural tube or neural folds past 7 somites (Fig. 2-1), Tspan18 does not normally regulate neural tube closure; however, when misexpressed, Tspan18 must affect proteins involved in neurepithelial morphogenesis. These likely include cadherins, as N-cadherin gain- or loss-of-function causes similar defects (Detrick et al., 1990; Fujimori et al., 1990; Nandadasa et al., 2009) and the dynamic regulation of AJ positioning is required for epithelial folding during *Drosophila* gastrulation (Wang et al., 2012).

*Tspan18* and *Cad6B* expression persist in the forebrain even after they are downregulated in the midbrain (Fig. 2-1D,H). As the rostral-most neural tube does not produce neural crest cells (Creuzet et al., 2005), it is possible that the expression of these epithelial markers is one factor that prevents neural crest migration from this region. Interestingly, Tspan18 knock down led to a statistically significant reduction of *Cad6B* mRNA expression in forebrain neural folds, despite *Cad6B* mRNA being unaffected in the midbrain of the majority of embryos (Fig. 2-2N). Meanwhile, Cad6B protein is more effectively diminished by Tspan18 knock down in the midbrain (Fig. 2-2E) than the forebrain (Fig. 2-2D'). This suggests regional complexity in Cad6B transcriptional and post-translational regulation, and the regulatory relationship between Tspan18 and Cad6B.

**Tspan18 post-translationally maintains Cad6B protein.**

Tspan18 loss-of-function impacts both Cad6B mRNA and protein levels, however our results suggest these effects are separable. First, Tspan18 knock down has a significant effect on Cad6B protein and minimal effects on *Cad6B* mRNA levels in the midbrain (Fig. 2-2). Second, Cad6B protein persists when Tspan18 is overexpressed despite temporally normal downregulation of *Cad6B* mRNA (Fig. 2-6H). Third, when Tspan18 is overexpressed, Cad6B protein persists only in the dorsal neural tube where it is normally expressed (Fig. 2-6C) indicating Tspan18 affects existing Cad6B protein rather than eliciting de novo expression. Altogether, these results suggest that Tspan18 maintains Cad6B protein levels post-translationally. Transcriptionally, we propose that Tspan18 knock down leads to *Cad6B* mRNA downregulation as a secondary consequence of AJ remodeling that results in increased nuclear β-catenin (Fig. 2-S7F-H).

The ability of Tspan18 to affect Cad6B post-translationally is consistent with existing knowledge of tetraspanins and cadherins. For example, in human cancer cells, the tetraspanin CD82 promotes E-cad-dependent cell-cell adhesion by stabilizing E-cad protein-protein interactions without markedly altering E-cad protein levels (Abe et al., 2008). However, in this study, CD82 was concluded to promote epithelial barrier formation to contain metastatic cells, rather than to antagonize EMT (Abe et al., 2008). Nevertheless, post-translational regulation of cadherins during EMT is not unprecedented. N-cad protein is cleared by processing during trunk neural crest EMT (Shoval et al., 2007). Moreover, during mouse gastrulation, p38 destabilizes and EPB41L5 alters the localization of E-cad, acting in conjunction with E-cad transcriptional repression to enable EMT (Hirano et al., 2008; Zohn et al., 2006). Thus, coupled

transcriptional and post-translational regulation of cadherin levels appears to be a common mechanism to tightly regulate AJ remodeling and cell adhesion during dynamic, rapid events like neural crest migration and gastrulation (Thiery et al., 2009).

The means by which Tspan18 maintains Cad6B protein levels is unclear. One possibility is that Cad6B is processed, and Tpsan18 protects Cad6B from processing enzymes to stabilize it at the membrane. Tetraspanins can associate with membrane proteases such as ADAM metalloproteases (Yanez-Mo et al., 2011), and Tspan18 could alter ADAM-dependent Cad6B processing. N-cad is processed in trunk neural crest cells by ADAM10 (Shoval et al., 2007), and cadherin-11 cleavage regulates *Xenopus* cranial neural crest migration (McCusker et al., 2009). However, Cad6B processing has not been defined, precluding evaluation of this scenario. Another possibility is that Tspan18 protects Cad6B from degradation. In either case, Tspan18 could interact with Cad6B directly, or it could promote the formation of a complex that stabilizes Cad6B. Evaluating these mechanisms are important future experiments.

**Tspan18 knock down does not ensure premature neural crest migration.**

Loss of Tspan18 does not promote early neural crest migration (Fig. 2-3) despite a consistent reduction in Cad6B protein levels (Fig. 2-2), an event that was previously shown to augment neural crest migration (Coles et al., 2007). There are several likely explanations for this. First and foremost, Tspan18 knock down may deplete Cad6B protein, but in a majority of embryos, *Cad6B* mRNA persists in the midbrain (Fig. 2-2N). Thus, in contrast to Cad6B knock down (Coles et al., 2007), new Cad6B protein will continue to be translated, barely detectable by immunofluorescence (see Fig. 2-2O) but

presumably sufficient to maintain adhesion. Only in the minority of cases where *Cad6B* mRNA is also lost in the midbrain would an effect on migration be anticipated. Incidentally, the frequency of embryos in which *Cad6B* mRNA is downregulated in the midbrain (Fig. 2-2N) is roughly equivalent to the frequency of embryos with precocious migration (Fig. 2-3G). Unfortunately we cannot visualize Cad6B mRNA levels in premigratory neural crest cells and subsequently assay those same cells for precocious migration in order to test this correlation directly.

It is unclear why only some Tspan18 morphant embryos show the more dramatic phenotype. One possibility is that severely affected embryos are those with neural folds uniformly targeted with high levels of MO. Tspan18 knock down is efficient (Fig. 2-S4), however, MO electroporation is by nature mosaic. Given that cadherins interact homophilically, when MO targeting is variable in the neural fold, cells containing low levels of TS18MO and residual Cad6B could stabilize AJs in adjacent, well-targeted cells, prevent β-catenin nuclear translocation (Fig. 2-S7F-H), and thus reduce the penetrance of the enhanced migration phenotype.

Another reason Tspan18 knock down may not reliably elicit precocious migration is that loss of an epithelial cadherin is not the sole feature of EMT; to emigrate from the neural tube, the basal lamina must also break down, and neural crest cells must remodel their AJs to include cadherins that allow mesenchymal cell-cell adhesion during collective cell migration (Friedl and Wolf, 2003; Park and Gumbiner, 2010; Theveneau and Mayor, 2012). Although Cad6B protein is lost prematurely following Tspan18 knock down, basal lamina break down and upregulation of the mesenchymal cadherin Cad7 still occur on the proper developmental timeline (Fig. 2-4). As neural crest cells will not

invade an intact basal lamina (Erickson, 1987), this likely prevents precocious neural crest migration. In this respect, Tspan18 and Cad6B knock down are similar: although Cad6B knock down leads to increased numbers of migratory neural crest cells, it has minimal effects on the extent of migration away from the neural tube (Coles et al., 2007), supporting this interpretation. The diversity and non-linearity of cellular behaviors during trunk neural crest emigration also suggest that it is not possible to change the time course of EMT by disrupting any one individual feature (Ahlstrom and Erickson, 2009).

Finally, it is also possible that Tspan18 knock down does not elicit premature cranial neural crest migration because of genetic redundancy. The tetraspanin family is large, including 33 members with broad, overlapping expression domains, and mutants often exhibit only minor defects (Rubinstein, 2011). In the chick embryo, Tspan18 is coexpressed with Tspan4 and CD9/Tspan29 during later development of the spinal cord, thus it is possible other tetraspanins compensate for Tspan18 loss of function during cranial neural crest development (Perron and Bixby, 1999). However, this would not explain why neural crest cells occasionally do migrate prematurely (Fig. 2-3), thus, it would seem that other mechanistic explanations are more likely.

### ***Tspan18*** **is downstream of FoxD3: a novel transcriptional input into cranial neural crest EMT.**

While they have similar temporal expression patterns (Fig. 2-1), and although Tspan18 maintains Cad6B protein levels (Fig. 2-6), transcriptional regulation of *Tspan18* and *Cad6B* is distinct: *Cad6B* is directly repressed by Snail2 in cranial neural crest cells (Taneyhill et al., 2007), and *Tspan18* is downstream of FoxD3 (Fig. 2-7). Although its

role in regulating neural crest multipotency and cell fate is well known (Kos et al., 2001; Lister et al., 2006; Mundell and Labosky, 2011; Sasai et al., 2001), a role for FoxD3 in EMT is not unexpected. When overexpressed in trunk neural tube cells, FoxD3 promotes cell adhesive changes associated with EMT, leading to loss of *N-cad* expression and upregulation of *Cad7* and *β1-integrin* in a Snail2-independent fashion (Cheung et al., 2005; Dottori et al., 2001). As downregulation of *Tspan18* is necessary for cranial neural crest cells to migrate (Fig. 2-5 and 2-7), our results show that FoxD3 is an indirect transcriptional regulator of cranial crest EMT that negatively affects *Tspan18* expression. Thus the action of Snail2 and FoxD3 converge to impact Cad6B transcriptionally and post-translationally (through downregulation of Tspan18), resulting in AJ remodeling during cranial neural crest migration. As only cranial neural crest cells express detectable *Tspan18* (Fig. 2-1), and as Snail2 transcriptionally downregulates Cad6B prior to cranial but not trunk neural crest migration (Park and Gumbiner, 2010; Taneyhill et al., 2007), it appears that this coordinated transcriptional and postranslational regulation of Cad6B is a cranial-specific mechanism. Additional experiments are currently underway to further characterize the transcriptional regulation of *Tspan18* by FoxD3.

**A new model for cranial neural crest EMT.**

Our study of Tspan18 provides new insight into the unique molecular mechanisms of cranial neural crest EMT (Fig. 2-8). Premigratory cranial neural crest cells express Tspan18 and Cad6B, two markers that distinguish their epithelial character. Our data indicate that, in premigratory cranial neural crest cells, Tspan18 maintains Cad6B-dependent AJs to antagonize EMT. During EMT, Snail2 downregulates *Cad6B*

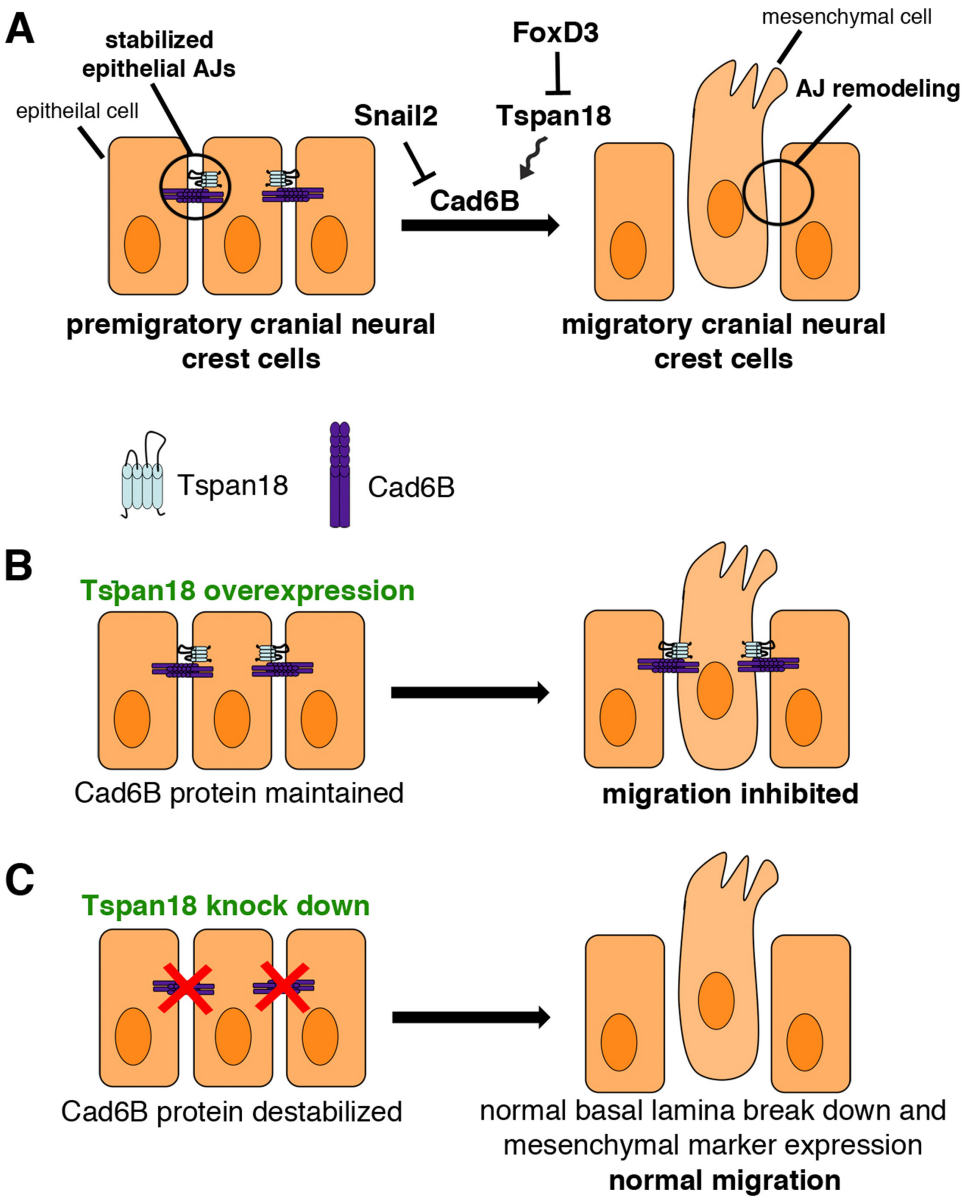
A
stabilized
epithelial AJs
epitheilal cell
Snail2
FoxD3
Tspan18
Cad6B
mesenchymal cell
AJ remodeling
premigratory cranial neural
crest cells
migratory cranial neural
crest cells
Tspan18
Cad6B
B
Tspan18 overexpression
Cad6B protein maintained
migration inhibited
C
Tspan18 knock down
Cad6B protein destabilized
normal basal lamina break down and
mesenchymal marker expression
normal migration

**Fig. 2-8. The role of Tspan18 in cranial neural crest EMT.**

(A) Epithelial, premigratory cranial neural crest cells are tightly joined by Tspan18-stabilized, Cad6B-containing adherens junctions (AJs). During EMT, neural crest cells transcriptionally downregulate Cad6B via Snail2 and post-translationally destabilize Cad6B by FoxD3-dependent downregulation of Tspan18 to remodel their AJs in preparation for migration. (B) Evidence for the role of Tspan18. Sustained expression of Tspan18 maintains Cad6B protein and promotes Cad6B-dependent AJs, inhibiting neural crest migration. (C) In contrast, loss of Tspan18 results in premature downregulation of Cad6B protein but normal cranial neural crest migration, presumably reflecting a need for coordinated transcriptional and post-translational regulation of Cad6B and temporally normal delamination and expression of mesenchymal markers. Thus, loss of Tspan18 is necessary, but not sufficient for cranial neural crest migration.

transcription (Taneyhill et al., 2007). In parallel, we demonstrate that FoxD3 downregulates *Tspan18* expression, alleviating Tspan18-dependent Cad6B stabilization. Together, Cad6B transcriptional repression and post-translational destabilization result in AJ remodeling that changes cell adhesion and allows for mesenchymal transition and subsequent neural crest migration (Fig. 2-8A). Tspan18 downregulation is necessary for EMT, as prolonging endogenous Tspan18 expression (Fig. 2-7) or driving exogenous Tspan18 expression in the neural folds (Fig. 2-5) maintains Cad6B protein levels and/or prevents migration (Fig. 2-8B). However, Tspan18 downregulation is not sufficient for migration: loss of Tspan18 (and destabilization of Cad6B protein) does not alter Cad6B transcription and fails to trigger neural crest migration in the majority of cases (Fig. 2-8C). This underscores the importance of coordinated transcriptional and post-translational regulation of cadherin expression during EMT, and emphasizes that while cadherin switching and AJ remodeling is a critical step in EMT, it is not the only step in the process of producing migratory neural crest cells (Ahlstrom and Erickson, 2009; Lim and Thiery, 2012). In summary, post-translational stabilization of Cad6B by Tspan18 that must be downregulated for cells to undergo EMT is a novel mechanism that provides new insight into the developmental function of tetraspanins and has important implications for cancer metastasis.

## 2.5 Supplemental Figures:

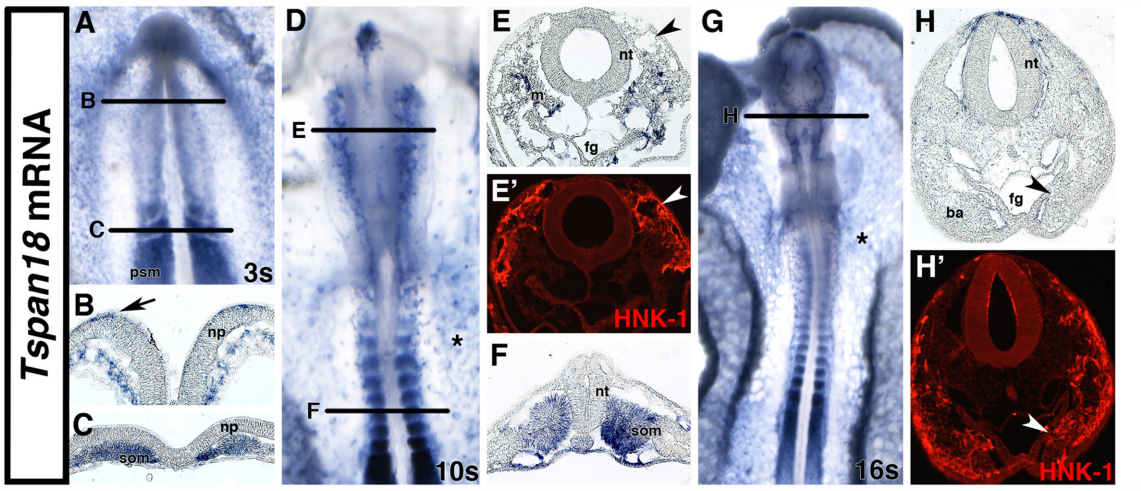

**Fig. 2-S1. *Tspan18* is expressed during early chick development, but is absent from cranial migratory neural crest cells.**

Whole mount in situ hybridization for *Tspan18* in 3 somite (s; A-C), 10s (D-F) and 16s (G,H) chick embryos (dorsal view with corresponding transverse sections at the levels indicated in A,D,G). In 3s embryos *Tspan18* is expressed in the dorsal neural plate (np; arrow in B), in the presomitic mesoderm (psm), and the newly formed, epithelial somites (som). At 10s, *Tspan18* is expressed in the developing vasculature (asterisk in D), the head mesenchyme (m) and epithelial somites (F). However, *Tspan18* is absent in migrating neural crest cells that express HNK-1 (arrowheads in E,E') and rostral, dissociated somites. At 16s, *Tspan18* mRNA persists in the vasculature (asterisk in G) and epithelial somites, but remains absent from HNK-1-positive migratory neural crest cells in the branchial arch (ba; arrowheads in H,H'). nt, neural tube; fg, foregut.

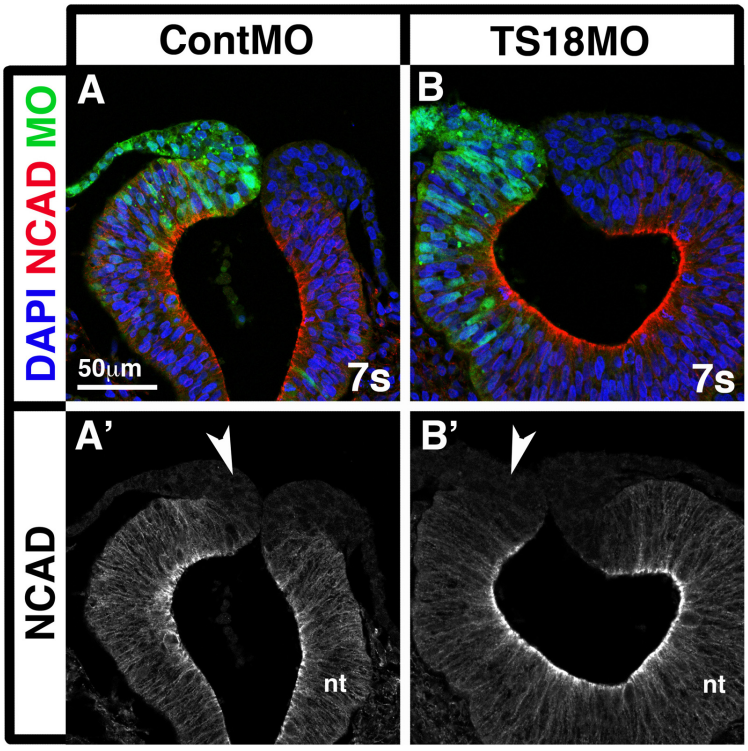
ContMO
TS18MO
DAPI NCAD MO
A
B
50μm
7s
7s
NCAD
A'
B'
nt
nt

**Fig. 2-S2. Tspan18 knock down does not affect N-cadherin protein levels.**

Embryos were unilaterally electroporated at HH4+ with ContMO (A, green) or TS18MO (B, green) and subsequently sectioned and immunostained for N-cad (A, B, red; A', B'). N-cad expression in the cranial neural tube at 7s, including its absence from cranial neural folds (Dady et al., 2012), is unaffected by ContMO (arrowhead in A') or TS18MO electroporation (arrowhead in B'). nt, neural tube; Scale bar in A= 50 μm.

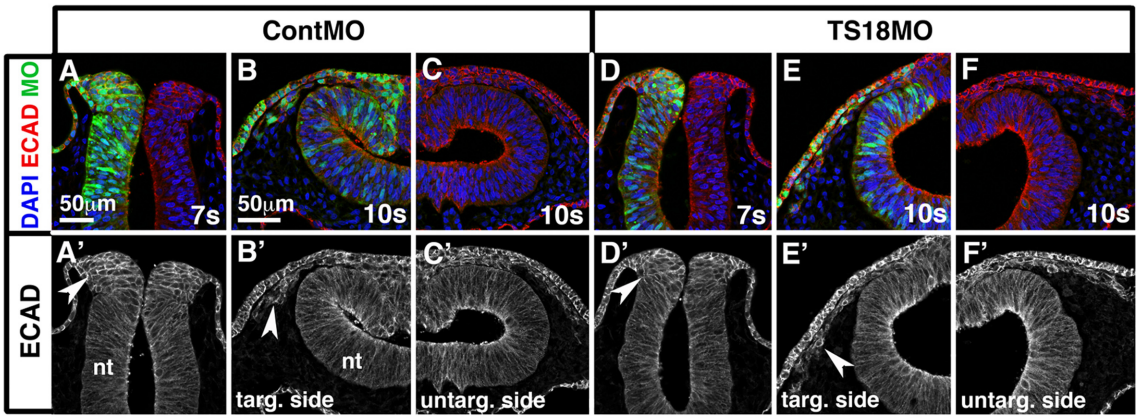
ContMO
TS18MO
DAPI ECAD MO
ECAD
A
B
C
D
E
F
50μm
7s
10s
A'
B'
C'
D'
E'
F'
nt
targ. side
untarg. side

**Fig. 2-S3. Tspan18 knock down does not affect E-cadherin protein levels.**

Embryos were unilaterally electroporated at HH4+ with ContMO (A, B, green) or TS18MO (D, E, green) and subsequently sectioned and immunostained for E-Cad (A-F, red; A'-F'). E-cad expression is unaffected by ContMO (arrowheads in A'-C') or TS18MO (arrowheads in D'-F') electroporation both in the cranial neural tube at 7s (A, D) and in migrating neural crest cells at 10s (B,C,E,F; Dady et.al., 2012). C and F are the unelectroporated halves of the embryos shown in B and E. nt, neural tube; Scale bars in A,B= 50μm.

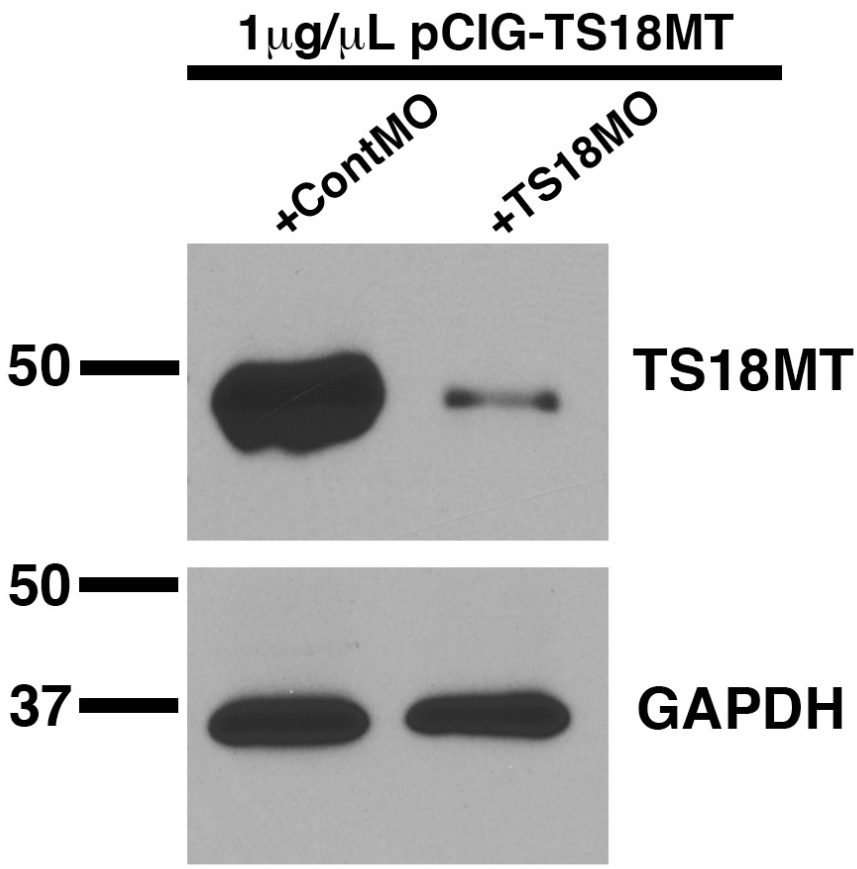
1μg/μL pCIG-TS18MT
+ContMO
+TS18MO
50
TS18MT
50
37
GAPDH

**Fig. 2-S4. TS18MO efficiently prevents Tspan18 protein synthesis.**

Embryos were bilaterally co-electroporated with 1 μg/μl pCIG-TS18MT (to express Tspan18 with a C-terminal 6x myc tag fusion) and either ContMO or TS18MO. Embryos were incubated to 7-10s and embryo heads with bright, equivalently targeted GFP fluorescence (indicating expression of the bicistronic message) were dissected. Embryo heads from 12 embryos were pooled, lysed, and analyzed by western blot with antibodies against myc tag (to detect TS18MT; 9E10; Developmental Studies Hybridoma Bank) or GAPDH (6C5; Life Technologies) as a loading control. Abundant TS18MT was detected following co-electroporation with ContMO. However, TS18MO drastically reduced the amount of TS18MT expressed from the pCIG-TS18MT plasmid, although some residual TS18MT was translated.

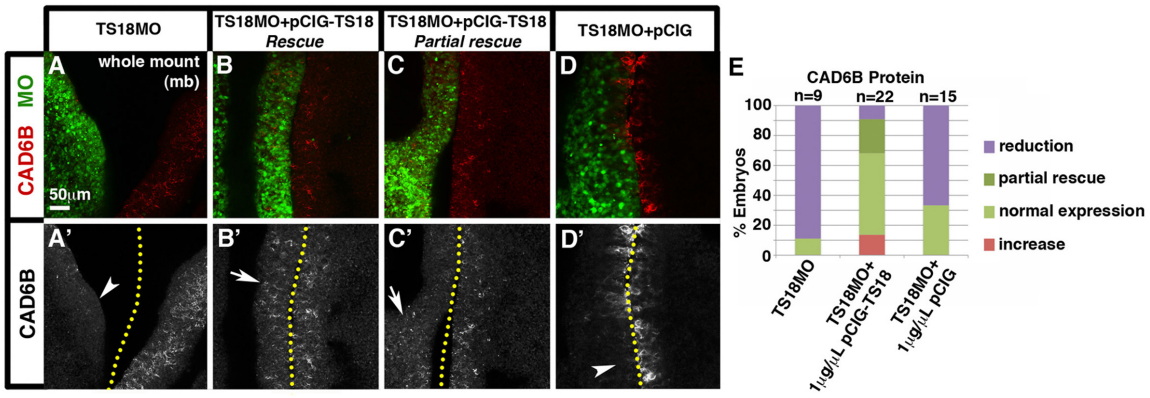
TS18MO
TS18MO+pCIG-TS18
Rescue
TS18MO+pCIG-TS18
Partial rescue
TS18MO+pCIG
MO
CAD6B
A
whole mount
(mb)
B
C
D
50μm
CAD6B
A'
B'
C'
D'
E
CAD6B Protein
n=9
n=22
n=15
% Embryos
100
80
60
40
20
0
reduction
partial rescue
normal expression
increase
TS18MO
TS18MO+
1μg/μL pCIG-TS18
TS18MO+
1μg/μL pCIG

**Fig. 2-S5. Co-electroporation of TS18MO with pCIG-TS18 rescues Cad6B protein levels.**

Embryos were unilaterally electroporated with TS18MO alone (A, green) or TS18MO mixed with 1μg/μl of pCIG-TS18 (B,C, green) or empty pCIG (D, green) and immunostained for Cad6B protein (A-D, red; A'-D'). As previously observed, Cad6B protein was largely absent in midbrain cells targeted with TS18MO (arrowhead in A'). Following co-electroporation of TS18MO and pCIG-TS18, Cad6B protein levels were normal or increased in 68% of embryos (arrow in B'), while Cad6B protein staining was speckled and partially rescued in another 23% (arrowhead in C'; $p=1.7x10^{-4}$, n=22). Co-electroporation of TS18MO with empty pCIG did not rescue Cad6B protein (arrowhead in D'; p=0.35, n=15). (E) A bar graph of the number of electroporated embryos showing a reduction, rescue, or increase in Cad6B protein levels. mb, midbrain. Scale bar in A= 50 μm. Dotted lines in A'-D' indicate embryo midline.

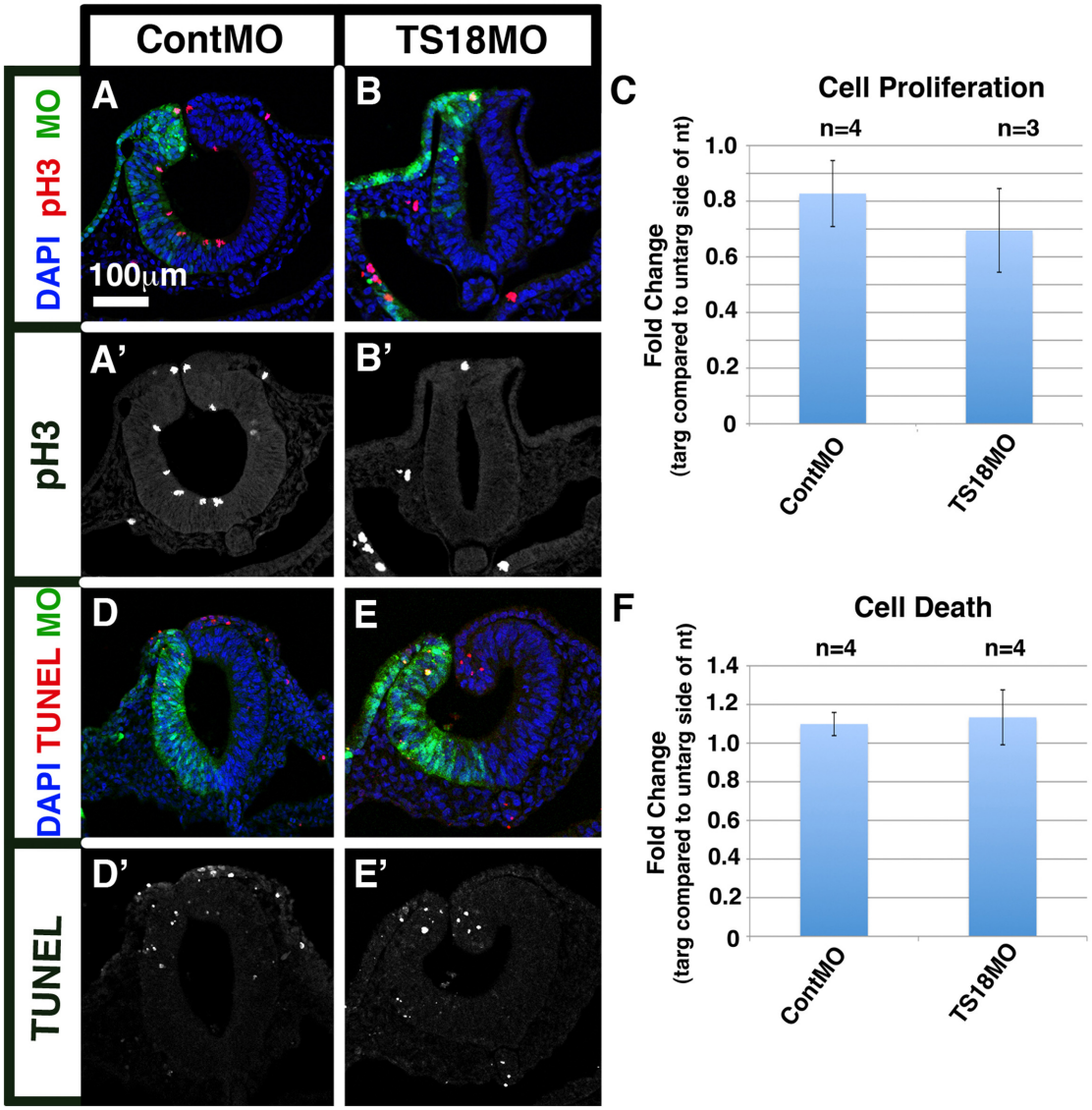
ContMO
TS18MO
DAPI pH3 MO
A
B
100μm
pH3
A'
B'
DAPI TUNEL MO
D
E
TUNEL
D'
E'
C
Cell Proliferation
n=4
n=3
Fold Change
(targ compared to untarg side of nt)
1.0
0.8
0.6
0.4
0.2
0
ContMO
TS18MO
F
Cell Death
n=4
n=4
Fold Change
(targ compared to untarg side of nt)
1.4
1.2
1.0
0.8
0.6
0.4
0.2
0
ContMO
TS18MO

**Fig. 2-S6. Tspan18 knockdown does not affect cell proliferation or death.**

Embryos unilaterally electroporated with ContMO (A,D) or TS18MO (B,E) were sectioned and immunostained for phosphohistone H3 (pH3; A,B, red; A', B') or labeled by TUNEL staining (D,E, red; D',E'; Roche Applied Science; Indianapolis, IN). There was no apparent difference in the number of pH3-positive cells on the targeted side of the neural tube, as compared to the untargeted side, in ContMO (A') or TS18MO (B') electroporated embryos. (C) Effects on proliferation were quantitated by counting the number of pH3-positive cells divided by the total number of cells in the dorsal quarter of the neural tube on the targeted and untargeted sides in 5 sections of 3 or 4 electroporated embryos ($p=0.270$). Likewise, there was no apparent difference in the relative number of TUNEL-positive cells on the targeted side of the neural tube in ContMO (D') or TS18MO (E') electroporated embryos. (F) Effects on cell death were quantitated by counting the number of TUNEL-positive cells divided by the total number of cells in the dorsal quarter of the neural tube on the targeted and untargeted sides in 5 sections of 4 electroporated embryos ($p=0.415$). Statistics were performed using the paired Student's *t* test in Excel (Microscoft). Error bars indicate +/- the standard error of the mean. nt, neural tube. Scale bar in A= 100 μm.

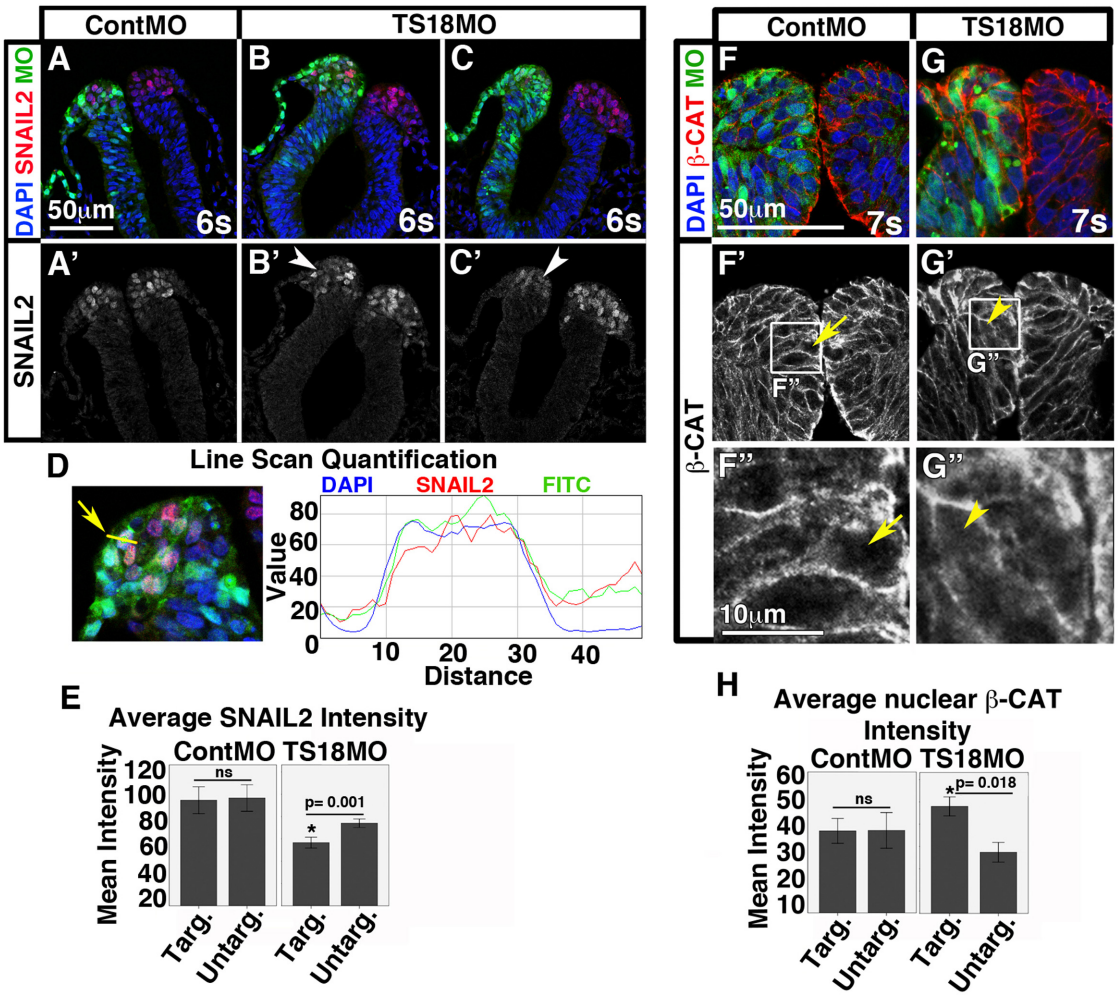
ContMO
TS18MO
DAPI SNAIL2 MO
SNAIL2
A
B
C
A'
B'
C'
50μm
6s
D
Line Scan Quantification
DAPI
SNAIL2
FITC
Value
Distance
E
Average SNAIL2 Intensity
ContMO TS18MO
Mean Intensity
ns
p= 0.001
Targ.
Untarg.
DAPI β-CAT MO
β-CAT
F
G
F'
G'
F''
G''
7s
10μm
H
Average nuclear β-CAT Intensity
p= 0.018

**Fig. 2-S7. Downregulation of *Cad6B* mRNA following Tspan18 knock down does not correlate with Snail2 but may be the consequence of increased nuclear β-catenin.**

Embryos unilaterally electroporated with ContMO (A,F) or TS18MO (B,C,G) were immunostained for Snail2 (A-C) or β-catenin (F, G). (A-C) Transverse midbrain sections of 6s embryos. Snail2 protein levels (red; A'-C') are unaffected by ContMO electroporation (A, green) but reduced on the targeted side in embryos electroporated with TS18MO (B',C', green; arrowheads). (D) A representative line scan used to measure the average immunofluorescence intensity in a nucleus (yellow arrow; same procedure used for Snail2 and β-catenin). (E) Nuclear Snail2 immunofluorescence was quantified by line scan, comparing cells of the targeted (targ) and untargeted (untarg) sides of the neural tube within individual sections (horizontal lines above the graphs) to control for experimental variations in staining between sections and embryos. These measurements verified that ContMO had no effect, while TS18MO electroporation led to reduced Snail2 levels (n=4; p=0.001). (F-G) Transverse midbrain sections of 6-7s embryos reveal abundant membrane-localized β-catenin in embryos electroporated with both ContMO (F') and TS18MO (G'). However, higher magnification images (box in F',G') suggest increased nuclear-localized β-catenin on the targeted (green) side of the neural tube in TS18MO-electroporated embryos (arrowheads in G") compared to ContMO-electroporated embryos (arrow in F"). (H) Nuclear β-catenin was quantified by line scan, comparing cells of the targeted (targ) and untargeted (untarg) sides of the neural tube within individual sections (horizontal lines above the graphs) to control for experimental variations in staining between sections and embryos. These measurements

documented a significant increase in nuclear-localized β-catenin on the targeted side of the neural tube in TS18MO-electroporated embryos (n=3; p=0.018). To quantify Snail2 and β-catenin, 10 nuclei were chosen from 3 sections per embryo (Snail2 n=4 embryos; β-catenin n=3 embryos). Nuclei were selected based on the following criteria: 1) in the dorsal-most quarter of the neural tube, 2) non-overlapping with other nuclei, 3) from cells containing detectable levels of MO. The RGB profiler plug-in in ImageJ was used to perform line scans (with 5 pixel lines) to measure the average intensity of the red channel within each DAPI-positive nucleus. Statistical evaluation of intensity measurements was performed using SPSS 16.0 for Windows (Chicago, IL) using paired comparisons in a MANOVA. A p value $< 0.05$ was considered statistically significant. Error bars indicate +/- the standard error of the mean. Scale bars in A, F= 50 μm; scale bar in F"=10 μm.

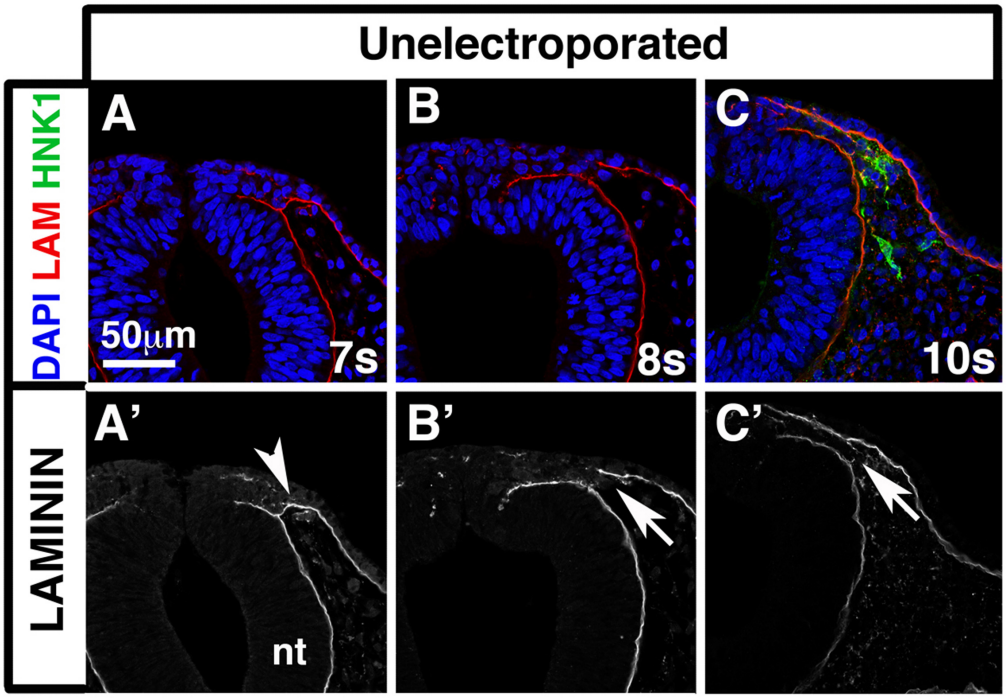
Unelectroporated
DAPI LAM HNK1
A
B
C
50μm
7s
8s
10s
LAMININ
A'
B'
C'
nt

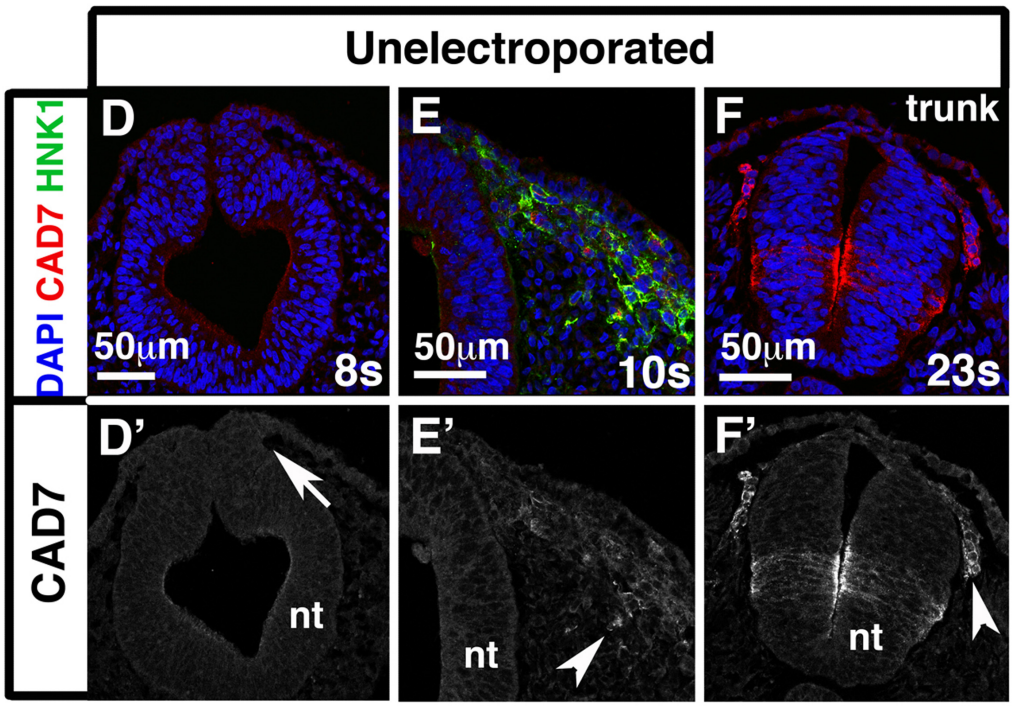
Unelectroporated
DAPI CAD7 HNK1
D
E
F
trunk
50μm
8s
50μm
10s
50μm
23s
CAD7
D'
E'
F'
nt
nt
nt

**Fig. 2-S8. Normal expression patterns of Laminin and Cad7 during EMT.**

Transverse midbrain sections of unelectroporated embryos immunostained for Laminin (A-C, red; A'-C') or Cad7 (D-F, red; D'-F'). (A-C) The intact basal lamina connecting the basal surface of the neural tube with the non-neural ectoderm at 7s (arrowhead in A') becomes discontinuous at 8s (arrow in B') in the region that HNK-1-positive cranial neural crest cells (green in C) exit the neural tube at 10s (arrow in C'). (D-F) Cad7 protein is undetectable in early migrating neural crest cells at 8s (arrow in D') but accumulates by 10s in HNK-1-positive migratory cranial neural crest cells (arrowhead in E'), similar to the pattern in 23s trunk migratory neural crest cells (arrowhead in F'; (Nakagawa and Takeichi, 1998)). nt, neural tube. Scale bars= 50 μm.

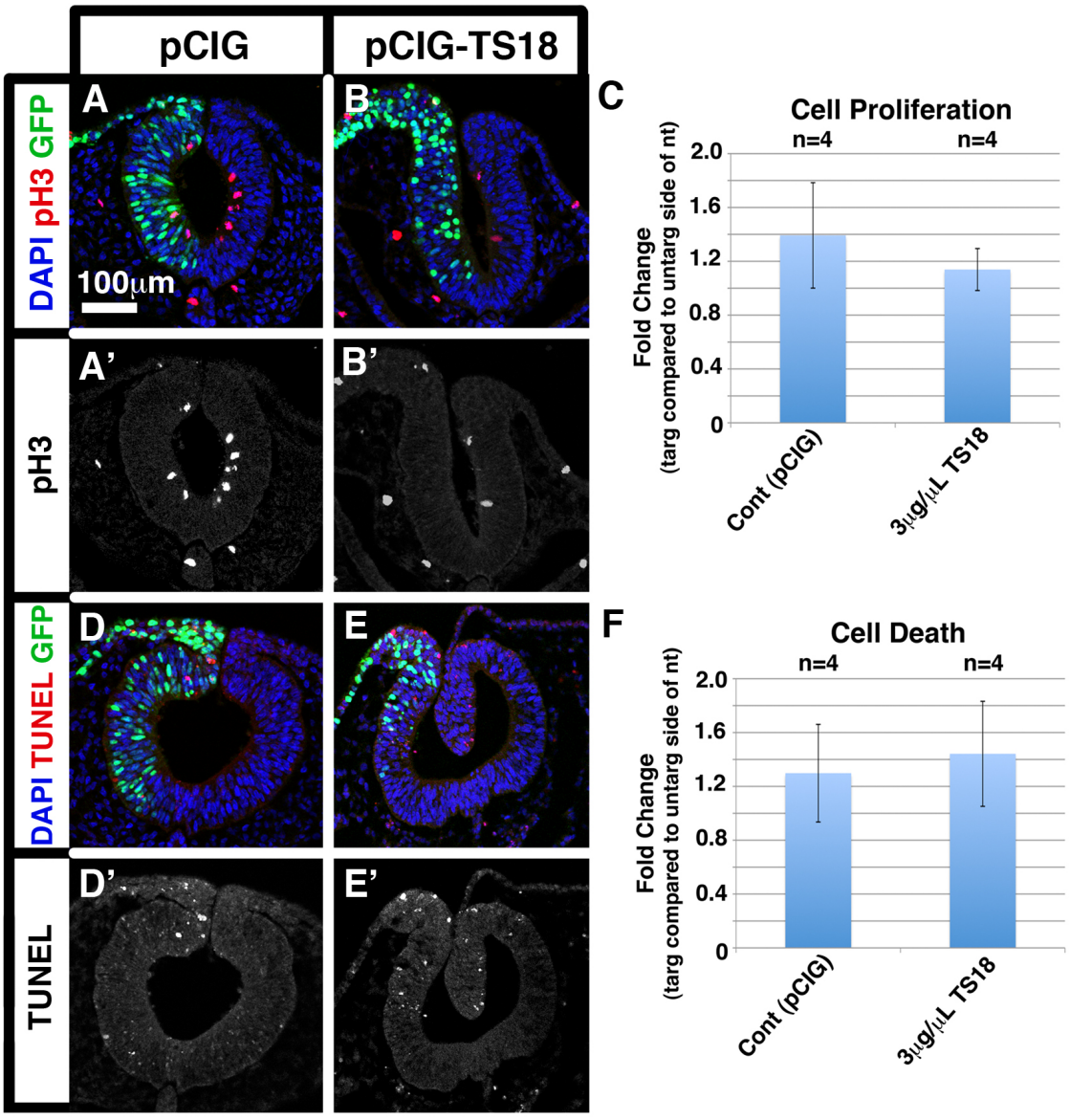
pCIG
pCIG-TS18
DAPI pH3 GFP
A
B
100μm
pH3
A'
B'
DAPI TUNEL GFP
D
E
TUNEL
D'
E'
C
Cell Proliferation
n=4
n=4
Fold Change
(targ compared to untarg side of nt)
2.0
1.6
1.2
0.8
0.4
0
Cont (pCIG)
3μg/μL TS18
F
Cell Death
n=4
n=4
Fold Change
(targ compared to untarg side of nt)
2.0
1.6
1.2
0.8
0.4
0
Cont (pCIG)
3μg/μL TS18

**Fig. 2-S9. Tspan18 overexpression does not affect cell proliferation or death.**

Embryos unilaterally electroporated with empty pCIG (A,D) or pCIG-TS18 (B,E) were sectioned and immunostained for phosphohistone H3 (pH3; A,B) or labeled by TUNEL staining (D,E). (C) There was no noticeable difference in the number of pH3-positive cells on the targeted side of the dorsal neural tube, as compared to the untargeted side, in pCIG (A') or pCIG-TS18 (B') electroporated embryos. Effects on proliferation were quantitated by counting the number of pH3-positive cells divided by the total number of cells in the dorsal quarter of the neural tube on the targeted and untargeted sides in 5 sections of 4 electroporated embryos ($p=0.285$). (F) Likewise, there was no noticeable difference in the number of TUNEL-positive cells on the targeted side of the neural tube in embryos electroporated with either empty pCIG (D') or pCIG-TS18 (E'). Effects on cell death were quantitated by counting the number of TUNEL-positive cells divided by the total number of cells in the dorsal quarter of the neural tube on the targeted and untargeted sides in 5 sections of 4 electroporated embryos ($p=0.398$). Statistics were performed using the paired Student's *t* test in Excel (Microscoft). Error bars indicate +/- the standard error of the mean. nt; neural tube. Scale bar in A= 100 μm.

## 2.6 Materials and Methods:

### Embryos

Fertile chicken embryos were incubated in a humidified incubator (G. Q. F. Manufacturing; Savannah, GA) at 37-38°C. Embryos were staged according to Hamburger and Hamilton, 1951 or by counting somite pairs.

### Morpholino design, DNA constructs, and electroporation

FITC-tagged, antisense morpholinos (MO) synthesized by GeneTools, LLC (Philomath, OR) included a Tspan18 translation blocking MO (TS18MO: 5'-TGCAGCTCAGACAGTCTCCCTCCAT-3'), a 5 base pair mismatch TS18MO (mmTS18MO: 5'-TGgAcCTCAcACAcTCTgCCTCCAT-3'), a FoxD3 translation blocking MO (FoxD3 MO: 5'-CGCTGCCGCCGCCCGATAGAGTCAT-3'; (Kos et al., 2001)) and a standard control MO (ContMO: 5'-CCTCTTACCTCAGTTACAATTTATA-3'). To produce pCIG-TS18 and pCIG-TS18MT, full length Tspan18 without or with 6x myc tags was cloned by PCR into the GFP bicistronic expression plasmid pCIG (Megason and McMahon, 2002) using 5-10s chick cDNA (RNA prepared by TRIZOL extraction, cDNA synthesized with Superscript III; Life Technologies, Carlsbad, CA) as a template. To produce pMES-FoxD3, full length FoxD3 (Kos et al., 2001) was cloned into the EcoRI site of the GFP bicistronic expression plasmid pMES (Swartz et al., 2001). FITC-tagged morpholinos at 750 μM (with 0.2 μg/μL pCS2+MycTag DNA as carrier) or DNA at the indicated concentrations were unilaterally electroporated into the presumptive neural crest at Hamburger and Hamilton (HH) stage 4+ as previously described (Gammill and Krull, 2011). After

electroporation, embryos were incubated until the desired stages and fixed in 4% paraformaldehyde at room temperature for 15 min (Snail2 experiments) or 1 hour (all other experiments) before washing with PBS + 0.1% Tween. FITC or GFP targeting was verified by fluorescent microscopy before embryos were either immediately used for whole mount immunofluorescence, dehydrated into methanol and stored at -20°C for in situ hybridization, or embedded and prepared for sectioning.

**In situ hybridization**

Whole-mount in situ hybridization was performed as previously described (Wilkinson, 1992). Digoxigenin-labeled RNA probes were transcribed from the following templates: *cTspan18* (Adams et al., 2008), *cCad6B* (Gammill and Bronner-Fraser, 2002), and *cSox10* (Cheng et al., 2000). After processing, embryos were imaged in whole mount using a Zeiss Discovery V8 stereoscope, then embedded in gelatin, sectioned using a Leica CM1900 cryostat at 12-18 μm, and imaged on a Zeiss AxioImager A1 with a Zeiss AxioCam MRc5 digital camera and Axiovision software.

**Immunohistochemistry**

Immunofluorescence was performed as previously described (Roffers-Agarwal et al., 2012) with the following antibodies: anti-HNK-1 (ATTC, Manassas, VA; 1:25), anti-Cad6B (DSHB, Iowa City, IA; clone CCD6B-1; 1:100 (Nakagawa and Takeichi, 1998)), anti-Laminin (DSHB clone 31 or 31-2; 1:50), anti-Cad7 (DSHB clone CCD7-1; 1:50 (Nakagawa and Takeichi, 1998)), anti-N-cad (DSHB clone 6B3; 1:100), anti-E-cad (BD Transduction Laboratories; 1:250 (Dady et al., 2012)), anti-Snail2 (DSHB clone 62.1E6;

1:100), anti-β-catenin (Ctnnb1, BD Transduction Laboratories; 1:200 (Matson et al., 2011)) and anti-phosphohistone H3 (pH3; Millipore; Billerica, MA; 1:250). Primary antibody was detected using donkey anti-mouse or donkey anti-rat secondary antibodies at 1:250 (Jackson Labs; West Grove, PA). Slides were mounted in PermaFluor (Thermo Fisher Scientific; Waltham, MA) containing 1 μg/mL DAPI and imaged on a Zeiss LSM 710 laser scanning confocal microscope. Images were processed in Photoshop (Adobe).

**Analysis**

The statistical significance of the observed phenotypes was calculated by Fisher's exact test in R (R Development Core Team, 2012). For all expression analyses, staining on the targeted and untargeted sides of the neural tube were compared in individual images to rule out any difference in exposure time or staining efficiency between images/sections. To quantify Cad6B fluorescence intensity, the mean gray value was calculated in ImageJ for the Cad6B expression domain of 3 sections per embryo (n=5 embryos). Statistical evaluation of intensity measurements was performed using SPSS 16.0 for Windows (Chicago, IL) using paired comparisons in a MANOVA. A p value $< 0.05$ was considered statistically significant. Error bars indicate +/- the standard error of the mean.

**Acknowledgments:**

We are grateful to Yi-Chuan Cheng, Sean Megason, Cathy Krull and Carol Erickson for the kind gift of plasmids. We thank Lisa Taneyhill for technical advice and collaboration. Many thanks to the members of the Gammill lab for their input and support and Wuming Gong and Rebecca Pulver for their help with statistical analysis. The monoclonal antibodies used in this study, developed by M. Takeichi and S. Nakagawa (Cad6B, N-Cad, Cad7) and D. Fambrough (Laminin), were obtained from the Developmental Studies Hybridoma Bank developed under the auspices of the NICHD and maintained by The University of Iowa, Department of Biology, Iowa City, IA 52242. This work was supported by the National Institutes of Health, award numbers F31 NRSA GM087951 (CLF) and K22 DE015309 (LSG), and by a University of Minnesota Grant-in-Aid .

## Chapter 3

# FoxD3 regulates cranial neural crest EMT via downregulation of Tetraspanin18 independent of its functions during neural crest formation.

Corinne L. A. Fairchild, Joseph P. Conway, Andrew T. Schiffmacher, Lisa A. Taneyhill, and Laura S. Gammill.

[This thesis chapter was submitted to *Developmental Neurobiology* for publication in June, 2013]

## 3.1 Summary:

The scaffolding protein tetraspanin18 (Tspan18) maintains epithelial cadherin-6B (Cad6B) to antagonize chick cranial neural crest epithelial-to-mesenchymal transition (EMT). For migration to take place, Tspan18 must be downregulated. Here, we characterize the role of the winged-helix transcription factor FoxD3 in the control of *Tspan18* expression. *Tspan18* mRNA persists several hours past the stage it would normally be downregulated in FoxD3-deficient neural folds, though *Tspan18* expression eventually declines. This indicates that FoxD3 is required for initial downregulation of *Tspan18*, although other factors subsequently impact *Tspan18* expression. Remarkably, the classical EMT transcription factor Snail2 is not one of these factors. As in other vertebrates, FoxD3 is required for chick cranial neural crest specification, survival and migration. Strikingly, Tspan18 knockdown rescues FoxD3-depdendent neural crest migration defects, although neural crest formation is still deficient. This indicates that FoxD3 regulates cranial neural crest migration by promoting *Tspan18* downregulation to allow EMT, independent of its activity during neural crest specification and survival.

**Key words:** neural crest, FoxD3, tetraspanin, epithelial-to-mesenchymal transition (EMT)

## 3.2 Introduction:

The neural crest is a transient population of multipotent cells that arises from the dorsal neural tube of vertebrate embryos, migrates, and eventually contributes to a wide range of adult structures, including the peripheral nervous system and craniofacial skeleton (LeDouarin and Kalcheim, 1999). Neural crest development begins during gastrulation, when secreted factors induce the expression of a cohort of transcription factors, known generally as neural crest specifiers (Betancur et al., 2010), in the neural folds (Stuhlmiller and Garcia-Castro, 2012a). Neural crest specifiers converge to regulate the activity of neural crest effector genes that control cell adhesion, motility, and fate (Betancur et al., 2010). By doing so, neural crest specifiers are crucial for neural crest cells to progress through epithelial-to-mesenchymal transition (EMT), migration, and differentiation into diverse adult neural crest derivatives. Unfortunately, since few targets of neural crest specifiers have been identified, we know little about the exact mechanism behind their cellular impacts.

The winged-helix transcription factor FoxD3 is a key neural crest specifier that has been implicated in multiple steps of neural crest development. FoxD3 is initially required for neural crest formation during early stages of neural crest development, including specification, multipotency, cell fate and survival (Hochgreb-Hagele and Bronner, 2013; Kos et al., 2001; Lister et al., 2006; Montero-Balaguer et al., 2006; Mundell and Labosky, 2011; Nitzan et al., 2013; Sasai et al., 2001; Stewart et al., 2006; Thomas and Erickson, 2009). Subsequently, neural crest cells fail to migrate in FoxD3 mutant zebrafish (Stewart et al., 2006). Furthermore, FoxD3 overexpression in the chick trunk neural tube alters cell-cell adhesion (Cheung et al, 2005) and increases the number

of emigrating neural crest cells (Dottori et al., 2001; Kos et al., 2001). While these results suggest that FoxD3 also regulates neural crest migration, it is not possible to distinguish whether FoxD3 is required for neural crest migration independent of its functions during neural crest formation, or whether migration is blocked as a secondary consequence of these earlier roles. Moreover, FoxD3 represses neural crest and cancer cell migration in other circumstances, leaving the role of FoxD3 in migration unclear (Drerup et al., 2009; Katiyar and Aplin, 2011). Altogether, these results emphasize the need for further investigation to reconcile conflicting observations and define FoxD3 function during migration.

At the start of neural crest EMT, altered expression of $Ca^{2+}$-dependent cell adhesion molecules called cadherins disrupts cell-cell adhesions (Meng and Takeichi, 2009; Nieto, 2011; Oda and Takeichi, 2011). In cranial neural crest cells, *cadherin-6B* (*Cad6B*) is directly repressed by the neural crest specifier and well-established EMT transcription factor, Snail2 (Coles et al., 2007; Taneyhill et al., 2007). However, Cad6B protein levels in cranial neural crest cells are not only subject to transcriptional control. In addition, the transmembrane scaffolding protein Tetraspanin18 (Tspan18) post-translationally maintains Cad6B protein levels and must be downregulated in order for cranial neural crest cells to migrate (Fairchild and Gammill, 2013). Intriguingly, premigratory cranial neural crest cells lacking FoxD3 retain *Tspan18* mRNA expression (Fairchild and Gammill, 2013). This finding, along with the observation that ectopic FoxD3 in chick trunk alters cell adhesion molecule expression (Cheung et al., 2005), suggests that FoxD3 may modulate cadherin levels during cranial neural crest EMT through its effects on *Tspan18*.

Although our previous study showed that FoxD3 knockdown sustained *Tspan18* expression (Fairchild and Gammill, 2013), it did not address whether this was an indirect consequence of altered neural crest specification, or whether *Tspan18* was downstream of FoxD3 during EMT. Thus, the aim of this study was to distinguish between these two scenarios. We report that FoxD3 is required for initial downregulation of *Tspan18*, as well as for chick cranial neural crest specification and migration. Importantly, we show that the FoxD3-dependent migration defect can be rescued by Tspan18 knockdown, indicating that FoxD3 promotes cranial neural crest migration at least in part through downregulation of *Tspan18*. Interestingly, although Tpsan18 knockdown rescued the distance FoxD3-deficient neural crest cells migrated away from the neural tube, the population of migratory neural crest cells was still reduced. Together, these results suggest that FoxD3 is required for chick cranial neural crest EMT, and that FoxD3 function during migration is independent of its role in other aspects of neural crest development.

## 3.3 Results:

### *FoxD3* and *Tspan18* expression overlap in premigratory cranial neural crest cells

The general expression pattern of *FoxD3* during chick cranial neural crest development has previously been described (Khudyakov and Bronner-Fraser, 2009; Kos et al., 2001; Simoes-Costa et al., 2012); however, for FoxD3 to regulate *Tspan18*, their expression domains must overlap in neural crest cells as they are undergoing EMT, specifically between 6 and 9 somites when *Tspan18* downregulation occurs (Fairchild and Gammill, 2013). To assess this, we visualized and compared *FoxD3* and *Tspan18* mRNA levels by *in situ* hybridization in whole mount and transverse sections. At 6 and 7 somites, *FoxD3* transcripts were detected exclusively in the cranial neural tube (arrowheads in Fig. 3-1A,B). Transverse sections confirmed that *FoxD3* was abundantly expressed in the dorsal neural tube at these stages (Fig. 3-1A',B'). At 8s, emigrating cranial neural crest cells expressed *FoxD3* mRNA, which persisted in the dorsal cranial neural tube (arrowhead in Fig. 3-1C), and additionally extended into the trunk (arrow in Fig. 3-1C). At 9s, *FoxD3* expression was still apparent in the cranial neural tube (arrowhead in Fig. 3-1D') and in the trunk (arrow in Fig. 3-1D), however, its expression was reduced in actively migrating neural crest cells (Fig. 3-1D,D'; asterisks). Like *FoxD3*, *Tspan18* mRNA expression in the cranial, dorsal neural tube was apparent at 6 and 7 somites (arrowheads in Fig. 3-1E, F); however, *Tspan18* expression was downregulated in the dorsal neural tube by 8s (asterisk in Fig. 3-1G), when neural crest cells emigrate (Fairchild and Gammill, 2013). Thus, *FoxD3* is expressed at the right time and in the correct location to regulate *Tspan18* expression.

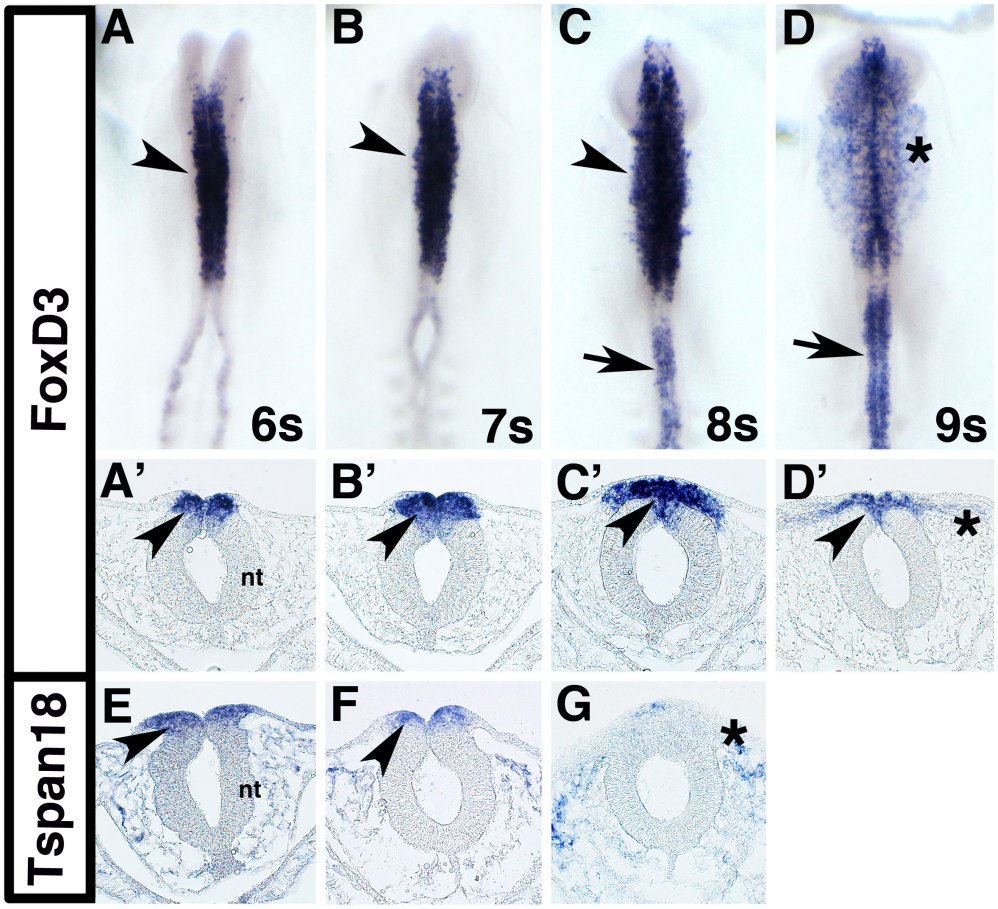
FoxD3
Tspan18
A
B
C
D
6s
7s
8s
9s
A'
B'
C'
D'
nt
E
F
G
nt

**Fig. 3-1. *FoxD3* and *Tspan18* expression domains overlap in premigratory cranial neural crest cells.**

Whole mount and transverse sections of chick embryos processed by *in situ* hybridization for *FoxD3* (A-D) and *Tspan18* (E-G) at 6 somites (s; A,A',E), 7s (B,B',F), 8s (C,C',G) and 9s (D,D'). (A,B) *FoxD3* was expressed in premigratory cranial neural crest cells at 6 and 7s (arrowheads, transverse sections in A',B'). (C) At 8s, FoxD3 expression persisted in early emigrating neural crest cells (arrowhead, transverse section in C') and extended into the trunk (arrow). (D) At 9s, *FoxD3* expression was reduced in migrating cranial neural crest cells (asterisks in D,D'), but retained in the dorsal neural tube (arrowhead in D') and in the trunk (arrow). (E-F) *Tspan18* was expressed in premigratory cranial neural crest cells at 6 and 7s (arrowheads). (G) *Tspan18* was downregulated at 8s (asterisk), when neural crest cells begin migrating. nt, neural tube.

**In the absence of FoxD3, *Tspan18* mRNA downregulation is delayed**

We previously reported that *Tspan18* mRNA fails to downregulate when FoxD3 is knocked down (Fairchild and Gammill, 2013). To determine the persistence and dynamics of this effect, we evaluated *Tspan18* expression over time in embryos electroporated with a FITC-tagged FoxD3 translation-blocking antisense morpholino oligonucleotide (FoxD3MO; (Kos et al., 2001)). FITC-tagged standard control MO (ContMO) or FoxD3MO was electroporated unilaterally into presumptive chick neural crest cells at stage HH4+, and resulting embryos at 8-9 or 10+ somites were processed by *in situ* hybridization to visualize *Tspan18* mRNA expression in whole mount or transverse sections. *Tspan18* mRNA was absent in the dorsal neural tube of embryos with 8 or more somites that had been electroporated with ContMO (Fig. 3-2A,A",B,B"; arrows), as expected (Fig. 3-1; (Fairchild and Gammill, 2013)). In contrast, at 8-9 somites, *Tspan18* mRNA persisted on the targeted side of the dorsal neural tube in embryos electroporated with FoxD3MO (Fig. 3-2C,C",E; arrowheads). However, by 10 somites, *Tspan18* transcripts were no longer visible in the dorsal neural tube of FoxD3MO-electroporated embryos (Fig. 3-2D,D"). These results suggest that FoxD3 is required for prompt, initial downregulation of *Tspan18* mRNA, but it is not the only factor regulating *Tspan18* mRNA expression.

One obvious candidate to contribute to *Tspan18* downregulation is the neural crest transcription factor, Snail2. Tspan18 antagonizes EMT by maintaining Cad6B protein (Fairchild and Gammill, 2013), and *Cad6B* is directly repressed by Snail2 (Taneyhill et al., 2007). Thus, we reasoned that *Tspan18* may also be regulated by Snail2. To determine if Snail2 directly regulates *Tspan18* in cranial neural crest cells, we

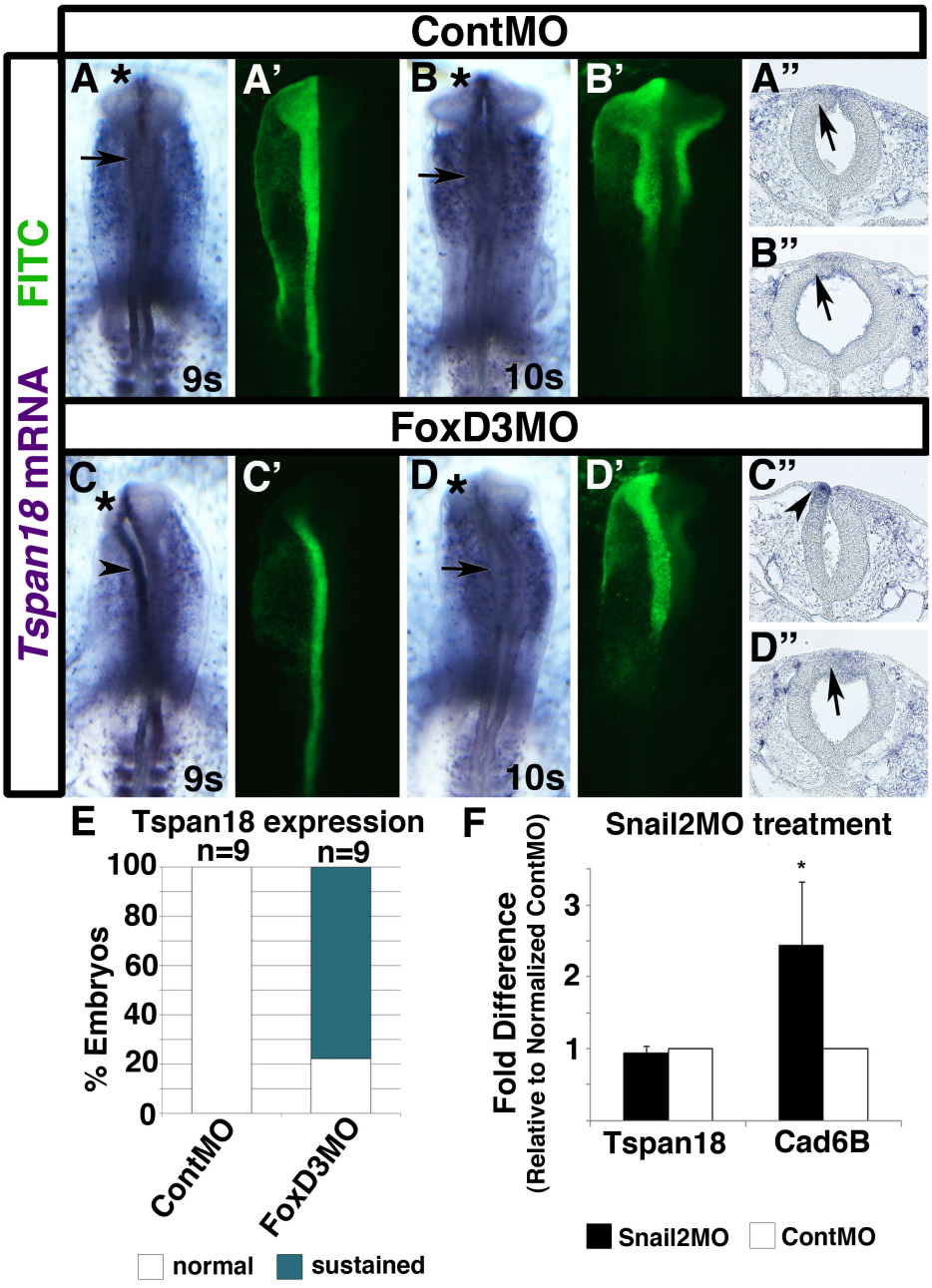
ContMO
FoxD3MO
Tspan18 mRNA
FITC
A *
A'
A''
B *
B'
B''
C *
C'
C''
D *
D'
D''
9s
10s
9s
10s
E
Tspan18 expression
n=9
n=9
100
80
60
40
20
0
% Embryos
ContMO
FoxD3MO
normal
sustained
F
Snail2MO treatment
Fold Difference
(Relative to Normalized ContMO)
3
2
1
*
Tspan18
Cad6B
Snail2MO
ContMO

**Fig. 3-2. *Tspan18* downregulation is delayed in the absence of FoxD3.**

Whole mount images (A-D, A'-D') and transverse sections (A"-D") of embryos unilaterally electroporated with ContMO (A,B) or FoxD3MO (C,D) after processing by *in situ* hybridization for *Tspan18*. At 9 somites (s; A) and 10s (B), *Tpsan18* mRNA is absent (arrows) on the targeted (asterisks; green in A',B') and untargeted sides of the dorsal neural tube in representative ContMO-electroporated embryos (A,B) and transverse sections (A",B"). At 9s, *Tspan18* expression is retained (arrowhead) on the FoxD3MO-targeted side of the neural tube (asterisk; C', green) in embryos (C) and transverse sections (C"). At 10s, *Tspan18* mRNA expression is downregulated (arrow), even on the FoxD3MO-targeted side (asterisk; F', green) of the neural tube in embryos (D) and transverse sections (D"). (E) Bar graph representing the frequency of 8-9s embryos exhibiting sustained *Tspan18* expression. (F) Quantification of *Tspan18* mRNA levels following MO-mediated depletion of Snail2. *Cad6B* levels were analyzed as a positive control (Taneyhill et al., 2007). Results are reported as fold difference relative to that obtained with ContMO normalized to 1. Means and standard errors of fold differences were generated from 3 independent experimental cDNA replicates. Asterisks (*) located above values denote a significant difference in the fold change between Snail2MO and ContMO levels ($p < 0.05$). Black bars, Snail2 MO; white bars, ContMO.

electroporated 5 to 6 somite embryos with either ContMO or Snail2MO, excised MO-targeted neural folds after 30 min, and quantified *Cad6B* (as a positive control) and *Tspan18* mRNA levels by QPCR. As expected, *Cad6B* mRNA levels were significantly increased in Snail2MO-electroporated embryos as compared to ContMO-electroporated embryos (Fig. 3-2F; approximately 2.5-fold increase, $p<0.05$, as previously described; (Taneyhill et al., 2007)), suggesting that Snail2MO was effective and efficiently reduced Snail2 protein levels. In contrast, *Tspan18* mRNA levels were similar in both Snail2MO- and ContMO-electroporated embryos (Fig. 3-2F). Thus, Snail2 is not one of the additional transcription factors that regulates *Tspan18* expression. The identity of these additional factors awaits further analysis.

**FoxD3 promotes cranial neural crest survival**

Because FoxD3 is required for neural crest cell survival (Stewart et al., 2006; Wang et al., 2011), we next determined whether FoxD3 knockdown altered cell death in chick cranial neural crest cells. To visualize dying cells, we immunostained FoxD3MO-electroporated embryos for the activated, cleaved form of the apoptotic enzyme caspase-3 (casp3) and counted the number of casp3-positive cells in the dorsal neural tube. While we electroporated FoxD3 MO at 1.0 mM previously (Fairchild and Gammill, 2013), cells electroporated with FoxD3MO at 1.0 mM were strongly and non-specifically apoptotic (C. Fairchild, unpublished). Electroporation of 0.5 mM FoxD3MO greatly mitigated this response. In 0.5 mM FoxD3MO-electroporated embryos, there were significantly more casp3 positive neural crest cells on the targeted side compared to the untargeted side of the dorsal neural tube (Fig. 3-3B,B',C; $p=0.003$). However, the incidence of casp3-

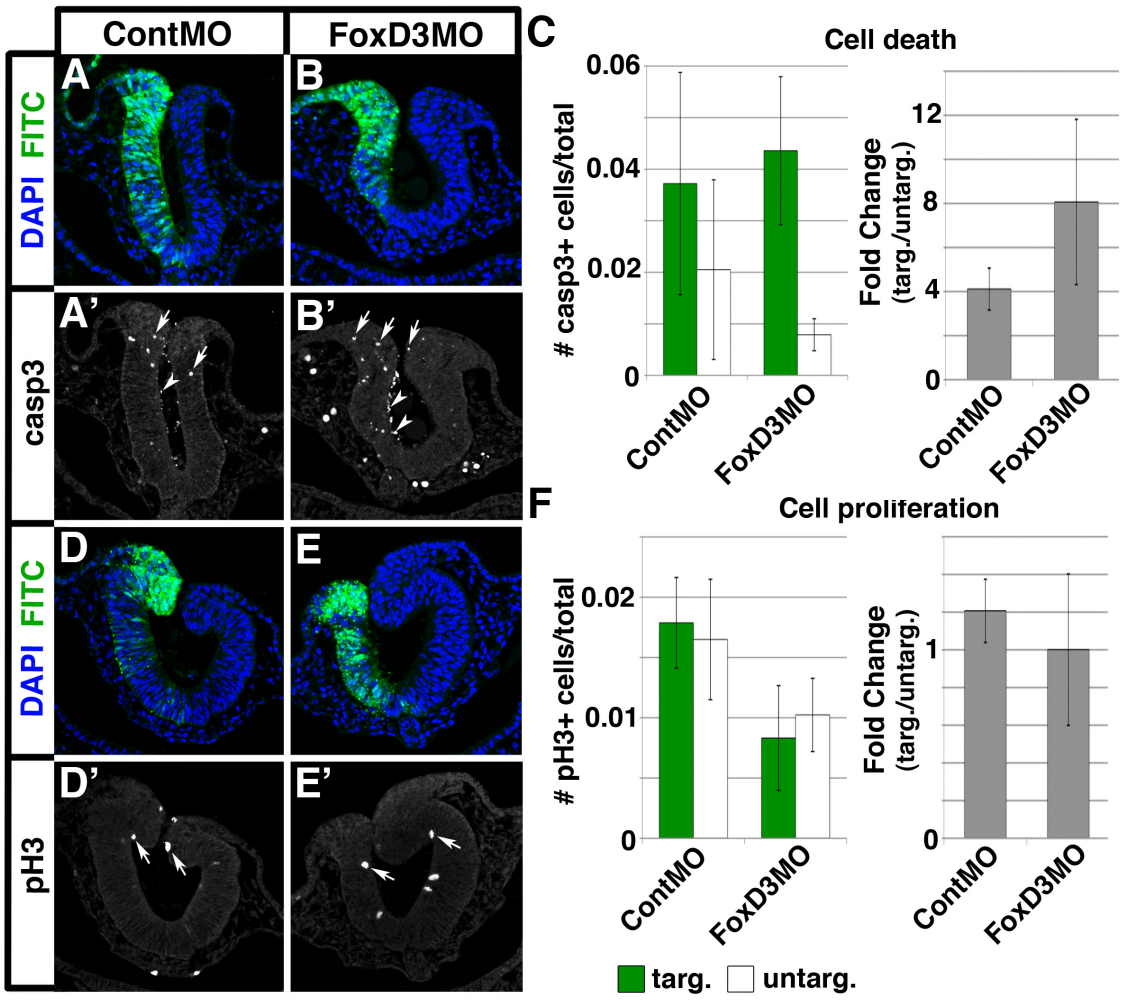
ContMO
FoxD3MO
DAPI FITC
casp3
pH3
A
B
A'
B'
D
E
D'
E'
C
Cell death
# casp3+ cells/total
0.06
0.04
0.02
0
Fold Change
(targ./untarg.)
12
8
4
0
ContMO
FoxD3MO
F
Cell proliferation
# pH3+ cells/total
0.02
0.01
1
targ.
untarg.

**Fig. 3-3. Cell survival, but not cell proliferation, is affected by FoxD3 knockdown.** Quantification of cell death (A-C) and proliferation (D-F) in embryos unilaterally electroporated with ContMO (A,D) or FoxD3MO (B,E). (A,B) Immunostaining for cleaved caspase-3 (casp3) reveals that there are more dying cells (arrows) on the targeted side of the neural tube (green) in FoxD3MO-electroporated embryos (B) as compared to the targeted side of control embryos (A). Casp3-positive cells were present in the lumen of the neural tube (arrowheads) under both conditions and were thus not counted during quantification. (C) Bar graphs representing the total number and the fold change of dying cells in electroporated embryos. (D,E) Immunostaining for phospho-histone H3 (pH3) reveals that there is an equal frequency of proliferating cells (arrows) on the targeted (green) and untargeted sides of the neural tube in embryos electroporated with either ContMO (D) or FoxD3MO (E). (F) Bar graphs representing the total number and the fold change of proliferating cells in electroporated embryos.

positive cells on the targeted side of ContMO- and FoxD3MO-electroporated embryos was similar (Fig. 3-3C), the actual number of dying cells was small (Fig. 3-3B'), and the fold change of the targeted compared to untargeted side of the neural tube was not significantly different between ContMO and FoxD3MO electroporated embryos (Fig. 3-3C), suggesting reduced cell survival is not a major contributor to the FoxD3 knock down phenotype. To ensure there was no reciprocal effect on proliferation, we immunostained for phospho-histone H3 and found that loss of FoxD3 did not alter the number of proliferating cells (Fig. 3-3D-F). Therefore, while FoxD3 knock down does lead to a low level of cell death, consistent with results in zebrafish (Stewart et al., 2006; Wang et al., 2011), the resulting decrease in neural crest cell number as well as the small number of cells affected cannot explain the maintenance of *Tspan18* mRNA expression throughout the neural fold (Fig. 3-2). This leads us to conclude that FoxD3's role in cell survival is independent of its role in regulating *Tspan18* mRNA expression.

**FoxD3 is required for premigratory *Sox10* expression and neural crest migration**

FoxD3 knockdown leads to transiently sustained *Tspan18* mRNA expression (Fig. 2). Our previous report concluded that downregulation of Tspan18 is a requirement for neural crest cells to migrate (Fairchild and Gammill, 2013). Thus, FoxD3MO electroporated cells would not be expected to migrate. To interpret the effects of FoxD3 knockdown in the context of early neural crest development, we electroporated stage HH4+ embryos with ContMO or FoxD3MO and visualized neural crest specification and migration by *in situ* hybridization for the key neural crest transcription factor and FoxD3-responsive gene *Sox10* (Prasad et al., 2012). *Sox10* mRNA expression levels were

unaffected at 6-7 somites in ContMO electroporated embryos (Fig. 3-4A,A"; arrow). However, *Sox10* mRNA expression was severely reduced on the targeted side of the neural tube in embryos electroporated with FoxD3MO (Fig. 3-4C,C",E; arrowhead), suggesting that FoxD3 knockdown prevents cranial neural crest specification in chick embryos. This is consistent with analyses of mutant mouse and zebrafish embryos, which show that FoxD3 is required for early neural crest specification and precursor maintenance (Hochgreb-Hagele and Bronner, 2013; Montero-Balaguer et al., 2006; Stewart et al., 2006; Teng et al., 2008; Wang et al., 2011). Furthermore, the FoxD3-deficient *Sox10*-positive neural crest cells that did form failed to migrate. While ContMO-targeted and untargeted *Sox10*-positive neural crest cells migrated an equivalent distance away from the neural tube at 9-10 somites (Fig. 3-4B,B"; arrows), FoxD3MO-electroporated neural crest cell migration distance was severely reduced relative to the untargeted side in the majority of embryos (Fig. 3-4D,D",F; arrowhead). These results indicate that FoxD3 is required for chick cranial neural crest formation (specification and survival) and subsequent migration.

**FoxD3 regulates cranial neural crest migration through its effects on *Tspan18***

Given that expression of Tspan18 is incompatible with migration (Fairchild and Gammill, 2013), it is possible that cranial neural crest cells fail to migrate in FoxD3 knockdown embryos (Fig. 3-4) because they retain *Tspan18* expression (Fig. 3-2; (Fairchild and Gammill, 2013)). If this were true, we reasoned that knockdown of Tspan18 should rescue the FoxD3 loss-of-function migration phenotype. To investigate this possibility, we co-electroporated embryos with FoxD3MO and either ContMO or

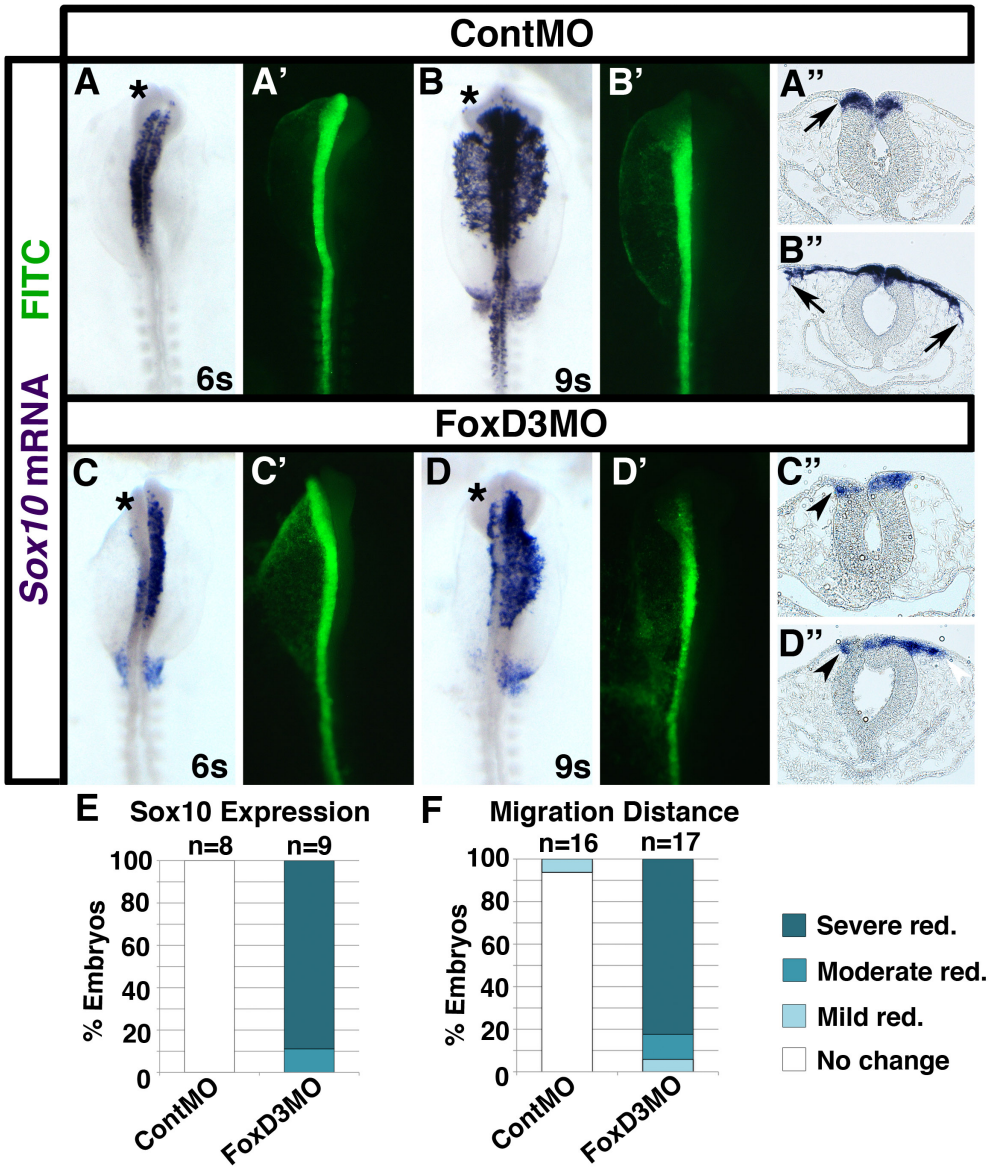
ContMO
FoxD3MO
Sox10 mRNA
FITC
A
A'
A''
B
B'
B''
C
C'
C''
D
D'
D''
6s
9s
E
Sox10 Expression
n=8
n=9
% Embryos
100
80
60
40
20
0
ContMO
FoxD3MO
F
Migration Distance
n=16
n=17
Severe red.
Moderate red.
Mild red.
No change

**Fig. 3-4. Chick FoxD3 is required for premigratory *Sox10* expression and neural crest migration.**

Whole mount images (A-D, A'-D') and transverse sections (A"-D") of embryos unilaterally electroporated with ContMO (A,B) or FoxD3MO (C,D) and processed by *in situ* hybridization for *Sox10*. In ContMO-electroporated embryos, *Sox10* expression (A,A") and the distance that *Sox10*-positive neural crest cells migrated (B,B") was even on targeted (asterisks; A',B', green) and untargeted sides of the neural tube. In contrast, *Sox10* expression was impaired (C,C") and migration distance was reduced (D,D") on the targeted side (asterisks; C',D', green) compared to the untargeted side of the neural tube of FoxD3MO-electroporated embryos. (E,F) Bar graphs representing the frequency of electroporated embryos exhibiting reduced premigratory *Sox10* expression (E) or reduced migration distance (F).

TS18MO, processed the resulting embryos by *in situ* hybridization for *Sox10* and measured the distance *Sox10*-positive neural crest cells had migrated away from the neural tube. Similar to embryos electroporated with FoxD3MO alone (Fig. 3-4D), in embryos co-electroporated with FoxD3MO and ContMO, neural crest migration distance was severely reduced on the targeted side of the neural tube in 7/9 (Fig. 3-5A,F) and moderately reduced in 2/9 (Fig.3-5D,F). Strikingly, in embryos co-electroporated with FoxD3MO and TS18MO, only 2/10 exhibited severe migration defects (Fig.3-5B,F), 4/10 were moderately reduced (Fig. 3-5C,F), and neural crest migration in 4/10 embryos was only mildly affected (Fig. 3-5E,F). Thus, knockdown of Tspan18 partially rescues the FoxD3 loss-of-function migration phenotype. Importantly, although co-electroporation of FoxD3MO and TS18MO largely rescued the failure to migrate, there were fewer *Sox10*-positive neural crest cells migrating away from the neural tube (see, for example Fig. 3-5E"; arrow). Therefore, Tspan18 knockdown does not rescue FoxD3-dependent features of neural crest formation (specification/cell survival). In sum, these results reveal that FoxD3 regulates cranial neural crest migration through its effects on *Tspan18* expression. Given that Tspan18 antagonizes EMT by maintaining Cad6B protein (Fairchild and Gammill, 2013), this suggests that FoxD3 is required to elicit Tspan18 downregulation and promote EMT for cranial neural crest migration. That Tspan18 knock down fails to rescue FoxD3-dependent cranial neural crest formation indicates that FoxD3 impacts target gene expression in addition to *Tspan18*, and that FoxD3 independently regulates cranial neural crest formation and migration.

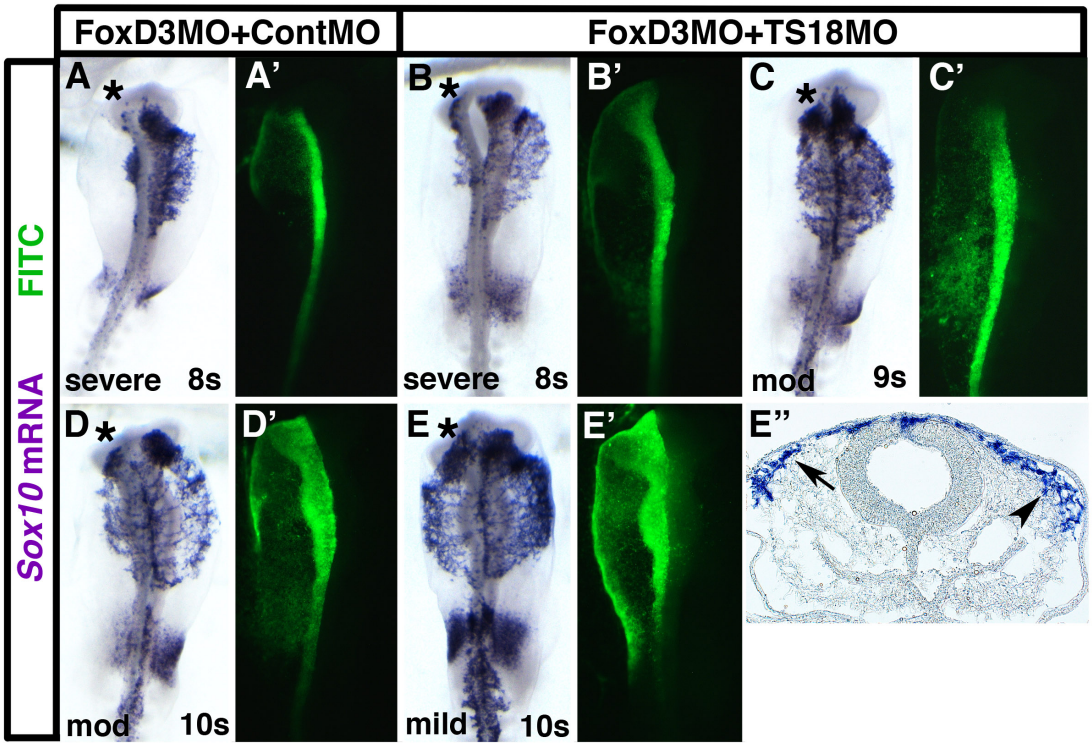
FoxD3MO+ContMO
FoxD3MO+TS18MO
FITC
Sox10 mRNA
A
A'
B
B'
C
C'
severe 8s
severe 8s
mod 9s
D
D'
E
E'
E''
mod 10s
mild 10s

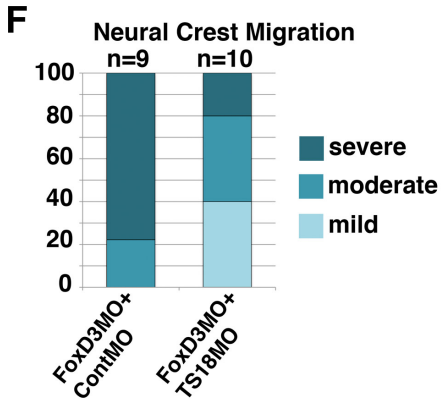
F
Neural Crest Migration
n=9
n=10
100
80
60
40
20
0
severe
moderate
mild
FoxD3MO+ ContMO
FoxD3MO+ TS18MO

**Fig. 5. Co-electroporation with TS18MO partially rescues the FoxD3 loss-of-function migration defect.**

Whole mount images and transverse sections of embryos unilaterally co-electroporated with FoxD3MO and either ContMO (A,D) or TS18MO (B,C,E) after processing by *in situ* hybridization for *Sox10*. (A-E) Following co-electroporation with FoxD3MO and ContMO, the distance of *Sox10*-positive cells migrated on the targeted side of the neural tube (asterisks; green in A'-E') is severely inhibited (A) in nearly all embryos with only a few moderately affected (D). Following co-electroporation with FoxD3 and TS18MO, the incidence of severely affected (B) embryos is greatly reduced and most embryos are moderately (C) or only mildly affected (E). (E") A transverse section of the mildly affected embryo in (E) reveals that while co-electroporation with FoxD3MO and TS18MO partially rescued migration distance, the size of the *Sox10*-positive migratory neural crest population is reduced (arrow) on the targeted side of the embryo, as compared to the untargeted side of the embryo (arrowhead). (F) Bar graph representing the frequency of electroporated embryos that exhibit a severe, moderate, or mild reduction in migration distance.

## 3.4 Discussion:

In this study, we have investigated the regulatory relationship between FoxD3 and Tspan18 and, in so doing, gained insight into the poorly understood role of FoxD3 in neural crest migration. From our FoxD3 knockdown experiments, we conclude that FoxD3 supports chick cranial neural crest specification, survival and migration, and specifically report that FoxD3 is required for initial downregulation of *Tspan18* mRNA expression. Strikingly, we reveal that the FoxD3 loss-of-function migration defects can be rescued by simultaneous knockdown of Tspan18, although neural crest formation is still defective. Together these data reveal separable requirements for FoxD3 during cranial neural crest formation and migration, and show that FoxD3 promotes EMT and migration through negative regulation of *Tspan18* expression.

### FoxD3 is required for initial *Tspan18* downregulation, though other factors contribute at later stages

Tspan18 is incompatible with migration (Fairchild and Gammill, 2013), and as such, *Tspan18* mRNA is absent later than 7 somites (Fig. 3-1). However, in embryos electroporated with FoxD3MO, *Tspan18* transcripts are still visible at 9 somites (Fig. 3-2C), indicating that FoxD3 is required for the initial downregulation of *Tspan18*. We have, to date, been unable to determine whether this is the consequence of FoxD3 directly binding to and repressing transcription from the *Tspan18* promoter. Experiments to address this crucial question will be the subject of future investigation.

Our results highlight the complexity of *Tspan18* transcriptional regulation. Notably, even in embryos that have been electroporated with FoxD3MO, *Tspan18*

mRNA is eventually downregulated (Fig. 3-2D). This finding suggests that FoxD3 is not the only factor that negatively regulates *Tspan18* mRNA expression. The identity of these additional factors is unclear, though Snail2 does not appear to contribute (Fig. 3-2F). Regulatory complexity is further suggested by continuous co-expression of *FoxD3* and *Tspan18* in premigratory neural crest cells (Fig. 3-1). This delayed action of a neural crest transcription factor is not unprecedented: Snail2, which represses *Cad6B* transcription to promote EMT, is co-expressed with Cad6B throughout premigratory neural crest development and modulated through altered rates of degradation (Taneyhill et al., 2007; Vernon and LaBonne, 2006). FoxD3 activity could also be post-translationally regulated, as is Sox10 (Taylor and Labonne, 2005). Alternatively, FoxD3 could require and/or affect the activity of a co-factor, for which there is also precedent. In the trunk neural crest, FoxD3 regulates the expression of the melanocyte marker *MITF*, but not through direct binding to the *MITF* promoter; instead FoxD3 binds to the transcriptional activator Pax3 and prevents Pax3 from binding to the *MITF* promoter (Thomas and Erickson, 2009). Identifying FoxD3-interactors would provide a better understanding of its regulation of *Tspan18* mRNA expression.

**FoxD3 promotes *Tspan18* downregulation to drive cranial neural crest EMT independent of its role in specification and survival**

The ability of Tspan18 to rescue FoxD3-dependent migration (Fig. 3-5) allowed us to separate the requirement for FoxD3 during formation and migration. Consistent with previous studies in *Xenopus*, zebrafish and mouse embryos (Hochgreb-Hagele and Bronner, 2013; Lister et al., 2006; Montero-Balaguer et al., 2006; Mundell and Labosky,

2011; Sasai et al., 2001; Stewart et al., 2006), FoxD3 knockdown in chick embryos inhibited neural crest specification (Fig. 3-4C) and survival (Fig. 3-3A-C). As a result, it was unclear whether FoxD3 knockdown affected migration (Fig. 3-4D) directly, or as a secondary consequence of these defects. This is a caveat of any sustained loss-of-function experiment: the inability to determine the dependence of late defects on early phenotypes. Although electroporation of older chick embryos in which neural crest specification has already occurred can circumvent this issue, late electroporation of a MO does not always elicit knockdown, because stable proteins do not turnover rapidly enough to allow the effects of inhibited translation to be revealed. Instead, we note that co-electroporation of TS18MO with FoxD3MO rescues migration distance despite the fact that the migratory population is reduced (see for example Fig. 3-5E"). This suggests that although fewer neural crest cells are specified and survive as a result of FoxD3 knockdown (in other words, specification/survival is not rescued), those that form are able to migrate as long as Tspan18 is absent. This indicates that FoxD3 regulates neural crest EMT/migration through downregulation of *Tspan18* and, because neural crest formation is still defective, provides the first evidence that FoxD3 plays independent roles in neural crest specification and migration.

As FoxD3 has been reported to both positively and negatively regulate neural crest migration, we propose that FoxD3 promotes EMT but is incompatible with motility. Our results in chick (Fig. 3-4) along with those in zebrafish (Stewart et al., 2006) indicate that FoxD3 is required for neural crest migration. However, expanded *FoxD3* expression in zebrafish cranial neural crest cells prevents migration (Drerup et al., 2009), and FoxD3 negatively regulates Rho-GTPase-induced cell motility in human metastatic melanoma

cells (Katiyar and Aplin, 2011). These contrary observations likely reflect temporal differences. FoxD3 knockdown sustains *Tspan18* expression (Fig. 3-2), which in turn maintains Cad6B protein levels that inhibit neural crest EMT (Coles et al., 2007; Fairchild and Gammill, 2013). Thus, at the start of neural crest migration, FoxD3 elicits *Tspan18* downregulation, which destabilizes Cad6B-dependent cell adhesions and promotes neural crest EMT. Later, in actively migrating neural crest cells, FoxD3 may disrupt Rho-based motility, as has been reported for melanoma cells (Katiyar and Aplin, 2011). This could explain why *FoxD3* expression declines after neural crest cells leave the neural tube (Fig. 3-1; (Khudyakov and Bronner-Fraser, 2009)).

While FoxD3 regulates cranial neural crest EMT through Tspan18, it must act through a different pathway in the trunk. Although Tspan18 is not detectable by in situ hybridization in trunk neural tube (Fairchild and Gammill, 2013), FoxD3 overexpression leads to altered expression of cell adhesion molecules (Cheung et al., 2005). Thus, FoxD3 must regulate the expression of other gene(s) that impact EMT. To understand the role of FoxD3 in neural crest migration, and specifically in EMT, it will be crucial to identify FoxD3 targets in the neural crest.

In conclusion, this report shows that FoxD3 is required for chick cranial neural crest migration because it promotes the downregulation of *Tspan18* and thus EMT. Moreover, this function of FoxD3 is independent of the requirement for FoxD3 during cranial neural crest specification and survival. Overall this study provides new insight into the dual role of FoxD3 for neural crest formation and migration, and also gives us a better understanding for how neural crest transcription factors impact the cellular behaviors that occur as neural crest cells undergo EMT and migrate.

## 3.5 Materials and Methods:

### Embryos

Fertile chicken embryos were incubated in a humidified incubator (G. Q. F. Manufacturing: Savannah, GA) at 37-38°C. Embryos were staged according to Hamburger and Hamilton (HH) (Hamburger and Hamilton, 1951) or by counting somite pairs.

### In situ hybridization

Whole mount in situ hybridization was performed as previously described (Wilkinson, 1992). Digoxigenin-labeled RNA probes were transcribed from the following templates: *FoxD3* (Kos et al., 2001), *Tspan18* (Gammill and Bronner-Fraser, 2002), and *Sox10* (Cheng et al., 2000). After processing, embryos were first imaged in whole mount using a Zeiss Discovery V8 stereoscope then infiltrated with 5% and 15% sucrose, embedded in gelatin, sectioned using a Leica CM1900 cryostat at 12-18 μm and imaged again using a Zeiss AxioImager A1. Images of whole mount embryos and transverse sections were taken with an AxioCam MRc5 digital camera and Axiovision software and assembled in Photoshop (Adobe).

### Morpholino design and electroporation

The following FITC-tagged, antisense morpholinos (MO) were designed and synthesized by GeneTools, LLC (Philomath, OR): FoxD3 translation blocking MO (FoxD3MO: 5'-CGCTGCCGCCGCCCGATAGAGTCAT-3'; (Kos et al., 2001)), Tspan18 translation blocking MO (TS18MO: 5'-TGCAGCTCAGACAGTCTCCCTCCAT-3'; (Fairchild and

Gammill, 2013)), and standard FITC control MO (ContMO: 5'-CCTCTTACCTCAGTTACAATTTATA-3'). For early embryo electroporations, morpholinos were unilaterally electroporated into the presumptive neural crest at HH stage $4^{+}$, as previously described (Gammill and Krull, 2011), at 500 μM (FoxD3 and ContMO) and 390 μM (TS18MO) with carrier DNA (0.2 μg/μL pCS2+MycTag DNA). After electroporation, embryos were re-incubated until the desired stages and fixed in 4% paraformaldehyde at room temperature for 1 hour then washed with PBS + 0.1% Tween. Targeting was verified by fluorescent microscopy for FITC before embryos were either immediately embedded and sectioned for immunofluorescence or dehydrated into methanol and stored at -20° for in situ hybridization.

**Quantitative polymerase chain reaction (QPCR)**

MO-mediated Snail2 depletion followed by QPCR was carried out as described (Taneyhill et al., 2007). Briefly, 6 somite embryos were electroporated in ovo with Snail2MO or ContMO and midbrain neural folds were excised after 30 minutes. Neural folds from six electroporated embryos were pooled and total RNA was isolated using the RNAqueous Total RNA Isolation Kit (Ambion-Life Technologies, Carlsbad, CA). cDNA was synthesized using random hexamers and the Superscript II RT-PCR system (Life technologies) according to the manufacturer's instructions. QPCR was performed using the ABI 7000 in a TaqMan or SYBR Green (Life Technologies) assay as described (Taneyhill and Bronner-Fraser, 2005). Briefly, 25 μl *Tspan18* QPCR reactions included 2X SYBR Green master mix, cDNA and 75 nM of each primer (Sense: 5′-GCTTGTTGCCAGCGAAAGCTCC-3′; Antisense: 5′-

TAGCAGCCCTGCCGGTTCTGA-3′). 18S QPCR reactions included 2x SYBR Green mastermix, cDNA and 150 nM each primer as previously described (Taneyhill and Bronner-Fraser, 2005). *Cad6B* QPCR reactions included TaqMan mastermix, cDNA, 150 nM of each primer, and 150 nM each Cad6B TaqMan probe, as described (Taneyhill et al., 2007). After normalization to a standard (chick 18S rRNA), fold upregulation or downregulation for each of three replicates was determined by dividing the relative expression value for the gene of interest in the presence of the Snail2MO by that obtained for the gene of interest in the presence of ContMO.

**Immunofluorescence and cell counting**

Immunofluorescence was performed using either anti-cleaved caspase3 (casp3, Cell Signaling; Danvers, MD: 1:200) or anti-phosho-histone H3 (pH3, Millipore; Billerica, MA: 1:250) primary antibody diluted into PBS + 0.1% Triton-X100 supplemented with 5% normal donkey serum followed by incubation with a donkey anti-rabbit secondary antibody at 1:250 (RRX conjugated; Jackson Labs, West Grove, PA). Slides were mounted in PermaFluor (Thermo Fisher Scientific; Waltham, MA) containing 1 μg/mL DAPI and imaged on a Zeiss LSM 710 laser scanning confocal microscope. Images were assembled in Photoshop (Adobe). Cell death and proliferation were quantitated by counting the number of casp3- or pH3-positive cells and dividing by the total number of cells in the dorsal quarter of the neural tube on the targeted and untargeted sides in at least 5 sections per embryo (n=3 embryos). Statistics were performed using the paired Student's *t* test in Excel (Microsoft).

**Assaying neural crest migration**

To consistently assay neural crest cell migration (Fig. 3-4), and thus clearly determine rescue (Fig. 3-5), we measured the distance neural crest cells migrated away from the untargeted side of the neural tube and compared that to the same measurement for the targeted side of the neural tube. We used this comparison to categorize phenotype severity. In severely affected embryos, neural crest cells on the targeted side had migrated 0-50 percent the distance of those on the untargeted side. In moderately affected embryos, neural crest cells on the targeted side had migrated 51-75 percent of the distance of those on the untargeted side. In mildly affected embryos, neural crest cells on the targeted side had migrated 76-95 percent of the distance of those on the untargeted side. Unaffected embryos displayed neural crest migration distances within 5 percent of each other on the targeted and untargeted sides of the neural tube.

**Acknowledgements**

We thank Yi-Chuan Cheng and Carol Erickson for the kind gift of plasmids. Many thanks to the members of the Gammill Lab for their input and support. This work was supported by the National Institutes of Health, award numbers F31 NRSA GM087951 (CLF), R00 HD055034 (LAT), and K22 DE015309 (LSG), as well as a University of Minnesota Grant-in-Aid.

**Author Contributions**

L.S.G and C.L.F conceived and designed the experiments. C.L.F. and J.P.C. performed the electroporation and in situ hybridization experiments. A.T.S. and L.A.T. performed and analyzed the QPCR experiments. L.S.G. and C.L.F. analyzed the data and wrote the paper.

# Chapter 4

## Conclusions, Future Directions and Significance

## 4.1 Summary:

Epithelial-to-mesenchymal transition (EMT) is the complex process during which adherent epithelial cells undergo drastic changes in cell polarity, cell-cell adhesion, and cytoskeletal arrangement to produce individual, invasive mesenchymal cells (Hay, 2005). EMT is involved in many of the intricate morphological events that occur during embryogenesis, including the formation of migratory neural crest cells (Thiery et al., 2009). Many of the cellular events that occur during neural crest EMT have been highly characterized and are generally conserved (Micalizzi et al., 2010; Nieto, 2011; Powell et al., 2013; Thiery et al., 2009). However some questions about how these cellular events are controlled remained unanswered. For example, neural crest cells remodel their cell adhesions by undergoing a cadherin switch, resulting in the disruption of epithelial cell adhesions in favor of more transient, mesenchymal cell adhesions (McKeown et al., 2013; Powell et al., 2013). But, how are neural crest cadherins transcriptionally and post-translationally regulated? Furthermore, the transcriptional outputs of neural crest gene regulatory network (GRN) transcription factors, and thus their impact on EMT, are not fully defined. Although we know that GRN transcription factors are required for the initial specification of neural crest cell fate (Betancur et al., 2010), are they independently required later, when neural crest cells be come migratory? What impact do they have on cellular behaviors like adhesion? This thesis has provided additional insight into some of these intriguing questions, and the main conclusions are outlined below.

## 4.2 Main conclusions and future directions:

### *Tspan18 post-translationally regulates cad6B protein and inhibits neural crest migration.*

In Chapter 2 I report that the transmembrane scaffolding protein Tetraspanin18 (Tspan18) post-translationally maintains the neural crest cell adhesion molecule cadherin-6B (Cad6B) and in turn prevents migration (Fairchild and Gammill, 2013). These results demonstrate that cranial neural crest migration requires the relief of Tspan18-dependent maintenance of Cad6B protein levels, in addition to the previously characterized transcriptional repression of *Cad6B* (Coles et al., 2007; Taneyhill et al., 2007). This is the first evidence for Cad6B post-translational regulation. The mechanism behind Tspan18's post-translational control of Cad6B protein levels is currently unknown. Identifying Tspan18 binding partners would greatly increase our understanding of this mechanism and would furthermore provide a new collection of genes to investigate for a more complete understanding of neural crest EMT. Such Tspan18 interaction studies are crucial future experiments and are currently underway.

Given that *Tspan18* mRNA expression in the neural crest is restricted to the cranial region (Fairchild and Gammill, 2013), the results of Chapter 2 have also provided additional insight into our knowledge of the distinct differences in cranial and trunk EMT. Morphologically speaking, the exit of cranial and trunk neural crest cells is very different (Theveneau and Mayor, 2012). Moreover, variations in cadherin expression and function in cranial versus trunk neural crest cells are striking molecular differences when comparing these two regions (McKeown et al., 2013). For example, Cad6B protein is present in migrating trunk neural crest cells and activates an intracellular signaling

cascade that actually promotes de-epithelialization (Park and Gumbiner, 2010; Park and Gumbiner, 2012). Meanwhile, Cad6B downregulation is required for cranial neural crest migration, and Cad6B protein is not detected in migrating cranial neural crest cells (Coles et al., 2007; Fairchild and Gammill, 2013). Proteolytic processing of neural crest cadherins by ADAM proteases affects intercellular signaling (Cavallaro and Dejana, 2011; McCusker et al., 2009; Shoval et al., 2007), and differences in ADAM-dependent processing of Cad6B may explain the specific function of Cad6B in cranial and trunk neural crest cells. Thus, it is intriguing to speculate whether Tspan18 may play an essential role in mediating cranial-specific Cad6B regulation, perhaps by modulating ADAM activity (see Appendix I), and subsequently cranial modes of migration. Continued investigation into this mechanism is essential.

In addition to regional variations in Cad6B, E-cad expression is also strikingly different in cranial and trunk regions (Dady et al., 2012). E-cad expression in the trunk is downregulated long before trunk neural crest migration commences (Dady et al., 2012). This is consistent with the extensive findings of many cancer EMT studies that suggest E-cad downregulation is crucial to promote cancer metastasis (Gheldof and Berx, 2013; Micalizzi et al., 2010). Interestingly, however, E-cad protein is clearly visible in premigratory cranial neural crest cells and persists after neural crest cells begin their migration (Dady et al., 2012). In Chapter 2 we suggest that Tspan18 specifically regulates Cad6B and found that E-cad protein levels were not affected by Tspan18 knockdown (Fairchild and Gammill, 2013). However, it is intriguing to ponder the presence of other tetraspanins that might similarly regulate E-cad. Identifying other tetraspanins present in cranial neural crest cells will help us understand if tetraspanin-mediated cadherin

regulation is a recurring theme of EMT, and may help elucidate the role of sustained E-cad protein in cranial neural crest cells.

***Tspan18 is downstream of the neural crest GRN transcription factor FoxD3.***

In Chapter 3, I report that downregulation of *Tspan18*, which is a prerequisite for migration (Fairchild and Gammill, 2013), requires the neural crest GRN transcription factor FoxD3. We show that FoxD3 knockdown sustains *Tspan18* mRNA expression and inhibits migration. FoxD3 chromatin immunoprecipitation (ChIP) experiments are crucial and currently underway, but we have not yet verified whether this regulatory relationship is direct. Moreover, our findings from Chapter 3 suggest that transcriptional downregulation of *Tspan18* requires more than FoxD3, since *Tspan18* expression is eventually downregulated, even when FoxD3 is absent. In depth promoter analysis studies of *Tspan18* would provide a more comprehensive understanding of *Tspan18* transcriptional regulation.

In addition to trasncriptional regulation, tetraspanin function is commonly regulated by post-translational mechanisms. For example, many tetraspanins are modified by the addition of the fatty acid palmitate via a process called palmitoylation (Baekkeskov and Kanaani, 2009; Fukata and Fukata, 2010; Levy and Shoham, 2005). Palmitoylation of tetraspanins, and their binding partners, impacts cellular localization and facilitates protein-protein interactions (Levy and Shoham, 2005). Thus it is important to evaluate whether Tspan18 is palmitoylated, and if it is, to determine whether such post-translational modification is essential for it's function in cranial neural crest cells. These experiments would provide a more comprehensive understanding of how Tspan18 itself is regulated during neural crest EMT.

Although neural crest GRN transcription factors have been implicated in both neural crest specification and migration (Betancur et al., 2010; Prasad et al., 2012), distinguishing a separable role for GRN members at these distinct developmental time points has proven difficult. Our findings in Chapter 3 provide evidence that FoxD3 independently regulates neural crest formation and migration. I report that Tspan18 knockdown rescues the FoxD3 loss-of-function migration defect, but does not rescue the FoxD3-dependent decrease in neural crest cell number. This indicates that FoxD3 regulates migration through its effects on Tspan18, independent of its role in neural crest specification and survival. In the trunk, FoxD3 overexpression causes changes in cell adhesion (Cheung et al., 2005), but the significance of this effect had not been investigated. Our results show that, in cranial neural crest cells, FoxD3 regulates *Tspan18,* which affects cell adhesion and in turn regulates EMT and cell migration. Thus, Chapter 3 provides new evidence for how neural crest GRN transcription factors impact the cellular events leading up to migration. FoxD3 ChIP-seq experiments would allow us to define a complete array of FoxD3 targets and would also allow us to test, in an un-biased manner, whether *Tspan18* is a direct target of FoxD3.

## 4.3 Significance:

The results I have presented in this thesis give us a better understanding of how cell-cell adhesions are dynamically regulated during EMT. Identifying Tspan18 binding partners will likely provide novel membrane-associated factors for investigating neural crest cell motility, polarity or invasiveness, and will thus help define the complex cellular events that occur during EMT. Additionally, characterizing the molecular players involved in this process in neural crest cells will help us understand cancer progression, since many of the cellular events that occur during neural crest EMT are similar to cellular changes characteristic of metastasis. More generally, this study provides new insight into how tetraspanins impact cell adhesions and EMT. An extensive number of recent studies are beginning to emphasize the vital role tetraspanins play in both suppressing and promoting cancer metastasis. Thus, understanding the mechanisms behind their action may help to identify novel targets for developing new cancer therapies.

## References


**Abe, M., Sugiura, T., Takahashi, M., Ishii, K., Shimoda, M. and Shirasuna, K.** (2008). A novel function of CD82/KAI-1 on E-cadherin-mediated homophilic cellular adhesion of cancer cells. *Cancer Lett* **266**, 163-70.

**Adams, M. S., Gammill, L. S. and Bronner-Fraser, M.** (2008). Discovery of transcription factors and other candidate regulators of neural crest development. *Dev Dyn* **237**, 1021-33.

**Ahlstrom, J. D. and Erickson, C. A.** (2009). The neural crest epithelial-mesenchymal transition in 4D: a 'tail' of multiple non-obligatory cellular mechanisms. *Development* **136**, 1801-12.

**Akitaya, T. and Bronner-Fraser, M.** (1992). Expression of cell adhesion molecules during initiation and cessation of neural crest cell migration. *Dev Dyn* **194**, 12-20.

**Alfandari, D., Cousin, H., Gaultier, A., Hoffstrom, B. G. and DeSimone, D. W.** (2003). Integrin alpha5beta1 supports the migration of Xenopus cranial neural crest on fibronectin. *Dev Biol* **260**, 449-64.

**Alfandari, D., Cousin, H., Gaultier, A., Smith, K., White, J. M., Darribere, T. and DeSimone, D. W.** (2001). Xenopus ADAM 13 is a metalloprotease required for cranial neural crest-cell migration. *Curr Biol* **11**, 918-30.

**Aoki, Y., Saint-Germain, N., Gyda, M., Magner-Fink, E., Lee, Y. H., Credidio, C. and Saint-Jeannet, J. P.** (2003). Sox10 regulates the development of neural crest-derived melanocytes in Xenopus. *Dev Biol* **259**, 19-33.

**Baekkeskov, S. and Kanaani, J.** (2009). Palmitoylation cycles and regulation of protein function (Review). *Mol Membr Biol* **26**, 42-54.

**Basch, M. L., Bronner-Fraser, M. and Garcia-Castro, M. I.** (2006). Specification of the neural crest occurs during gastrulation and requires Pax7. *Nature* **441**, 218-22.

**Bass, R., Werner, F., Odintsova, E., Sugiura, T., Berditchevski, F. and Ellis, V.** (2005). Regulation of urokinase receptor proteolytic function by the tetraspanin CD82. *J Biol Chem* **280**, 14811-8.

**Berditchevski, F.** (2001). Complexes of tetraspanins with integrins: more than meets the eye. *J Cell Sci* **114**, 4143-51.

**Berndt, J. D., Clay, M. R., Langenberg, T. and Halloran, M. C.** (2008). Rho-kinase and myosin II affect dynamic neural crest cell behaviors during epithelial to mesenchymal transition in vivo. *Dev Biol* **324**, 236-44.

**Betancur, P., Bronner-Fraser, M. and Sauka-Spengler, T.** (2010). Assembling neural crest regulatory circuits into a gene regulatory network. *Annu Rev Cell Dev Biol* **26**, 581-603.

**Blobel, C. P.** (2005). ADAMs: key components in EGFR signalling and development. *Nat Rev Mol Cell Biol* **6**, 32-43.

**Borchers, A., David, R. and Wedlich, D.** (2001). Xenopus cadherin-11 restrains cranial neural crest migration and influences neural crest specification. *Development* **128**, 3049-60.

**Bronner-Fraser, M. and Fraser, S. E.** (1988). Cell lineage analysis reveals multipotency of some avian neural crest cells. *Nature* **335**, 161-4.

**Carmona-Fontaine, C., Matthews, H. K., Kuriyama, S., Moreno, M., Dunn, G. A., Parsons, M., Stern, C. D. and Mayor, R.** (2008). Contact inhibition of locomotion in vivo controls neural crest directional migration. *Nature* **456**, 957-61.

**Carmona-Fontaine, C., Theveneau, E., Tzekou, A., Tada, M., Woods, M., Page, K. M., Parsons, M., Lambris, J. D. and Mayor, R.** (2011). Complement fragment C3a controls mutual cell attraction during collective cell migration. *Dev Cell* **21**, 1026-37.

**Cavallaro, U. and Dejana, E.** (2011). Adhesion molecule signalling: not always a sticky business. *Nat Rev Mol Cell Biol* **12**, 189-97.

**Chairoungdua, A., Smith, D. L., Pochard, P., Hull, M. and Caplan, M. J.** (2010). Exosome release of beta-catenin: a novel mechanism that antagonizes Wnt signaling. *J Cell Biol* **190**, 1079-91.

**Chapman, S. C., Collignon, J., Schoenwolf, G. C. and Lumsden, A.** (2001). Improved method for chick whole-embryo culture using a filter paper carrier. *Dev Dyn* **220**, 284-9.

**Chattopadhyay, N., Wang, Z., Ashman, L. K., Brady-Kalnay, S. M. and Kreidberg, J. A.** (2003). alpha3beta1 integrin-CD151, a component of the cadherin-catenin complex, regulates PTPmu expression and cell-cell adhesion. *J Cell Biol* **163**, 1351-62.

**Cheng, Y., Cheung, M., Abu-Elmagd, M. M., Orme, A. and Scotting, P. J.** (2000). Chick sox10, a transcription factor expressed in both early neural crest cells and central nervous system. *Brain Res Dev Brain Res* **121**, 233-41.

**Cheung, M., Chaboissier, M. C., Mynett, A., Hirst, E., Schedl, A. and Briscoe, J.** (2005). The transcriptional control of trunk neural crest induction, survival, and delamination. *Dev Cell* **8**, 179-92.

**Chizhikov, V. V. and Millen, K. J.** (2004). Control of roof plate formation by Lmx1a in the developing spinal cord. *Development* **131**, 2693-705.

**Chu, Y. S., Eder, O., Thomas, W. A., Simcha, I., Pincet, F., Ben-Ze'ev, A., Perez, E., Thiery, J. P. and Dufour, S.** (2006). Prototypical type I E-cadherin and type II cadherin-7 mediate very distinct adhesiveness through their extracellular domains. *J Biol Chem* **281**, 2901-10.

**Coles, E. G., Taneyhill, L. A. and Bronner-Fraser, M.** (2007). A critical role for Cadherin6B in regulating avian neural crest emigration. *Dev Biol* **312**, 533-44.

**Creuzet, S., Couly, G. and Le Douarin, N. M.** (2005). Patterning the neural crest derivatives during development of the vertebrate head: insights from avian studies. *J Anat* **207**, 447-59.

**Dady, A., Blavet, C. and Duband, J. L.** (2012). Timing and kinetics of E- to N-cadherin switch during neurulation in the avian embryo. *Dev Dyn*.

**Deardorff, M. A., Tan, C., Saint-Jeannet, J. P. and Klein, P. S.** (2001). A role for frizzled 3 in neural crest development. *Development* **128**, 3655-63.

**Detrick, R. J., Dickey, D. and Kintner, C. R.** (1990). The effects of N-cadherin misexpression on morphogenesis in Xenopus embryos. *Neuron* **4**, 493-506.

**Dickinson, M. E., Selleck, M. A., McMahon, A. P. and Bronner-Fraser, M.** (1995). Dorsalization of the neural tube by the non-neural ectoderm. *Development* **121**, 2099-106.

**Dorey, K. and Amaya, E.** (2010). FGF signalling: diverse roles during early vertebrate embryogenesis. *Development* **137**, 3731-42.

**Dottori, M., Gross, M. K., Labosky, P. and Goulding, M.** (2001). The winged-helix transcription factor Foxd3 suppresses interneuron differentiation and promotes neural crest cell fate. *Development* **128**, 4127-38.

**Drerup, C. M., Wiora, H. M., Topczewski, J. and Morris, J. A.** (2009). Disc1 regulates foxd3 and sox10 expression, affecting neural crest migration and differentiation. *Development* **136**, 2623-32.

**Duband, J. L.** (2006). Neural crest delamination and migration: integrating regulations of cell interactions, locomotion, survival and fate. *Adv Exp Med Biol* **589**, 45-77.

**Duband, J. L., Volberg, T., Sabanay, I., Thiery, J. P. and Geiger, B.** (1988). Spatial and temporal distribution of the adherens-junction-associated adhesion molecule A-CAM during avian embryogenesis. *Development* **103**, 325-44.

**Dufour, S., Beauvais-Jouneau, A., Delouvee, A. and Thiery, J. P.** (1999). Differential function of N-cadherin and cadherin-7 in the control of embryonic cell motility. *J Cell Biol* **146**, 501-16.

**Duong, T. D. and Erickson, C. A.** (2004). MMP-2 plays an essential role in producing epithelial-mesenchymal transformations in the avian embryo. *Dev Dyn* **229**, 42-53.

**Edwards, D. R., Handsley, M. M. and Pennington, C. J.** (2008). The ADAM metalloproteinases. *Mol Aspects Med* **29**, 258-89.

**Erickson, C. A.** (1987). Behavior of neural crest cells on embryonic basal laminae. *Dev Biol* **120**, 38-49.

**Etchevers, H. C., Amiel, J. and Lyonnet, S.** (2006). Molecular bases of human neurocristopathies. *Adv Exp Med Biol* **589**, 213-34.

**Etienne-Manneville, S. and Hall, A.** (2002). Rho GTPases in cell biology. *Nature* **420**, 629-35.

**Fairchild, C. L. and Gammill, L. S.** (2013). Tetraspanin18 is a FoxD3-responsive antagonist of cranial neural crest epithelial to mesenchymal transition that maintains Cadherin6B protein. *J Cell Sci* **126**, 1464-76.

**Faure, S. and Fort, P.** (2011). Atypical RhoV and RhoU GTPases control development of the neural crest. *Small GTPases* **2**, 310-313.

**Fort, P., Guemar, L., Vignal, E., Morin, N., Notarnicola, C., de Santa Barbara, P. and Faure, S.** (2011). Activity of the RhoU/Wrch1 GTPase is critical for cranial neural crest cell migration. *Dev Biol* **350**, 451-63.

**Friedl, P. and Wolf, K.** (2003). Tumour-cell invasion and migration: diversity and escape mechanisms. *Nat Rev Cancer* **3**, 362-74.

**Fujimori, T., Miyatani, S. and Takeichi, M.** (1990). Ectopic expression of N-cadherin perturbs histogenesis in Xenopus embryos. *Development* **110**, 97-104.

**Fukata, Y. and Fukata, M.** (2010). Protein palmitoylation in neuronal development and synaptic plasticity. *Nat Rev Neurosci* **11**, 161-75.

**Gammill, L. S. and Bronner-Fraser, M.** (2002). Genomic analysis of neural crest induction. *Development* **129**, 5731-41.

**Gammill, L. S. and Krull, C. E.** (2011). Embryological and genetic manipulation of chick development. In *Methods Mol Biol*, vol. 770, pp. 119-37.

**Garcia-Castro, M. I., Marcelle, C. and Bronner-Fraser, M.** (2002). Ectodermal Wnt function as a neural crest inducer. *Science* **297**, 848-51.

**Garnett, A. T., Square, T. A. and Medeiros, D. M.** (2012). BMP, Wnt and FGF signals are integrated through evolutionarily conserved enhancers to achieve robust expression of Pax3 and Zic genes at the zebrafish neural plate border. *Development* **139**, 4220-31.

**Gheldof, A. and Berx, G.** (2013). Cadherins and epithelial-to-mesenchymal transition. *Prog Mol Biol Transl Sci* **116**, 317-36.

**Greco, C., Bralet, M. P., Ailane, N., Dubart-Kupperschmitt, A., Rubinstein, E., Le Naour, F. and Boucheix, C.** (2010). E-cadherin/p120-catenin and tetraspanin Co-029 cooperate for cell motility control in human colon carcinoma. *Cancer Res* **70**, 7674-83.

**Groysman, M., Shoval, I. and Kalcheim, C.** (2008). A negative modulatory role for rho and rho-associated kinase signaling in delamination of neural crest cells. *Neural Dev* **3**, 27.

**Gupta, P. B., Kuperwasser, C., Brunet, J. P., Ramaswamy, S., Kuo, W. L., Gray, J. W., Naber, S. P. and Weinberg, R. A.** (2005). The melanocyte differentiation program predisposes to metastasis after neoplastic transformation. *Nat Genet* **37**, 1047-54.

**Gutierrez-Lopez, M. D., Gilsanz, A., Yanez-Mo, M., Ovalle, S., Lafuente, E. M., Dominguez, C., Monk, P. N., Gonzalez-Alvaro, I., Sanchez-Madrid, F. and Cabanas, C.** (2011). The sheddase activity of ADAM17/TACE is regulated by the tetraspanin CD9. *Cell Mol Life Sci* **68**, 3275-92.

**Haining, E. J., Yang, J., Bailey, R. L., Khan, K., Collier, R., Tsai, S., Watson, S. P., Frampton, J., Garcia, P. and Tomlinson, M. G.** (2012). The TspanC8 subgroup of tetraspanins interacts with A disintegrin and metalloprotease 10 (ADAM10) and regulates its maturation and cell surface expression. *J Biol Chem* **287**, 39753-65.

**Hall, B. K.** (2000). The neural crest as a fourth germ layer and vertebrates as quadroblastic not triploblastic. *Evol Dev* **2**, 3-5.

**Hall, R. J. and Erickson, C. A.** (2003). ADAM 10: an active metalloprotease expressed during avian epithelial morphogenesis. *Dev Biol* **256**, 146-59.

**Hamburger, V. and Hamilton, H. L.** (1951). A series of normal stages in the development of the chick embryo. *Journal of Morphology* **88**, 231-72.

**Harrison, M., Abu-Elmagd, M., Grocott, T., Yates, C., Gavrilovic, J. and Wheeler, G. N.** (2004). Matrix metalloproteinase genes in Xenopus development. *Dev Dyn* **231**, 214-20.

**Hatta, K. and Takeichi, M.** (1986). Expression of N-cadherin adhesion molecules associated with early morphogenetic events in chick development. *Nature* **320**, 447-9.

**Hay, E. D.** (1968). Organization and fine structure of epithelium and mesenchyme in the developing chick embryos. In *Epithelial-Mesenchymal Interactions: 18th Hahnemann Symposium* (ed. R. Fleischmajer), pp. 31-35. Baltimore: Williams & Wilkins: RE Billingham.

**Hay, E. D.** (2005). The mesenchymal cell, its role in the embryo, and the remarkable signaling mechanisms that create it. *Dev Dyn* **233**, 706-20.

**Hemler, M. E.** (2003). Tetraspanin proteins mediate cellular penetration, invasion, and fusion events and define a novel type of membrane microdomain. *Annu Rev Cell Dev Biol* **19**, 397-422.

**Hemler, M. E.** (2005). Tetraspanin functions and associated microdomains. *Nat Rev Mol Cell Biol* **6**, 801-11.

**Heuberger, J. and Birchmeier, W.** (2010). Interplay of cadherin-mediated cell adhesion and canonical Wnt signaling. *Cold Spring Harb Perspect Biol* **2**, a002915.

**Hirano, M., Hashimoto, S., Yonemura, S., Sabe, H. and Aizawa, S.** (2008). EPB41L5 functions to post-transcriptionally regulate cadherin and integrin during epithelial-mesenchymal transition. *J Cell Biol* **182**, 1217-30.

**Hochgreb-Hagele, T. and Bronner, M. E.** (2013). A novel FoxD3 gene trap line reveals neural crest precursor movement and a role for FoxD3 in their specification. *Dev Biol* **374**, 1-11.

**Hong, C. S., Park, B. Y. and Saint-Jeannet, J. P.** (2008). Fgf8a induces neural crest indirectly through the activation of Wnt8 in the paraxial mesoderm. *Development* **135**, 3903-10.

**Hong, C. S. and Saint-Jeannet, J. P.** (2007). The activity of Pax3 and Zic1 regulates three distinct cell fates at the neural plate border. *Mol Biol Cell* **18**, 2192-202.

**Honore, S. M., Aybar, M. J. and Mayor, R.** (2003). Sox10 is required for the early development of the prospective neural crest in Xenopus embryos. *Dev Biol* **260**, 79-96.

**Huang, C. L., Liu, D., Masuya, D., Kameyama, K., Nakashima, T., Yokomise, H., Ueno, M. and Miyake, M.** (2004). MRP-1/CD9 gene transduction downregulates Wnt signal pathways. *Oncogene* **23**, 7475-83.

**Huber, O., Korn, R., McLaughlin, J., Ohsugi, M., Herrmann, B. G. and Kemler, R.** (1996). Nuclear localization of beta-catenin by interaction with transcription factor LEF-1. *Mech Dev* **59**, 3-10.

**Jamora, C., DasGupta, R., Kocieniewski, P. and Fuchs, E.** (2003). Links between signal transduction, transcription and adhesion in epithelial bud development. *Nature* **422**, 317-22.

**Johnson, J. L., Winterwood, N., DeMali, K. A. and Stipp, C. S.** (2009). Tetraspanin CD151 regulates RhoA activation and the dynamic stability of carcinoma cell-cell contacts. *J Cell Sci* **122**, 2263-73.

**Kalcheim, C. and Burstyn-Cohen, T.** (2005). Early stages of neural crest ontogeny: formation and regulation of cell delamination. *Int J Dev Biol* **49**, 105-16.

**Kam, Y. and Quaranta, V.** (2009). Cadherin-bound beta-catenin feeds into the Wnt pathway upon adherens junctions dissociation: evidence for an intersection between beta-catenin pools. *PLoS One* **4**, e4580.

**Kasemeier-Kulesa, J. C., Kulesa, P. M. and Lefcort, F.** (2005). Imaging neural crest cell dynamics during formation of dorsal root ganglia and sympathetic ganglia. *Development* **132**, 235-45.

**Katiyar, P. and Aplin, A. E.** (2011). FOXD3 regulates migration properties and Rnd3 expression in melanoma cells. *Mol Cancer Res* **9**, 545-52.

**Kerosuo, L. and Bronner-Fraser, M.** (2012). What is bad in cancer is good in the embryo: importance of EMT in neural crest development. *Semin Cell Dev Biol* **23**, 320-32.

**Khudyakov, J. and Bronner-Fraser, M.** (2009). Comprehensive spatiotemporal analysis of early chick neural crest network genes. *Dev Dyn* **238**, 716-23.

**Kopan, R.** (2012). Notch signaling. *Cold Spring Harb Perspect Biol* **4**.

**Kos, R., Reedy, M. V., Johnson, R. L. and Erickson, C. A.** (2001). The winged-helix transcription factor FoxD3 is important for establishing the neural crest lineage and repressing melanogenesis in avian embryos. *Development* **128**, 1467-79.

**Kozma, R., Ahmed, S., Best, A. and Lim, L.** (1995). The Ras-related protein Cdc42Hs and bradykinin promote formation of peripheral actin microspikes and filopodia in Swiss 3T3 fibroblasts. *Mol Cell Biol* **15**, 1942-52.

**Kulesa, P. M. and Fraser, S. E.** (2000). In ovo time-lapse analysis of chick hindbrain neural crest cell migration shows cell interactions during migration to the branchial arches. *Development* **127**, 1161-72.

**Kuo, B. R. and Erickson, C. A.** (2010). Regional differences in neural crest morphogenesis. *Cell Adh Migr* **4**, 567-85.

**Kuphal, F. and Behrens, J.** (2006). E-cadherin modulates Wnt-dependent transcription in colorectal cancer cells but does not alter Wnt-independent gene expression in fibroblasts. *Exp Cell Res* **312**, 457-67.

**LaBonne, C. and Bronner-Fraser, M.** (1998). Neural crest induction in Xenopus: evidence for a two-signal model. *Development* **125**, 2403-14.

**Lander, R., Nordin, K. and LaBonne, C.** (2011). The F-box protein Ppa is a common regulator of core EMT factors Twist, Snail, Slug, and Sip1. *J Cell Biol* **194**, 17-25.

**Le Lievre, C. S. and Le Douarin, N. M.** (1975). Mesenchymal derivatives of the neural crest: analysis of chimaeric quail and chick embryos. *J Embryol Exp Morphol* **34**, 125-54.

**LeDouarin, N. and Kalcheim, C.** (1999). The Neural Crest. Cambridge: Cambridge University Press.

**Levy, S. and Shoham, T.** (2005). Protein-protein interactions in the tetraspanin web. *Physiology (Bethesda)* **20**, 218-24.

**Lewis, J. L., Bonner, J., Modrell, M., Ragland, J. W., Moon, R. T., Dorsky, R. I. and Raible, D. W.** (2004). Reiterated Wnt signaling during zebrafish neural crest development. *Development* **131**, 1299-308.

**Li, B., Kuriyama, S., Moreno, M. and Mayor, R.** (2009). The posteriorizing gene Gbx2 is a direct target of Wnt signalling and the earliest factor in neural crest induction. *Development* **136**, 3267-78.

**Liem, K. F., Jr., Tremml, G. and Jessell, T. M.** (1997). A role for the roof plate and its resident TGFbeta-related proteins in neuronal patterning in the dorsal spinal cord. *Cell* **91**, 127-38.

**Liem, K. F., Jr., Tremml, G., Roelink, H. and Jessell, T. M.** (1995). Dorsal differentiation of neural plate cells induced by BMP-mediated signals from epidermal ectoderm. *Cell* **82**, 969-79.

**Lim, J. and Thiery, J. P.** (2012). Epithelial-mesenchymal transitions: insights from development. *Development* **139**, 3471-86.

**Lin, J., Luo, J. and Redies, C.** (2010). Molecular characterization and expression analysis of ADAM12 during chicken embryonic development. *Dev Growth Differ* **52**, 757-69.

**Lin, J., Redies, C. and Luo, J.** (2007). Regionalized expression of ADAM13 during chicken embryonic development. *Dev Dyn* **236**, 862-70.

**Lister, J. A., Cooper, C., Nguyen, K., Modrell, M., Grant, K. and Raible, D. W.** (2006). Zebrafish Foxd3 is required for development of a subset of neural crest derivatives. *Dev Biol* **290**, 92-104.

**Liu, J. P. and Jessell, T. M.** (1998). A role for rhoB in the delamination of neural crest cells from the dorsal neural tube. *Development* **125**, 5055-67.

**MacDonald, B. T., Tamai, K. and He, X.** (2009). Wnt/beta-catenin signaling: components, mechanisms, and diseases. *Dev Cell* **17**, 9-26.

**Marchant, L., Linker, C., Ruiz, P., Guerrero, N. and Mayor, R.** (1998). The inductive properties of mesoderm suggest that the neural crest cells are specified by a BMP gradient. *Dev Biol* **198**, 319-29.

**Matson, C. K., Murphy, M. W., Sarver, A. L., Griswold, M. D., Bardwell, V. J. and Zarkower, D.** (2011). DMRT1 prevents female reprogramming in the postnatal mammalian testis. *Nature* **476**, 101-4.

**Matthews, H. K., Marchant, L., Carmona-Fontaine, C., Kuriyama, S., Larrain, J., Holt, M. R., Parsons, M. and Mayor, R.** (2008). Directional migration of neural crest cells in vivo is regulated by Syndecan-4/Rac1 and non-canonical Wnt signaling/RhoA. *Development* **135**, 1771-80.

**Mayor, R., Guerrero, N. and Martinez, C.** (1997). Role of FGF and noggin in neural crest induction. *Dev Biol* **189**, 1-12.

**McCawley, L. J. and Matrisian, L. M.** (2001). Matrix metalloproteinases: they're not just for matrix anymore! *Curr Opin Cell Biol* **13**, 534-40.

**McCusker, C., Cousin, H., Neuner, R. and Alfandari, D.** (2009). Extracellular cleavage of cadherin-11 by ADAM metalloproteases is essential for Xenopus cranial neural crest cell migration. *Mol Biol Cell* **20**, 78-89.

**McKeown, S. J., Wallace, A. S. and Anderson, R. B.** (2013). Expression and function of cell adhesion molecules during neural crest migration. *Dev Biol* **373**, 244-57.

**McKinney, M. C., Fukatsu, K., Morrison, J., McLennan, R., Bronner, M. E. and Kulesa, P. M.** (2013). Evidence for dynamic rearrangements but lack of fate or position restrictions in premigratory avian trunk neural crest. *Development* **140**, 820-30.

**McLennan, R., Dyson, L., Prather, K. W., Morrison, J. A., Baker, R. E., Maini, P. K. and Kulesa, P. M.** (2012). Multiscale mechanisms of cell migration during development: theory and experiment. *Development* **139**, 2935-44.

**Megason, S. G. and McMahon, A. P.** (2002). A mitogen gradient of dorsal midline Wnts organizes growth in the CNS. *Development* **129**, 2087-98.

**Meng, W. and Takeichi, M.** (2009). Adherens junction: molecular architecture and regulation. *Cold Spring Harb Perspect Biol* **1**, a002899.

**Menke, A. and Giehl, K.** (2012). Regulation of adherens junctions by Rho GTPases and p120-catenin. *Arch Biochem Biophys* **524**, 48-55.

**Meulemans, D. and Bronner-Fraser, M.** (2004). Gene-regulatory interactions in neural crest evolution and development. *Dev Cell* **7**, 291-9.

**Micalizzi, D. S., Farabaugh, S. M. and Ford, H. L.** (2010). Epithelial-mesenchymal transition in cancer: parallels between normal development and tumor progression. *J Mammary Gland Biol Neoplasia* **15**, 117-34.

**Monsonego-Ornan, E., Kosonovsky, J., Bar, A., Roth, L., Fraggi-Rankis, V., Simsa, S., Kohl, A. and Sela-Donenfeld, D.** (2012). Matrix metalloproteinase 9/gelatinase B is required for neural crest cell migration. *Dev Biol* **364**, 162-77.

**Monsoro-Burq, A. H., Fletcher, R. B. and Harland, R. M.** (2003). Neural crest induction by paraxial mesoderm in Xenopus embryos requires FGF signals. *Development* **130**, 3111-24.

**Monsoro-Burq, A. H., Wang, E. and Harland, R.** (2005). Msx1 and Pax3 cooperate to mediate FGF8 and WNT signals during Xenopus neural crest induction. *Dev Cell* **8**, 167-78.

**Montero-Balaguer, M., Lang, M. R., Sachdev, S. W., Knappmeyer, C., Stewart, R. A., De La Guardia, A., Hatzopoulos, A. K. and Knapik, E. W.** (2006). The mother superior mutation ablates foxd3 activity in neural crest progenitor cells and depletes neural crest derivatives in zebrafish. *Dev Dyn* **235**, 3199-212.

**Moulton, J. D. and Yan, Y. L.** (2008). Using Morpholinos to control gene expression. *Curr Protoc Mol Biol* **Chapter 26**, Unit 26 8.

**Moury, J. D. and Jacobson, A. G.** (1990). The origins of neural crest cells in the axolotl. *Dev Biol* **141**, 243-53.

**Mundell, N. A. and Labosky, P. A.** (2011). Neural crest stem cell multipotency requires Foxd3 to maintain neural potential and repress mesenchymal fates. *Development* **138**, 641-52.

**Nakagawa, S. and Takeichi, M.** (1995). Neural crest cell-cell adhesion controlled by sequential and subpopulation-specific expression of novel cadherins. *Development* **121**, 1321-32.

**Nakagawa, S. and Takeichi, M.** (1998). Neural crest emigration from the neural tube depends on regulated cadherin expression. *Development* **125**, 2963-71.

**Nakamura, H. and Ayer-le Lievre, C. S.** (1982). Mesectodermal capabilities of the trunk neural crest of birds. *J Embryol Exp Morphol* **70**, 1-18.

**Nandadasa, S., Tao, Q., Menon, N. R., Heasman, J. and Wylie, C.** (2009). N- and E-cadherins in Xenopus are specifically required in the neural and non-neural ectoderm, respectively, for F-actin assembly and morphogenetic movements. *Development* **136**, 1327-38.

**Nieto, M. A.** (2011). The ins and outs of the epithelial to mesenchymal transition in health and disease. *Annu Rev Cell Dev Biol* **27**, 347-76.

**Nishimura, T. and Takeichi, M.** (2009). Remodeling of the adherens junctions during morphogenesis. *Curr Top Dev Biol* **89**, 33-54.

**Nitzan, E., Krispin, S., Pfaltzgraff, E. R., Klar, A., Labosky, P. A. and Kalcheim, C.** (2013). A dynamic code of dorsal neural tube genes regulates the segregation between neurogenic and melanogenic neural crest cells. *Development*.

**Nobes, C. D. and Hall, A.** (1995). Rho, rac, and cdc42 GTPases regulate the assembly of multimolecular focal complexes associated with actin stress fibers, lamellipodia, and filopodia. *Cell* **81**, 53-62.

**Nohe, A., Keating, E., Knaus, P. and Petersen, N. O.** (2004). Signal transduction of bone morphogenetic protein receptors. *Cell Signal* **16**, 291-9.

**Nose, A., Nagafuchi, A. and Takeichi, M.** (1988). Expressed recombinant cadherins mediate cell sorting in model systems. *Cell* **54**, 993-1001.

**Notarnicola, C., Le Guen, L., Fort, P., Faure, S. and de Santa Barbara, P.** (2008). Dynamic expression patterns of RhoV/Chp and RhoU/Wrch during chicken embryonic development. *Dev Dyn* **237**, 1165-71.

**Oda, H. and Takeichi, M.** (2011). Evolution: structural and functional diversity of cadherin at the adherens junction. *J Cell Biol* **193**, 1137-46.

**Onder, T. T., Gupta, P. B., Mani, S. A., Yang, J., Lander, E. S. and Weinberg, R. A.** (2008). Loss of E-cadherin promotes metastasis via multiple downstream transcriptional pathways. *Cancer Res* **68**, 3645-54.

**Orsulic, S., Huber, O., Aberle, H., Arnold, S. and Kemler, R.** (1999). E-cadherin binding prevents beta-catenin nuclear localization and beta-catenin/LEF-1-mediated transactivation. *J Cell Sci* **112 ( Pt 8)**, 1237-45.

**Overduin, M., Harvey, T. S., Bagby, S., Tong, K. I., Yau, P., Takeichi, M. and Ikura, M.** (1995). Solution structure of the epithelial cadherin domain responsible for selective cell adhesion. *Science* **267**, 386-9.

**Pan, D. and Rubin, G. M.** (1997). Kuzbanian controls proteolytic processing of Notch and mediates lateral inhibition during Drosophila and vertebrate neurogenesis. *Cell* **90**, 271-80.

**Park, K. S. and Gumbiner, B. M.** (2010). Cadherin 6B induces BMP signaling and de-epithelialization during the epithelial mesenchymal transition of the neural crest. *Development* **137**, 2691-701.

**Park, K. S. and Gumbiner, B. M.** (2012). Cadherin-6B stimulates an epithelial mesenchymal transition and the delamination of cells from the neural ectoderm via LIMK/cofilin mediated non-canonical BMP receptor signaling. *Dev Biol*.

**Peinado, H., Portillo, F. and Cano, A.** (2004). Transcriptional regulation of cadherins during development and carcinogenesis. *Int J Dev Biol* **48**, 365-75.

**Perron, J. C. and Bixby, J. L.** (1999). Tetraspanins expressed in the embryonic chick nervous system. *FEBS Lett* **461**, 86-90.

**Pokutta, S., Herrenknecht, K., Kemler, R. and Engel, J.** (1994). Conformational changes of the recombinant extracellular domain of E-cadherin upon calcium binding. *Eur J Biochem* **223**, 1019-26.

**Polyak, K. and Weinberg, R. A.** (2009). Transitions between epithelial and mesenchymal states: acquisition of malignant and stem cell traits. *Nat Rev Cancer* **9**, 265-73.

**Powell, D. R., Blasky, A. J., Britt, S. G. and Artinger, K. B.** (2013). Riding the crest of the wave: parallels between the neural crest and cancer in epithelial-to-mesenchymal transition and migration. *Wiley Interdiscip Rev Syst Biol Med*.

**Prasad, M. S., Sauka-Spengler, T. and LaBonne, C.** (2012). Induction of the neural crest state: control of stem cell attributes by gene regulatory, post-transcriptional and epigenetic interactions. *Dev Biol* **366**, 10-21.

**Prox, J., Willenbrock, M., Weber, S., Lehmann, T., Schmidt-Arras, D., Schwanbeck, R., Saftig, P. and Schwake, M.** (2012). Tetraspanin15 regulates cellular trafficking and activity of the ectodomain sheddase ADAM10. *Cell Mol Life Sci* **69**, 2919-32.

**Przybylo, J. A. and Radisky, D. C.** (2007). Matrix metalloproteinase-induced epithelial-mesenchymal transition: tumor progression at Snail's pace. *Int J Biochem Cell Biol* **39**, 1082-8.

**Ragland, J. W. and Raible, D. W.** (2004). Signals derived from the underlying mesoderm are dispensable for zebrafish neural crest induction. *Dev Biol* **276**, 16-30.

**Ridley, A. J. and Hall, A.** (1992). The small GTP-binding protein rho regulates the assembly of focal adhesions and actin stress fibers in response to growth factors. *Cell* **70**, 389-99.

**Ridley, A. J., Paterson, H. F., Johnston, C. L., Diekmann, D. and Hall, A.** (1992). The small GTP-binding protein rac regulates growth factor-induced membrane ruffling. *Cell* **70**, 401-10.

**Roffers-Agarwal, J., Hutt, K. J. and Gammill, L. S.** (2012). Paladin is an antiphosphatase that regulates neural crest cell formation and migration. *Dev Biol*.

**Rogers, C. D., Jayasena, C. S., S., N. and M.E., B.** (2012). Neural crest specification: Tissues, signals, and transcription factors. *WIREs Developmental Biology 2012* **1**, 52-68.

**Rollhauser-ter Horst, J.** (1979). Artificial neural crest formation in amphibia. *Anat Embryol (Berl)* **157**, 113-20.

**Rubinstein, E.** (2011). The complexity of tetraspanins. *Biochem Soc Trans* **39**, 501-5.

**Saint-Jeannet, J. P., He, X., Varmus, H. E. and Dawid, I. B.** (1997). Regulation of dorsal fate in the neuraxis by Wnt-1 and Wnt-3a. *Proc Natl Acad Sci U S A* **94**, 13713-8.

**Sakai, D., Tanaka, Y., Endo, Y., Osumi, N., Okamoto, H. and Wakamatsu, Y.** (2005). Regulation of Slug transcription in embryonic ectoderm by beta-catenin-Lef/Tcf and BMP-Smad signaling. *Dev Growth Differ* **47**, 471-82.

**Sasai, N., Mizuseki, K. and Sasai, Y.** (2001). Requirement of FoxD3-class signaling for neural crest determination in Xenopus. *Development* **128**, 2525-36.

**Sato, T., Sasai, N. and Sasai, Y.** (2005). Neural crest determination by co-activation of Pax3 and Zic1 genes in Xenopus ectoderm. *Development* **132**, 2355-63.

**Savagner, P.** (2001). Leaving the neighborhood: molecular mechanisms involved during epithelial-mesenchymal transition. *Bioessays* **23**, 912-23.

**Selleck, M. A. and Bronner-Fraser, M.** (1995). Origins of the avian neural crest: the role of neural plate-epidermal interactions. *Development* **121**, 525-38.

**Selleck, M. A., Garcia-Castro, M. I., Artinger, K. B. and Bronner-Fraser, M.** (1998). Effects of Shh and Noggin on neural crest formation demonstrate that BMP is required in the neural tube but not ectoderm. *Development* **125**, 4919-30.

**Shimoyama, Y., Tsujimoto, G., Kitajima, M. and Natori, M.** (2000). Identification of three human type-II classic cadherins and frequent heterophilic interactions between different subclasses of type-II classic cadherins. *Biochem J* **349**, 159-67.

**Shoval, I. and Kalcheim, C.** (2012). Antagonistic activities of Rho and Rac GTPases underlie the transition from neural crest delamination to migration. *Dev Dyn* **241**, 1155-68.

**Shoval, I., Ludwig, A. and Kalcheim, C.** (2007). Antagonistic roles of full-length N-cadherin and its soluble BMP cleavage product in neural crest delamination. *Development* **134**, 491-501.

**Shtutman, M., Levina, E., Ohouo, P., Baig, M. and Roninson, I. B.** (2006). Cell adhesion molecule L1 disrupts E-cadherin-containing adherens junctions and increases scattering and motility of MCF7 breast carcinoma cells. *Cancer Res* **66**, 11370-80.

**Simoes-Costa, M. S., McKeown, S. J., Tan-Cabugao, J., Sauka-Spengler, T. and Bronner, M. E.** (2012). Dynamic and differential regulation of stem cell factor FoxD3 in the neural crest is Encrypted in the genome. *PLoS Genet* **8**, e1003142.

**Sternlicht, M. D. and Werb, Z.** (2001). How matrix metalloproteinases regulate cell behavior. *Annu Rev Cell Dev Biol* **17**, 463-516.

**Steventon, B., Araya, C., Linker, C., Kuriyama, S. and Mayor, R.** (2009). Differential requirements of BMP and Wnt signalling during gastrulation and neurulation define two steps in neural crest induction. *Development* **136**, 771-9.

**Stewart, R. A., Arduini, B. L., Berghmans, S., George, R. E., Kanki, J. P., Henion, P. D. and Look, A. T.** (2006). Zebrafish foxd3 is selectively required for neural crest specification, migration and survival. *Dev Biol* **292**, 174-88.

**Stuhlmiller, T. J. and Garcia-Castro, M. I.** (2012a). Current perspectives of the signaling pathways directing neural crest induction. *Cell Mol Life Sci* **69**, 3715-37.

**Stuhlmiller, T. J. and Garcia-Castro, M. I.** (2012b). FGF/MAPK signaling is required in the gastrula epiblast for avian neural crest induction. *Development* **139**, 289-300.

**Swartz, M. E., Eberhart, J., Pasquale, E. B. and Krull, C. E.** (2001). EphA4/ephrin-A5 interactions in muscle precursor cell migration in the avian forelimb. *Development* **128**, 4669-80.

**Takeichi, M., Hatta, K., Nose, A. and Nagafuchi, A.** (1988). Identification of a gene family of cadherin cell adhesion molecules. *Cell Differ Dev* **25 Suppl**, 91-4.

**Taneyhill, L. A. and Bronner-Fraser, M.** (2005). Dynamic alterations in gene expression after Wnt-mediated induction of avian neural crest. *Mol Biol Cell* **16**, 5283-93.

**Taneyhill, L. A., Coles, E. G. and Bronner-Fraser, M.** (2007). Snail2 directly represses cadherin6B during epithelial-to-mesenchymal transitions of the neural crest. *Development* **134**, 1481-90.

**Taylor, K. M. and Labonne, C.** (2005). SoxE factors function equivalently during neural crest and inner ear development and their activity is regulated by SUMOylation. *Dev Cell* **9**, 593-603.

**Teng, L., Mundell, N. A., Frist, A. Y., Wang, Q. and Labosky, P. A.** (2008). Requirement for Foxd3 in the maintenance of neural crest progenitors. *Development* **135**, 1615-24.

**Theveneau, E., Duband, J. L. and Altabef, M.** (2007). Ets-1 confers cranial features on neural crest delamination. *PLoS One* **2**, e1142.

**Theveneau, E. and Mayor, R.** (2012). Neural crest delamination and migration: From epithelium-to-mesenchyme transition to collective cell migration. *Dev Biol* **366**, 34-54.

**Thiery, J. P., Acloque, H., Huang, R. Y. and Nieto, M. A.** (2009). Epithelial-mesenchymal transitions in development and disease. *Cell* **139**, 871-90.

**Thiery, J. P. and Sleeman, J. P.** (2006). Complex networks orchestrate epithelial-mesenchymal transitions. *Nat Rev Mol Cell Biol* **7**, 131-42.

**Thomas, A. J. and Erickson, C. A.** (2009). FOXD3 regulates the lineage switch between neural crest-derived glial cells and pigment cells by repressing MITF through a non-canonical mechanism. *Development* **136**, 1849-58.

**Tomlinson, M. L., Guan, P., Morris, R. J., Fidock, M. D., Rejzek, M., Garcia-Morales, C., Field, R. A. and Wheeler, G. N.** (2009). A chemical genomic approach identifies matrix metalloproteinases as playing an essential and specific role in Xenopus melanophore migration. *Chem Biol* **16**, 93-104.

**Tosney, K. W.** (1978). The early migration of neural crest cells in the trunk region of the avian embryo: an electron microscopic study. *Dev Biol* **62**, 317-33.

**Tosney, K. W.** (1982). The segregation and early migration of cranial neural crest cells in the avian embryo. *Dev Biol* **89**, 13-24.

**Tousseyn, T., Jorissen, E., Reiss, K. and Hartmann, D.** (2006). (Make) stick and cut loose--disintegrin metalloproteases in development and disease. *Birth Defects Res C Embryo Today* **78**, 24-46.

**Tribulo, C., Aybar, M. J., Nguyen, V. H., Mullins, M. C. and Mayor, R.** (2003). Regulation of Msx genes by a Bmp gradient is essential for neural crest specification. *Development* **130**, 6441-52.

**Tsai, Y. C. and Weissman, A. M.** (2011). Dissecting the diverse functions of the metastasis suppressor CD82/KAI1. *FEBS Lett* **585**, 3166-73.

**Turner, D. L. and Weintraub, H.** (1994). Expression of achaete-scute homolog 3 in Xenopus embryos converts ectodermal cells to a neural fate. *Genes Dev* **8**, 1434-47.

**Vallin, J., Girault, J. M., Thiery, J. P. and Broders, F.** (1998). Xenopus cadherin-11 is expressed in different populations of migrating neural crest cells. *Mech Dev* **75**, 171-4.

**Vallin, J., Thuret, R., Giacomello, E., Faraldo, M. M., Thiery, J. P. and Broders, F.** (2001). Cloning and characterization of three Xenopus slug promoters reveal direct regulation by Lef/beta-catenin signaling. *J Biol Chem* **276**, 30350-8.

**VanSaun, M. N. and Matrisian, L. M.** (2006). Matrix metalloproteinases and cellular motility in development and disease. *Birth Defects Res C Embryo Today* **78**, 69-79.

**Vega, F. M. and Ridley, A. J.** (2007). SnapShot: Rho family GTPases. *Cell* **129**, 1430.

**Vernon, A. E. and LaBonne, C.** (2006). Slug stability is dynamically regulated during neural crest development by the F-box protein Ppa. *Development* **133**, 3359-70.

**Villanueva, S., Glavic, A., Ruiz, P. and Mayor, R.** (2002). Posteriorization by FGF, Wnt, and retinoic acid is required for neural crest induction. *Dev Biol* **241**, 289-301.

**Wakabayashi, T., Craessaerts, K., Bammens, L., Bentahir, M., Borgions, F., Herdewijn, P., Staes, A., Timmerman, E., Vandekerckhove, J., Rubinstein, E. et al.** (2009). Analysis of the gamma-secretase interactome and validation of its association with tetraspanin-enriched microdomains. *Nat Cell Biol* **11**, 1340-6.

**Wang, W. D., Melville, D. B., Montero-Balaguer, M., Hatzopoulos, A. K. and Knapik, E. W.** (2011). Tfap2a and Foxd3 regulate early steps in the development of the neural crest progenitor population. *Dev Biol* **360**, 173-85.

**Wang, Y. C., Khan, Z., Kaschube, M. and Wieschaus, E. F.** (2012). Differential positioning of adherens junctions is associated with initiation of epithelial folding. *Nature* **484**, 390-3.

**Weber, S. and Saftig, P.** (2012). Ectodomain shedding and ADAMs in development. *Development* **139**, 3693-709.

**Wennerberg, K. and Der, C. J.** (2004). Rho-family GTPases: it's not only Rac and Rho (and I like it). *J Cell Sci* **117**, 1301-12.

**Wheelock, M. J., Shintani, Y., Maeda, M., Fukumoto, Y. and Johnson, K. R.** (2008). Cadherin switching. *J Cell Sci* **121**, 727-35.

**Wilkinson, D.** (1992). Whole mount in situ hybridization of vertebrate embryos. In *In Situ Hybridization: A practical Approach*, pp. 75-83. Oxford: Oxford University Press.

**Wilson, P. A. and Hemmati-Brivanlou, A.** (1995). Induction of epidermis and inhibition of neural fate by Bmp-4. *Nature* **376**, 331-3.

**Winterwood, N. E., Varzavand, A., Meland, M. N., Ashman, L. K. and Stipp, C. S.** (2006). A critical role for tetraspanin CD151 in alpha3beta1 and alpha6beta4 integrin-dependent tumor cell functions on laminin-5. *Mol Biol Cell* **17**, 2707-21.

**Xu, D., Sharma, C. and Hemler, M. E.** (2009). Tetraspanin12 regulates ADAM10-dependent cleavage of amyloid precursor protein. *FASEB J* **23**, 3674-81.

**Yanez-Mo, M., Barreiro, O., Gordon-Alonso, M., Sala-Valdes, M. and Sanchez-Madrid, F.** (2009). Tetraspanin-enriched microdomains: a functional unit in cell plasma membranes. *Trends Cell Biol* **19**, 434-46.

**Yanez-Mo, M., Gutierrez-Lopez, M. D. and Cabanas, C.** (2011). Functional interplay between tetraspanins and proteases. *Cell Mol Life Sci* **68**, 3323-35.

**Yang, J. and Weinberg, R. A.** (2008). Epithelial-mesenchymal transition: at the crossroads of development and tumor metastasis. *Dev Cell* **14**, 818-29.

**Yonemura, S.** (2011). Cadherin-actin interactions at adherens junctions. *Curr Opin Cell Biol* **23**, 515-22.

**Zohn, I. E., Li, Y., Skolnik, E. Y., Anderson, K. V., Han, J. and Niswander, L.** (2006). p38 and a p38-interacting protein are critical for downregulation of E-cadherin during mouse gastrulation. *Cell* **125**, 957-69.

**Zoller, M.** (2009). Tetraspanins: push and pull in suppressing and promoting metastasis. *Nat Rev Cancer* **9**, 40-55.

# Appendix I

## Preliminary data investigating the mechanism behind Tspan18-dependent Cad6B maintenance: Does Tspan18 effect Cad6B processing by ADAMs?

[The data in this Appendix were collected in collaboration with Drs. D. Alfandari and L.A. Taneyhill.]

**Introduction:**

Epithelial-to-mesenchymal transition (EMT) is a complex, multiple step process during which tightly adherent epithelial cells undergo dynamic rearrangements in cell polarity and cell-cell adhesion and become individual, invasive mesenchymal cells (Hay, 2005). EMT is essential to produce the intricate adult body plan that forms during embryogenesis, including during the formation of the migratory neural crest (Nieto, 2011; Thiery et al., 2009). Neural crest cells originate from the dorsal portion of the developing vertebrate neural tube, but unlike their epithelial neighbors, they leave the neural tube and disperse throughout the embryo to eventually form the peripheral nervous system, craniofacial skeleton, and melanocytes (LeDouarin and Kalcheim, 1999). Although their migration is crucial to the formation of essential vertebrate structures, the regulation of neural crest EMT is not fully understood.

One aspect of EMT involves "cadherin switching", or altering the cell surface expression of $Ca^{2++}$-dependent adhesion molecules of the cadherin family (Wheelock et al., 2008). The production of migratory neural crest cells in the chick embryo includes a number of cadherin switches. For example, premigratory cranial neural crest cells downregulate N-cadherin (N-cad) early during their development and begin to express cadherin-6B (Cad6B) while they remain within the dorsal neural tube (Dady et al., 2012; Duband et al., 1988; Hatta and Takeichi, 1986; Nakagawa and Takeichi, 1995). Later, as cranial neural crest cells exit the neural tube they downregulate Cad6B and subsequently induce the expression of cadherin-7 during active migration (Fairchild and Gammill, 2013; Nakagawa and Takeichi, 1995). Preventing cadherin switching inhibits neural crest migration (Coles et al., 2007; Nakagawa and Takeichi, 1998; Shoval et al., 2007),

emphasizing the importance of regulated changes in cell adhesion for EMT. Thus, it is crucial to understand how the expression of cadherins relevant to neural crest EMT is regulated.

During EMT, cadherin levels are controlled by a number of diverse transcriptional and post-translational mechanisms (Gheldof and Berx, 2013; Kerosuo and Bronner-Fraser, 2012; McKeown et al., 2013). The transcriptional control of *cad6B* in cranial neural crest cells has been well established. In the cranial neural crest, *cad6B* is directly repressed by the EMT transcription factor Snail2 (Taneyhill et al., 2007). In addition, Cad6B protein levels are post-translationally maintained by a scaffolding protein of the tetraspanin transmembrane protein family, Tetraspanin18 (Tspan18)(Fairchild and Gammill, 2013). In fact, downregulation of *Cad6B* mRNA expression without the concomitant loss of Tspan18 is incompatible with migration (Fairchild and Gammill, 2013). Thus, coordinated transcriptional and post-translational mechanisms control Cad6B levels during neural crest EMT. Determining the mechanism by which Tspan18 maintains Cad6B protein levels will allow us to understand how cell adhesion is regulated as cranial neural crest cells become migratory.

Membrane-bound and secreted matrix metalloproteases, including those of the ADAM (a disintegrin and metalloproteinase) family, cleave a variety of transmembrane proteins including cell adhesion molecules like cadherins (Edwards et al., 2008; Tousseyn et al., 2006; VanSaun and Matrisian, 2006). This process, typically called ectodomain shedding, dynamically alters the function of cell adhesion molecules and can affect cell signaling during various developmental processes (Weber and Saftig, 2012). Chick neural crest cells, as well as surrounding tissues, express a handful of ADAMs,

including ADAM10, 12, 13 and 33 (Hall and Erickson, 2003; Lin et al., 2010; Lin et al., 2007; McLennan et al., 2012). In the trunk, ADAM10 cleaves N-cad and promotes trunk neural crest cell migration by both relieving N-cad dependent cell adhesions and affecting intracellular signaling, as the N-cad C-terminal fragment regulates the transcription of downstream targets of the Wnt signaling pathway (Shoval et al., 2007). Although ADAM13 has been implicated in cadherin-11 cleavage during cranial neural crest migration in *Xenopus* embryos (Alfandari et al., 2001; McCusker et al., 2009), the role of ADAMs in cad6B regulation has yet to be determined.

Recent studies have shown that tetraspanins can directly regulate ADAM activity by altering ADAM maturation and localization (Gutierrez-Lopez et al., 2011; Haining et al., 2012; Prox et al., 2012; Xu et al., 2009). These observations led me to hypothesize that Tspan18 modulates the activity of ADAMs that process Cad6B in premigratory cranial neural crest cells. In this chapter, I have outlined preliminary experiments I performed, in collaboration with the Alfandari and Taneyhill laboratories, to gain insight into the mechanism behind the ability of Tspan18 to maintain Cad6B protein levels (Fairchild and Gammill, 2013). Our preliminary data suggest that Tspan18 may regulate ADAM maturation, at least in *Xenopus* embryos, and furthermore emphasize the importance of future studies investigating whether Tspan18 regulates ADAM-dependent Cad6B processing.

## Results and Discussion:

### Tspan18 does not interact with Cad6B in chick fibroblasts

Forced expression of Tspan18 maintains Cad6B protein levels, without affecting *Cad6B* mRNA expression, and inhibits migration (Fairchild and Gammill, 2013), suggesting that Tspan18 stabilizes Cad6B protein levels post-translationally. In order to determine the mechanism behind this post-translational control, we first aimed to verify whether Tspan18 and Cad6B interact biochemically. To this end, we co-transfected chick embryonic fibroblast (DF1) cells with pCS2-TS18+MycTag (TS18MT) and pCS2-Cad6B+FlagTag (Cad6BFT) to evaluate an interaction by co-immunoprecipitation. At 32 hours post-transfection, TS18MT and cad6BFT were clearly detectable in whole cell lysates by western blotting with anti-Flag and anti-MycTag antibodies (Fig. 1A), suggesting that both constructs were efficiently expressed in DF1 cells. After immunoprecipitation using anti-Flag magnetic beads, Cad6BFT was clearly detectable by western blotting with anti-Flag (Fig. 1B), suggesting that the flag magnetic beads efficiently pull down flag-tagged cad6B. However, we could not detect TS18MT by western blotting with the anti-MycTag antibody (Fig. 1B). Together these data suggest that Tspan18 and Cad6B do not interact in DF1 cells. However, it is important to note that these experiments were performed outside of the context of the embryo. It is possible that Tspan18 and Cad6B interact indirectly, perhaps via associated cofactors that are present in the embryo and not in DF1 cells. Repeating these biochemical experiments after co-electroporation of similar tagged constructs into the embryo are important future experiments.

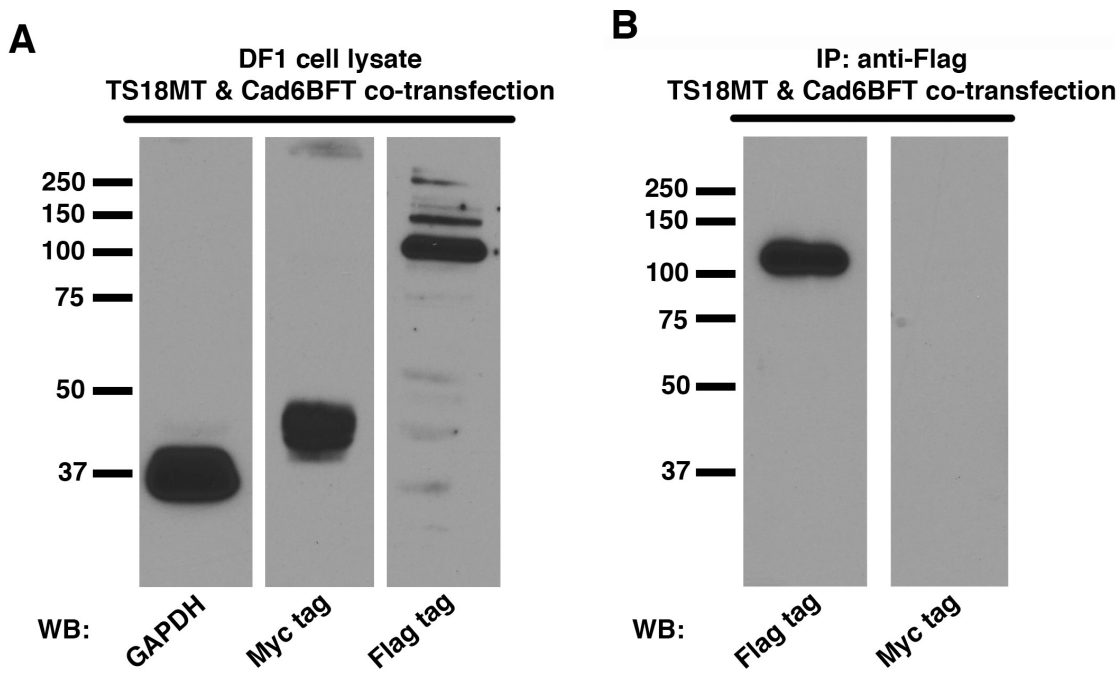
A
DF1 cell lysate
TS18MT & Cad6BFT co-transfection
250
150
100
75
50
37
WB:
GAPDH
Myc tag
Flag tag
B
IP: anti-Flag
TS18MT & Cad6BFT co-transfection
250
150
100
75
50
37
WB:
Flag tag
Myc tag

**Fig. 1. Tspan18 and Cad6B do not interact in DF1 cells.**

(A) Total cell lysate from DF1 cells co-transfected with TS18MT and Cad6BFT. GAPDH (36 kDa), TS18MT (39 kDa), and Cad6BFT (99 kDa) are all detectable by western blot with the appropriate primary antibodies. (B) Anti-flag immunoprecipitation using total cell lysate from DF1 cells co-transfected with TS18MT and Cad6BFT. Cad6BFT was detected in the immunoprecipitate following western blot with an anti-Flag tag primary antibody (note presence of 99 kDa band). However TS18MT was not detected following western blot using an anti-Myc Tag antibody.

**Although Tspan18 interacts with xADAM13 and xADAM19, it does not interact with cADAM19 in DF1 cells**

One possible reason Tspan18 did not interact with Cad6B in DF1 cells (Fig. 1) is that Tspan18 may affect Cad6B protein levels by indirectly interacting with, and/or controlling the activity of, other membrane proteins that are responsible for cad6B post-translational regulation. ADAMs regulate cadherin processing during neural crest development in the trunk (Shoval et al., 2007) and in *Xenopus* embryos (McCusker et al., 2009). Moreover, a handful of tetraspanins have been shown to regulate ADAM activity (Gutierrez-Lopez et al., 2011; Haining et al., 2012; Prox et al., 2012; Xu et al., 2009). Although ADAM processing of Cad6B has not been demonstrated, we reasoned that Cad6B may also be regulated by ADAMs, and furthermore reasoned that Tspan18 may modulate this regulation. In order to investigate this possibility we first wanted to determine whether Tspan18 interacts biochemically with two ADAMs that are potentially relevant to chick cranial neural crest development: cADAM10 and cADAM19 (A. Schiffmacher, unpublished data). DF1 cells were transfected with either pCIG-ADAM10+HATag (cA10HA) or pCIG-ADAM19+HATag (cA19HA) with or without pCS2-Tspan18 (TS18FT). 32 hours after transfection, we assayed the expression of cA10HA, cA19HA and TS18FT in DF1 cells by western blot. We found that TS18FT was abundantly expressed in both conditions (Fig 2A). Furthermore, we detected cA19HA in DF1 cells that were transfected with cA19HA alone and in cells co-transfected with TS18FT, although the amount of cA19HA was notably lower when co-transfected with TS18FT (Fig. 2B). Unfortunately we did not detect cA10HA in DF1

cells under any condition examined (Fig. 2B), suggesting that in these experiments, cA10HA is not being efficiently expressed.

Given that we could detect cA19HA, we next performed a co-immunoprecipitation experiment to determine whether cA19HA interacted with TS18FT. Following immunoprecipitation with anti-flag magnetic beads, we could clearly detect TS18FT by western blot using an anti-flag antibody (Fig. 2C), suggesting that TS18FT was being efficiently immunoprecipitated by the anti-flag magnetic beads. However, cA19HA was not apparent by western blot using an anti-HA antibody (Fig. 2C). This was unexpected, considering that Tspan18 does interact with both *Xenopus* ADAM19 (xADAM19) and *Xenopus* ADAM13 (xADAM13) in 293T cells (D. Alfandari, personal communication). However, it is possible that Tspan18 only interacts with cADAM19 under certain conditions, and that these conditions were not met in our culture system. Thus, it is essential to repeat these experiments in other culture conditions, or perhaps more appropriately, within the context of the chick embryo. Different ADAMs could be relevant to neural crest development in the chick embryo, and the function of an individual ADAM ortholog may not necessarily be the same when comparing chick and *Xenopus* embryos. Exploring the interaction between Tspan18 and other ADAMs, including those that have yet to be characterized in the neural crest, are intriguing future experiments.

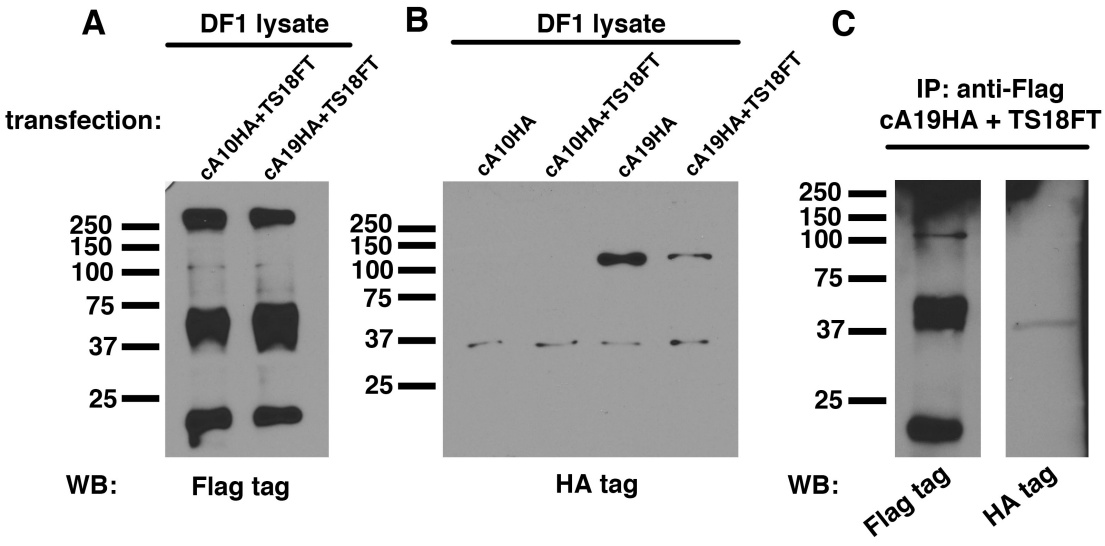
A
DF1 lysate
transfection:
cA10HA+TS18FT
cA19HA+TS18FT
250
150
100
75
37
25
WB:
Flag tag
B
DF1 lysate
cA10HA
cA10HA+TS18FT
cA19HA
cA19HA+TS18FT
250
150
100
75
37
25
HA tag
C
IP: anti-Flag
cA19HA + TS18FT
250
150
100
75
37
25
WB:
Flag tag
HA tag

**Fig. 2. Tspan18 does not interact with chick ADAM19 in DF1 cells.**

(A) Total cell lysate from DF1 cells transfected with TS18FT and either cA10HA or cA19HA. TS18FT (39 kDa) is detectable by western blot using anti-Flag tag antibody. (B) Total cell lysate from DF1 cells transfected with cA10HA alone or with TS18FT and cA19HA alone or with TS18FT. cA10HA is not detectable in either condition, but cA19HA is detectable by western blot using an anti-HA tag primary antibody. (C) Anti-Flag immunoprecipitation using cell lysate from DF1 cells co-transfected with cA19HA and TS18FT. TS18FT was detected in the immunoprecipitate by western blot using an anti-Flag tag antibody (note the presence of the 39 kDa band). However, cA19HA was not present in the immunoprecipitate following western blot using an anti-HA tag antibody.

**Tspan18 does not alter the ability of xADAM13 to cleave PAPC in vitro, but may affect ADAM maturation**

Tetraspanins have previously been shown to directly regulate ADAM activity in various cell types (Gutierrez-Lopez et al., 2011; Haining et al., 2012; Prox et al., 2012; Xu et al., 2009). Although Tspan18 did not interact with cADAM19 in DF1 cells (Fig. 2), it did interact with xADAM13 and xADAM19 in 293T cells (D. Alfandari, personal communication). We therefore wanted to determine whether Tspan18 alters the ability of xADAM13 to cleave *Xenopus* paraxial protocadherin (PAPC) in vitro. The results of these experiments, as performed by the Alfandari lab in collaboration with me, are shown in Fig. 3. In culture supernatants from cells transfected with wild-type xA13 (lane 1), a distinct band corresponding to the "shedded" version of PAPC (shedd PAPC) was clearly visible by western blot (Fig. 3A, arrowhead). In contrast, the band corresponding to shedd PAPC was absent in supernatants from cells transfected with a mutant, kinase-dead form of xA13 (E/A13; lane 3), suggesting that PAPC is not cleaved in the presence of E/A13 and, importantly, xA13 activity can be assed by the presence of this band. Interestingly, when wild-type xA13 was co-transfected with full-length Tspan18, shedd PAPC was present (Fig. 3A; lane2), suggesting that Tspan18 does not interfere with the ability of xA13 to cleave PAPC. Similar studies investigating the affect Tspan18 had on xADAM19-dependent cleavage of the ampheregulin receptor showed similar results (D. Alfandari, personal communication). Together these experiments suggest that Tspan18 does not directly regulate xADAM13 or xADAM19 activity.

One interesting observation, however, was that expression of Tspan18 did appear to decrease the amount of xADAM13 (Fig. 3C; lane 2) present in these cells. This is

consistent with our earlier finding, which suggested that expression of Tspan18 decreased the amount of cADAM19 expressed in DF1 cells (Fig. 2B). Furthermore, expression of Tspan18 altered the ratio of the mature form of xADAM13 produced (bottom arrow in Fig. 3C) compared to the immature form (top arrow in Fig. 3C). Specifically, in cells expressing only wild-type xA13, the amount of mature and immature isoforms of xA13 was approximately equal (Fig. 3C, lane 1), however, in cells co-transfected with Tspan18 there was much less of the mature form present, as compared to the immature form (Fig. 3C, lane 2). This could indicate that Tspan18 affects ADAM maturation, however additional control experiments are required to determine if this is a specific consequence of Tspan18 expression as compared to a general effect on translation. Furthermore, to assess whether Tspan18 regulates Cad6B processing, these experiments will need to be repeated *in vivo* using chick embryos. Unfortunately, no information regarding Cad6B processing is currently available, making these proposed experiments difficult. However, ADAM function is also regulated by intercellular trafficking (Edwards et al., 2008), thus an intriguing first step would be to determine whether Tspan18 knock down alters the localization of ADAMs expressed in chick cranial neural crest cells.

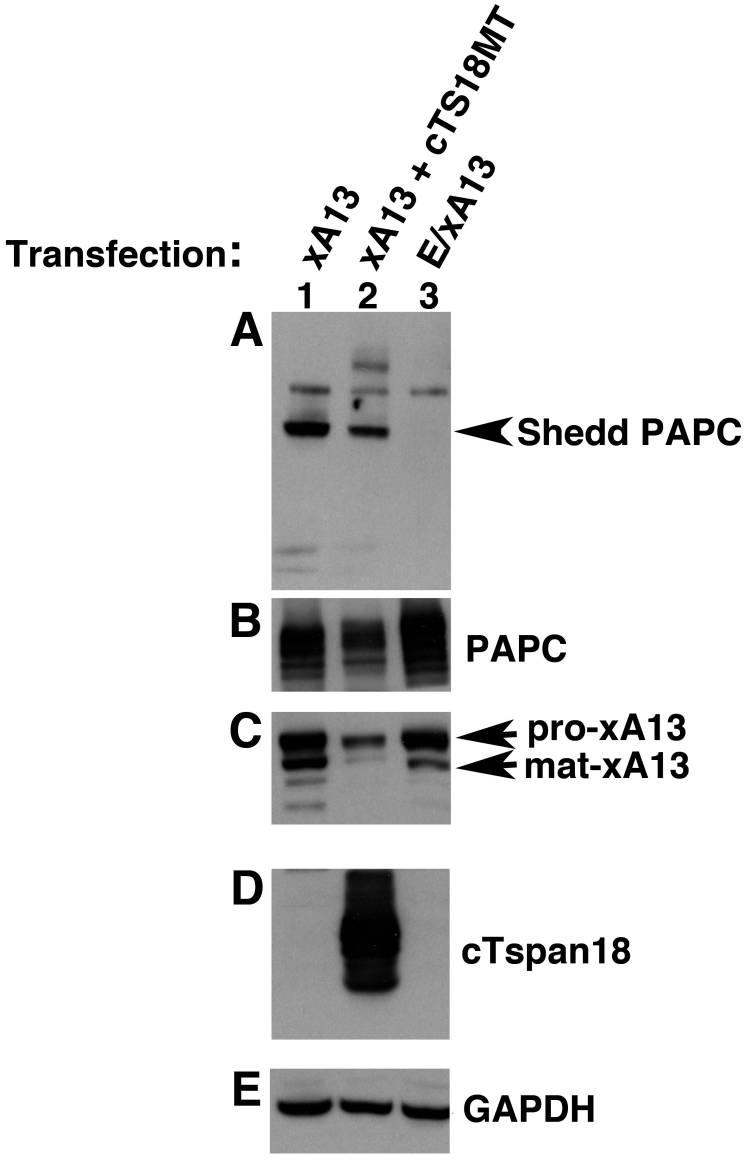
Transfection:
xA13
xA13 + cTS18MT
E/xA13
1
2
3
A
Shedd PAPC
B
PAPC
C
pro-xA13
mat-xA13
D
cTspan18
E
GAPDH

**Fig. 3. Tspan18 does not interfere with PAPC ectodomain shedding by xADAM13, but may affect xADAM13 maturation.**

PAPC ectodoamin shedding in cells transfected with xA13, alone (lane 1) or with cTS18MT (lane 2), and E/xA13 (lane 3), a catalytically inactive version of xA13. (A) The ectodomain of PAPC (shedd PAPC; arrowhead) is present in the cell culture supernatant from cells transfected with xA13, both with and without cTS18MT (note the presence of shedd PAPC in both of these conditions). In contrast, shedd PAPC is not detectable in cell supernatants from cells transfected with E/xA13. (B) The presence of PAPC in total cell lysate from transfected cells. (C) The presence of xA13 isoforms within total cell lysate from transfected cells. When xA13 is co-transfected with cTS18MT (lane 2), there is proportionally more of the immature form of xA13 (top arrow; pro-xA13) than there is the mature form of xA13 (bottom arrow; mat-xA13) as compared to cells transfected with xA13 alone (lane 1). (D) The presence of Tspan18 in total cell lysate from transfected cells. (E) The presence of GAPDH in total cell lysate from transfected cells.

**Evaluating the ability of *in vivo* ADAM inhibition to rescue Cad6B protein levels when Tspan18 is knocked down**

Knockdown of Tspan18 leads to a premature loss of Cad6B protein levels in the dorsal neural tube of developing chick embryos (Fairchild and Gammill, 2013). While the aforementioned experiments assayed the interplay of Tspan18 and ADAMs *in vitro*, they did not necessarily reflect *in vivo* conditions. Thus, our next aim was to determine whether Tspan18 maintains Cad6B protein levels via an ADAM-dependent mechanism in chick embryos. We hypothesized that Tspan18 might protect Cad6B from processing by ADAMs in cranial neural crest cells, and reasoned that if this were true, inhibiting ADAM activity using the general ADAM inhibitor marimastat should rescue the premature loss of Cad6B protein levels observed after Tspan18 knockdown (Fairchild and Gammill, 2013). To investigate this, we electroporated HH stage $4^{+}$ embryos with either a control (ContMO) or a Tspan18 translation-blocking morpholino (TS18MO) and later bathed the cranial neural folds of electroporated embryos with 1 mM marimastat (in 10% DMSO) at 2-3 somites. At 5-7 somites, embryos were processed by whole mount immunofluorescence to visualize Cad6B protein levels. As expected, Cad6B protein levels were unaffected in embryos electroporated with ContMO and treated with either DMSO or marimastat (Fig. 4A,B). In contrast, embryos injected with TS18MO and treated with DMSO exhibited a premature loss of Cad6B protein, as previously described (Fig. 4C; (Fairchild and Gammill, 2013). Likewise, in embryos electroporated with TS18MO and treated with marimastat, Cad6B protein levels were reduced on the targeted side of the embryo (Fig. 4D). Thus, under these conditions, marimastat treatment does

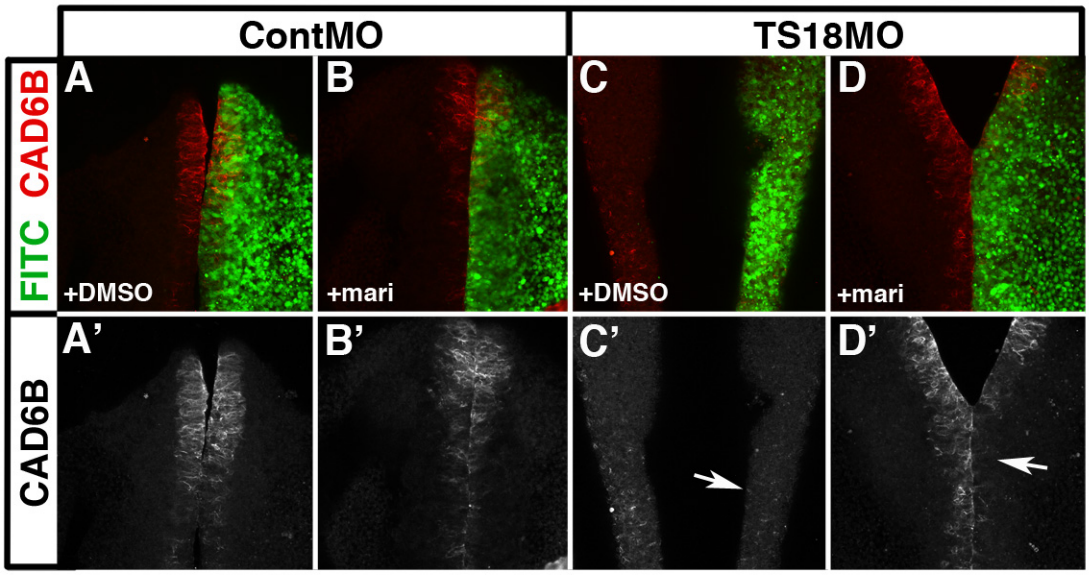
ContMO
TS18MO
FITC CAD6B
A
B
C
D
+DMSO
+mari
+DMSO
+mari
CAD6B
A'
B'
C'
D'

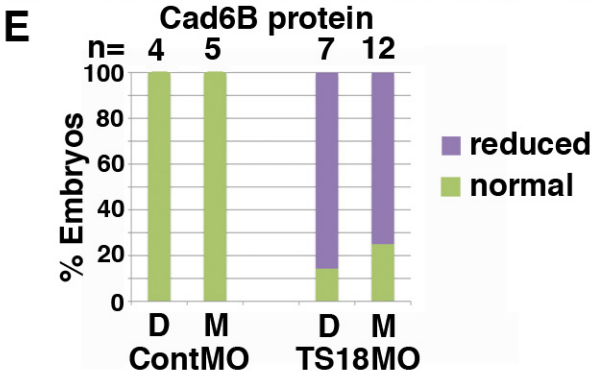
E
Cad6B protein
n= 4 5 7 12
100
80
60
40
20
0
% Embryos
D M D M
ContMO TS18MO
reduced
normal

**Fig. 4. Treatment with marimastat does not rescue the premature loss of Cad6B protein levels following Tspan18 knockdown.**

(A-D) Whole mount images of embryos electroporated with either ContMO (A,B) or TS18MO (C,D), treated with DMSO (A,C) or the general ADAM inhibitor marimastat (B,D) and immunostained for Cad6B protein. Embryos electroporated with ContMO (green in A,B) exhibit normal Cad6B protein levels (A'B'; and red in A,B) regardless of treatment with DMSO or marimastat. In contrast, electroporation with TS18MO (green in C,D) reduced Cad6B protein levels (C',D'; and red in C,D) regardless of treatment with DMSO or marimastat. (E) Bar graph representing the frequency of electroporated embryos exhibiting reduced v.s. normal Cad6B protein levels.

not rescue the premature loss of Cad6B protein levels that occurs following Tspan18 knockdown.

One possible explanation for why marimastat fails to rescue the Tspan18 loss-of-function Cad6B phenotype is that marimastat may not be efficiently delivered into the neural folds. In our experiments, electroporated stage $4^{+}$ embryos must be cultured ventral side up on agar-albumin (Chapman et al., 2001). This introduces two limitations. First, marimastat must be injected through ventral tissue to reach the dorsal neural tube, which easily damages the embryos. Second, even upon viable delivery of marimastat into the neural tube, the drug quickly dissipates into the agar-albumin culture substrate, drawing the marimastat away from the neural folds and preventing sustained incubation. Unfortunately, repositioning embryos dorsal side up after their initial incubation tears the delicate embryonic tissue of early embryos and is therefore not feasible (data not shown). Trying alternate culture systems, for example by incubating electroporated embryos in liquid culture containing marimastat, or using pluronic gel to more effectively localize and retain marimastat to the developing neural tube, may help correct these technical issues.

It is also possible that our results reflect a valid mechanistic finding. The absence of rescue in these experiments could indicate that we were incorrect in our hypothesis that Tspan18 regulates Cad6B through an ADAM-dependent post-translational mechanism; however, we currently lack a positive control for ADAM activity in the chick cranial neural folds to make this conclusion. Moreover, a recent study supports the idea that ADAM regulation by tetraspanins may be more complex than we have presently considered in this preliminary study. In particular, tetraspanin15 regulates ADAM10

activity at multiple levels, including initial maturation, trafficking to the cell surface, maintenance at the plasma membrane, and sheddase activity (Prox et al., 2012). Thus, it is possible that Tspan18 regulates ADAM maturation and/or localization in neural crest cells at a step in the process not addressed by these experiments. Identifying Tspan18 binding partners may identify proteins responsible for ADAM trafficking and/or maturation, and could potentially fill some of these gaps in our knowledge. Moreover, investigating Tspan18 binding partners would also allow us to indentify other potential mechanisms causing Tspan18-dependent maintenance of Cad6B. Such experiments are crucial and currently underway.

In conclusion, our preliminary data provides additional insight into the mechanism by which Tspan18 maintains cad6B protein. Our results suggest that Tspan18 indirectly regulates Cad6B levels, potentially by affecting ADAM metalloproteases. Our preliminary *in vitro* data with *Xenopus* ADAMs suggests that Tspan18 may be capable of altering ADAM maturation. However, because little is known about ADAM involvement during chick cranial neural crest migration, our chick experiments have been technically difficult and require further investigation. Identifying Tspan18 binding partners is an important next step in understanding the mechanism of how Tspan18 controls Cad6B, and more generally cell adhesion, during cranial neural crest EMT.

## Materials and Methods:

### Cell culture, vectors, and transfection

Chick embryonic fibroblasts (DF1; ATCC, Manassas, VA) were cultured in DMEM (high glucose; Life Technologies, Carlsbad, CA) supplemented with 10% fetal bovine serum (Life Technologies, Carlsbad, CA), 2.5 μg/μL plasmocin (InvivoGen, San Diego, CA), and penicillin/streptomycin at 37°C with 5% atmospheric $CO_2$. Chick Tspan18 and Cad6B were cloned into pCS2+ (Turner and Weintraub, 1994) containing either a C-terminal Myc Tag or Flag Tag as previously described (Fairchild and Gammill, 2013). pCIG-ADAM10 and pCIG-ADAM19 plasmids were provided by L.A. Taneyhill. 12 μg of each vector was transfected into DF1 cells using Lipofectamine 2000 (Life Technologies, Carlsbad, CA) according to manufacturer's protocol. 32 hours after transfection, cells were removed from the culture dish by scraping, and washed twice in sterile PBS, and either immediately frozen or lysed for immunoblotting or immunoprecipitation.

### Western Blotting and Immunoprecipitation

Transfected cells were lysed in ice-cold TBS containing 1% Brij-99 (Sigma Aldrich, St. Louis, MO) and Complete protease inhibitors (Roche, Indianapolis, IN). Following lysis insoluble proteins were removed by centrifugation at 15,000 rpm for 10 min at 4°C. For western blotting, cell lysates were run on hand poured 10% SDS-PAGE gels, transferred to nitrocellulose (Bio-Rad, Hercules, CA), and incubated overnight at 4°C with the appropriate primary antibodies: anti-Myc Tag (DSHB, Iowa City, IA) at 1:100, anti-Flag M2 (Sigma) at one 1:500, or anti-HA tag (clone 12CA5; Roche) at 1:100 followed by an

HRP-conjugated goat anti-mouse secondary antibody (Jackson Labs, West Grove, PA). Western blots were developed using the SuperSignal West Pico Chemiluminescent Substrate kit (Thermo Scientific, Rockford, IL) according to manufacturer's instruction. For immunoprecipitation, cell lysates were diluted in 1% Brij-99 lysis buffer, incubated with anti-Flag M2 magnetic beads (Sigma) overnight at 4°C, washed 3 times in PBS and eluted by boiling in 4X SDS-PAGE loading buffer with BME according to the Sigma protocol. To detect protein-protein interactions, immunoprecipitated proteins were then run on SDS-PAGE gels and visualized by western blot as described above.

**Embryos**

Fertile chicken embryos were incubated in a humidified incubator (G. Q. F. Manufacturing; Savannah, GA) at 37-38°C. Embryos were staged according to Hamburger and Hamilton, 1951 or by counting somite pairs.

**Embryo electroporation and marimastat treatment**

Stage $4^{+}$ embryos were electroporated with FITC-tagged standard control or Tspan18 translation-blocking morpholino oligonucleotides (MOs) according to (Gammill and Krull, 2011) as previously described (Fairchild and Gammill, 2013). After electroporation, embryos were incubated on agar albumin plates until 2-3 somites, and 1 mM marimastat in 10% DMSO (or 10% DMSO alone) was injected into the developing neural tube. Following reincubation to 5-6 somites, embryos were fixed in 4% paraformaldehyde and immediately processed for whole mount immunofluorescence.

**Whole mount immunofluorescence**

To detect Cad6B protein in electroporated embryos, whole embryos were incubated with anti-Cad6B primary antibody (DSHB) and appropriate RRX-conjugated secondary antibody as previously described (Fairchild and Gammill, 2013). Whole mount immunostained embryos were then imaged on a Zeiss 710 confocal microscope using LSM software. Images were adjusted in Photoshop (Adobe).